A STUDY OF THE DEPHOSPHORIZATION OF KOTON KARFE IRON ORE BY ACIDIC LEACHING.

BY

Ferdinard ASUKE (B. ENG, M.Sc)

(Ph.D/ENG/02133/2008 – 2009)

A PROJECT DISSERTATION SUBMITTED TO THE SCHOOL OF POSTGRADUATE STUDIES, AHMADU BELLO UNIVERSITY, ZARIA.

IN PARTIAL FULFILMENT FOR THE AWARD

OF A DOCTOR OF PHILOSOPHY (Ph.D)

IN METALLURGICAL AND MATERIALS ENGINEERING.

DEPARTMENT OF METALLURGICAL AND MATERIALS ENGINEERING

FACULTY OF ENGINEERING

AHMADU BELLO UNIVERSITY, ZARIA

NIGERIA

MAY, 2014.

DECLARATION

I declare that the work in this project dissertation entitled "A study of the dephosphorization of Koton-karfe iron ore by acidic leaching" has been carried out by me in the Department of Metallurgical and Materials Engineering, Ahmadu Bello University, Zaria. The information derived from the literature has been duly acknowledged in the text and a list of references provided. No part of this project dissertation was previously presented for another degree or diploma in this or any other Institution.

Ferdinard ASUKE _____ _____

Signature Date

CERTIFICATION

This project dissertation entitled 'A STUDY OF THE DEPHOSPHORIZATION OF KOTON KARFE IRON ORE BY ACIDIC LEACHING' by Ferdinard ASUKE meets the regulations governing the award of the degree of Doctor of philosophy (Ph.D) Metallurgical and Materials Engineering of the Ahmadu Bello University and is approved for its contributions to knowledge and literary presentation.

Prof. S. A. Yaro Chairman, Supervisory Committee	_____ Signature	_____ Date
Dr. A.P.I. Poopola Member, Supervisory Committee	_____ Signature	_____ Date
Dr. O. Aponbiede Member, Supervisory Committee	_____ Signature	_____ Date
Prof. S.A Yaro Head of Department	_____ Signature	_____ Date
Prof. A. A. Joshua Dean, School of Postgraduate Studies	_____ Signature	_____ Date

DEDICATION

This project dissertation is dedicated to the memory of my late father, Mr. James Asuke. Daddy continue to rest in peace.

ACKNOWLEDGEMENT

Thanks be to God Almighty who gave me the strength, understanding, favor, wisdom, health of mind and body to carry out this research.

My gratitude goes to the management of the Ahmadu Bello University, Zaria for the support given to me through the award of the 2010 Education Trust Fund (ETF) scholarship and the management of the Tshwane University of Technology (TUT) Pretoria, South Africa for providing me the bench space with which I carried out this research.

I appreciate my supervisors, Prof. S.A Yaro who encouraged, supported and directed me through this research and Dr. A.P.I Popoola who was also my host out there in South Africa during my bench work and provided most of the consumables used for this research, and ensured that I had a conducive environment to work; and Dr. O Aponbiede for your guidance and encouragement. I am forever grateful to you all and I pray that God will reward you. I also thank all the academic and non academic members of staff in the department for their contributions, advice and support.

Thank you Prof. Rob Makringle for your statistical optimization guide. To Janette Dykstra the X-ray fluorescent analysis expert and Wiebke Grote the X-ray Diffraction expert, I am grateful for your guidance and analysis.

To my friends Dr. V.S Aigbodion, Dr. M. Abdulwahab, Dr. A Kassim, Dr. B Akpor, O.S.I Fayomi, T. Loto, Kentse and Mercy Ramakokovhu, I appreciate your contributions to the success of this research.

I appreciate all my family members, my wife Mrs M. Asuke and my mum Mrs. M.I Asuke for their support, love, understanding, encouragement and prayers; my brothers Engr. Ben, Dr. Sunday, Dr. Dominic and my sisters Christy, Amina, Celestina, Georgina, Edith, Evelyn and Betty. Thank you all for your prayers and support.

Finally to all those that have contributed to this work that I have not mentioned, I pray that God may bless and reward you all abundantly. Thank you.

ABSTRACT

In this work an attempt was made to dephosphorize Koton-karfe iron ore by leaching with Sulphuric (H_2SO_4), Hydrochloric (HCl) and Citric ($C_6H_8O_7$) acids. The work involved carrying out chemical and mineralogical characterization of the ore, size/assay analysis (+355µm to -50µm) followed by leaching at different particle sizes (-355 +250 and -180 +125µm) and varying time (20 – 120minutes at an interval of 20 minutes), concentration of the acids (0.5M – 2.5M at an interval of 0.5M for hydrochloric and citric acid and 0.15 – 1.2M for sulphuric), temperature (30 - 80^oC at an interval of 10^oC) and agitation (100 – 500rpm at an interval of 100rpm) in order to develop the optimum leaching conditions for the acids under study. The ore after calcinations at 700, 800 and 900^oC was also leached at optimum conditions attained. The results of the chemical analysis revealed that the iron ore head sample had a total iron content of 46.91% Fe (67.02% Fe_2O_3) and phosphorus content of 0.79% P (1.81% P_2O_5). The results of the mineralogical analysis reveal that Goethite (FeO(OH)), Quartz (SiO_2), Alumina(Al_2O_3) and Phosphorus are the minerals present in the ore while Magnetite (Fe_3O_4), Hematite(Fe_2O_3) e.t.c are present in minute amounts. The mineralogical analysis also showed that the phosphorus is uniformly distributed in the iron ore in the form of berlinite ($AlPO_4$) and in solid solution with goethite. The leaching shows that the highest percentages of phosphorus removal prior to calcination of 45.40, 35.31 and 29.73% were attained at particle size fraction -180 +125µm for sulphuric, hydrochloric and citric acids respectively.

Generally calcination of the iron ore prior to leaching increased the rate of removal of Phosphorus from the ore. The kinetic study of the leaching mechanism of the phosphorus removal by the acids revealed that leaching with citric acid has an activation energy of 12.6KJ/mol, and hence it is diffusion controlled, while leaching mechanism of the phosphorus by hydrochloric and sulphuric acids are intermediate (chemical and diffusion) controlled with activation energies of 29.56 and 26.9KJ/mol respectively. Based on the results obtained, it can be concluded that Sulphuric acid gave the best results with 73.51% of the total phosphorus in the ore being removed.

TABLE OF CONTENT

TITLE PAGE- - - - - - - -i

DECLARATION PAGE- - - - - - - -ii

CERTIFICATION- - - - - - - -iii

DEDICATION- - - - - - - - -iv

ACKNOWLEDGEMENT- - - - - - -v

ABSTRACT- - - - - - - - -vii

TABLE OF CONTENT- - - - - - - -ix

LIST OF TABLES- - - - - - - - xvii

LIST OF FIGURES- - - - - - - -xxii

LIST OF PLATES- - - - - - - - xxviii

LIST OF APENDIX- - - - - - - -xxix

CHAPTER ONE

1.0 Introduction - - - - - - - - 1

1.1 Mineral Resources in Nigeria- - - - - - - 2

1.2 Nigerian Iron Ores- - - - - - - - 2

1.3 Research Problem- - - - - - - - 6

1.4 Objectives- - - - - - - - - 8

1.5 Justification- - - - - - - - - 9

1.6 Scope of work - - - - - - - - - 9

1.7 Contribution to knowledge - - - - - - - 10

CHAPTER TWO

2.0 Literature Review- - - - - - - - 11

2.1 Geology of Koton-karfe Iron Ore- - - - - - 11

2.2 Previous works on the upgrading of the Koton-karfe Iron ore- - 11

2.3 Phosphorous in Iron Ores- - - - - - - 12

2.4 Phosphorous in Goethite- - - - - - - 13

2.5 Phosphorous in Pig iron- - - - - - - 13

2.6 Leaching Process- - - - - - - - 15

2.6.1 Types of Leaching Processes- - - - - - 15

2.6.2 Choice of Leaching Agents- - - - - - 16

2.7 Sulfuric Acid- - - - - - - - - 18

2.8 Hydrochloric Acid- - - - - - - - 20

2.9 Citric Acid- - - - - - - - - 22

2.10 Leaching Techniques- - - - - - - 24

2.11 Mechanism of Leaching- - - - - - - 25

2.12 Factors influencing leaching kinetics- - - - - 25

2.13 Determination of leaching rate- - - - - - 28

2.14 Kinetic equation expressed as fraction leached- - - 29

2.15 Determination of Activation Energy- - - - - 30

2.16 Method for removal of phosphorous from iron ores- - - 31

2.16.1 Physical separation- - - - - - - 31

2.16.2 Chemical leaching- - - - - - - 32

2.16.3 Phosphorous reduction before, during and after steel Making- - - - - - - - 32

2.16.3.1 Reduction of phosphorous during iron making- - - 32

2.16.3.2 Dephosphorization during steelmaking- - - - 33

2.17 Previous studies on the leaching of iron ores- - - 37

2.18 Statistical design and development of mathematical Model-- - - - - - - - 46

CHAPTER THREE

3.0 Materials and Methods- - - - - - - 48

3.1 Equipment- - - - - - - - - 48

3.2 Materials- - - - - - - - - 48

3.2.1 Material collection and preparation- - - - - 48

3.3 Chemical Characterization of the head sample- - - - 49

3.3.1 Determination of the chemical composition of the head sample- - - - - - - 49
3.4 Mineralogical characterization of the head sample- - - 49
3.4.1 X-Ray diffractometer (XRD) characterization- - - 50
3.4.2 Scanning emission microscopy/energy dispersion spectrum (SEM/EDS)- - - - - - 50
3.5. The leaching process- - - - - - 51
3.5.1 Leaching reagents used- - - - - - 51
3.5.2 Leaching procedures- - - - - - 52
3.6 Determination of phosphorous content before and after leaching the ore- - - - - - - 53
3.7 Determination of the amount of phosphorous removed during leaching with acids- - - - - - 54
3.8 Analysis of the acids before leaching and the leached Liquor- - - - - - - - 54
3.8.1 Determination of acid content before leaching and in the leached solution- - - - - - 54
3.8.2 Analysis using inductively coupled plasma optical Emission spectrometry (ICP/OES)- - - - - 54
3.9 pH Measurement- - - - - - - 55
3.10 Determination of the Amounts of Iron dissolved in acid during Leaching- - - - - - 56

3.11 Determination of leaching rate constant - - - 56

3.12 Determination of Activation Energy- - - - 57

3.13 Statistical validation of the optimum Leaching

Condition- - - - - - - - 58

CHAPTER FOUR

4.0 Results- - - - - - - - 59

4.1 Characterization of the head sample- - - - - 59

4.2 Distribution of minerals in the various particle sizes of

the iron ore- - - - - - - - 67

4.3 Further analysis of -335 +250µm particle size- - - 68

4.4 Further analysis of -180+125µm particle size- - - 75

4.5 Results for leaching of -355+250µm particle size- - - 80

4.5.1 Effect of the variation of agitation on the leaching of

-355+250µm particle size- - - - - 80

4.5.2 Effect of the variation of temperature on the leaching of

-335+250µm particle size- - - - - 81

4.5.3 Effect of the variation of concentration and time on

the leaching of -355+250µm particle size- - - 83

4.6 Factorial design for developed leaching conditions with

-355+250 particle size- - - - - - 86

4.7 Leaching of -180+125µm particle size- - - - 91

4.8 Calcination of Iron ore- - - - - - 92

4.9 XRD Results after calcination at different
Temperature- - - - - - - 94
4.10 Leaching of the calcined iron ore- - - - 98
4.11 Comparison of optimum leaching conditions- - - 100
4.12 Determination of loses to the leach solution- - - 101
4.13 Determining of the pH values of acids before and after
Leaching- - - - - - - - 103
4.14 Kinetics of leaching- - - - - - 105
4.14.1 Determination of rate constants(k) and the activation
energy (E) for the Optimum leaching conditions- - 105

CHAPTER FIVE

5.0 Discussion of Results- - - - - - 107
5.1 X-Ray Fluorescent (XRF) analysis of Head sample- - - 107
5.2 X-Ray diffraction (XRD) pattern of Head Sample- - 107
5.3 Scanning electron micrograph (SEM) of Head sample- - 107
5.4 X-Ray Fluorescent (XRF) analysis of the various
particle size- - - - - - - - 108
5.5 X-Ray Diffraction (XRD) pattern of the selected
particle sizes- - - - - - - - 109
5.6 Scanning electron microscopy (SEM) image of the selected
particle size- - - - - - - - 109

5.7 Distribution of phosphorous within the head sample and selected particle sizes for leaching- - - - 110

5.8 Leaching of -355+250µm particle size- - - - 111

5.8.1 Variation of Agitation of leaching of -355+250µm particle size- - - - - - - 111

5.8.2 Variation of Temperature on leaching of -355+255µm particle size- - - - - - - 112

5.8.3 Variation of concentration and time on leaching of -355+250µm particle size- - - - - 113

5.9 Factorial Design for the Leaching Rate of -355+250 particle size and the various acids used- - - - - 114

5.10 Leaching of -180+125 Particle size- - - - 116

5.11 Calculation of the Iron Ore- - - - - 116

5.12 XRD results after calcination- - - - - 117

5.13 Leaching of calcined iron ore- - - - - 118

5.14 Comparison of optimum phosphorus leached for the various particle sizes and the acid used- - - - - 119

5.15 Ionization of Acids used for leaching- - - - 120

5.16 Equations of reaction- - - - - - 121

5.17 Dissolution of iron during leaching- - - - 121

5.18 pH values of acid after leaching- - - - - 122

5.19 Kinetics of leaching- - - - - - 123

5.19.1 The rate constant (k) and the activation energy (E) for the optimum leaching condition- - - - 123

5.20 Acid consumption cost- - - - - - 124

CHAPTER SIX

6.0 Conclusion and recommendation- - - - - 125

6.1 Conclusions- - - - - - - - 125

6.2 Recommendations- - - - - - - 127

REFERENCES- - - - - - - - 128

APPENDICES- - - - - - - - 139

LIST OF TABLES

Table 1.1: The Nigerian iron ore deposits and the proven reserves (in million tonnes)- - - - - - - 3

Table 1.2: Chemical composition of some Nigerian iron ores- - - 6

Table 2.1: A summary of commonly used leaching agent and their Applications- - - - - - - - 17

Table 3.1:Level of factors for the leaching process- - - - 58

Table 3.2: Design layout and response data for the various acids used as a Leachant- - - - - - - 58

Table 4.1: XRF analysis head sample showing constituents oxides and percentage composition- - - - - - 59

Table 4.2: The relative phase amounts (weights%) as estimated by the Rietveld method - - - - - - - 61

Table 4.3: Summary of the count of the individual element on the Head Sample- - - - - - - - 66

Table 4.4: XRF analysis of the various particle sizes- - - - 67

Table 4.5: The relative phase amounts (weight%) of the -355+250 Particle size, as estimated by the Rietveld method - - - 69

Table 4.6: Summary of the count of the individual elements of the SEM of the -355 +255 particle size- - - - - 74

Table 4.7: The relative phase amounts (weights %) of the -180+125 particle size as estimated by the Rietveld method - - - 76

Table 4.8: Summary of the count of the individual elements on the SEM of the -180+125 particle size- - - - - 79
Table 4.9: The effect of agitation on the leaching of -355+250 particle Size with the different acids used- - - - - 80
Table 4.10: Variation of temperature on the leaching rate of the different acid used - - - - - - - 82
Table 4.11: Variation of sulphuric acid concentration and time on the leaching of phosphorus in the -355+250 particle size- - 83
Table 4.12: Variation of Hydrochloric acid concentration and time on the Leaching of phosphorus in the -355+250 particle size- - 84
Table 4.13: Variation of citric acid concentration and time on the leaching of phosphorous in the -355+250 particle size- - 85
Table 4.14: Design layout and response data for sulphuric acid as a Leachant- - - - - - - - 87
Table 4.15: Design layout and response data for hydrochloric acid as a leachant - - - - - - - 87
Table 4.16: Design layout and response data for citric acid as a leachant - - - - - - - - 87
Table 4.17: ANOVA design of leaching rate of sulphuric acid at boundary conditions of concentration and time- - - 88
Table 4.18: ANOVA design of leaning rate with Hydrochloric acid at boundary conditions of concentration and time- - - 88

Table 4.19: ANOVA design of leaching rate with citric acid at Boundary conditions of concentration and time- - - 89
Table 4.20: Result of leaching of -180+125 particle size with optimum leaching condition generated for the different acids- - 91
Table 4.21: XRF result obtained after calcination of -355+250 particle size of Iron ore at 600,800 and 900^0C- - - - 92
Table 4.22: XRF result obtained after calcination of -180+125 particle size of Iron ore at 600,800 and 900^0C- - - - 93
Table 4.23: The relative phase amount (weight%) of the -355+250 particle size, as estimated by the Rietveld method after calcination- - - - - - 96
Table 4.24: The relative phase amounts (weight%) of the -180+250 particle size, as estimated by the Rietveld method after calcination- - - - - - 98
Table 4.25: Results of leaching of the -355+250 particle size with optimum leaching conditions after calcination- - - 98
Table 4.26:Results of leaching of the -180+125 particle size with the optimum leaching conditions after calcination- - - 99
Table 4.27: Summary of optimum leaching conditions for the various particle Sizes- - - - - - - 100
Table 4.28: ICPOES analysis of citric acid before and after leaching at optimum leaching concentration- - - 102

Table 4.29: ICPOES analysis of hydrochloric acid before and after leaching at optimum leaching concentration- - - 102
Table 4.30: ICPOES analysis of sulphuric acid before and after leaching at optimum leaching concentration- - - 103
Table 4.31: pH values of acid before and after initial leaching at optimum conditions for -355 +250µm particle size. (19.3^{o}C)- - - - - - - 103
Table 4.32: pH values of acid before and after Initial leaching at optimum conditions for -180 +125µm particle size. (2.17 ^{o}C)- - - - - - - 104
Table 4.33: pH values of acid before and after leaching at optimum conditions for -355 +250µm particle size after calcinations at 900^{o}C. (2.17 ^{o}C)- - - - - - - 104
Table 4.34: pH values of acid before and after leaching at optimum conditions for -180 +125µm particle size after calcinations at 900^{o}C.. (2.17 ^{o}C)- - - - - - - 104
Table 4.35: The rate constants (k) and the Activation energy (E_a) for Citric Acid as a leachant- - - - - - 105
Table 4.36: The rate constants (k) and the Activation energy (E_a) for Hydrochloric Acid as a leachant- - - - - 105
Table 4.37: The rate constants (k) and the Activation energy (E_a) for Sulphuric Acid as a leachant- - - - - - 106

Table 5.1: The developed optimum leaching conditions for the selective leaching of Phosphorus from -355 +250 particle size of the Koton-karfe iron ore- - - - 114

LIST OF FIGURES

Figure 1.1 : Geological Sketch Map of Nigeria Showing the Location of Koton Karfe Iron Ore Deposit- - - - - .4

Figure 2.1: The Zero Slag Process (ZSP) process flow at the NKK's Fukuyama's works- - - - - - - 37

Figure 4.1 : The X- ray Diffraction (XRD) pattern of the Head sample- - 60

Figure 4.2a: Energy Dispersion Spectroscopy (EDS) spectrum of Point 1 on the head sample in the SEM micrograph - - 62

Figure 4.2b: Energy Dispersion Spectroscopy (EDS) spectrum of Point 2 on the head sample in the SEM micrograph- - 62

Figure 4.2c: Energy Dispersion Spectroscopy (EDS) spectrum of Point 3 on the head sample in the SEM micrograph- - 63

Figure 4.2d: Energy Dispersion Spectroscopy (EDS) spectrum of Point 4 on the head sample in the SEM micrograph- - 63

Figure 4.2e: Energy Dispersion Spectroscopy (EDS) spectrum of Point 5 on the head sample in the SEM micrograph- - 64

Figure 4.3: The X- ray Diffraction (XRD) pattern of the

-355 +250µm particle size- - - - - - 68

Figure 4.4a: Energy Dispersion Spectroscopy (EDS) spectrum of

Point 1 on the SEM image of the -355 +250µm

particle size -- - - - - - - 70

Figure 4.4b: Energy Dispersion Spectroscopy (EDS) spectrum of

Point 2 on the SEM image of the -355 +250µm

particle size - - - - - - - 70

Figure 4.4c: Energy Dispersion Spectroscopy (EDS) spectrum of

Point 3 on the SEM image of the -355 +250µm

particle size- - - - - - - - 71

Figure 4.4d: Energy Dispersion Spectroscopy (EDS) spectrum of

Point 4 on the SEM image of the -355 +250µm

particle size- - - - - - - - 71

Figure 4.4e: Energy Dispersion Spectroscopy (EDS) spectrum of

Point 5 on the SEM image of the -355 +250µm

particle size - - - - - - - - 72

Figure 4.5: The X- ray Diffraction (XRD) pattern of the -180 +125µm particle size- - - - - - - - 75

Figure 4.6a: Energy Dispersion Spectroscopy (EDS) spectrum of Point 1 on the SEM image of -180 +125µm particle size- - - - - - - - 77

Figure 4.6b: Energy Dispersion Spectroscopy (EDS) spectrum of Point 2 on the SEM image of -180 +125µm particle size- - - - - - - - 77

Figure 4.6c: Energy Dispersion Spectroscopy (EDS) spectrum of Point 3 on the SEM image of -180 +125µm particle size -- - - - - - - 78

Figure 4.6d: Energy Dispersion Spectroscopy (EDS) spectrum of Point 4 on the SEM image of -180 +125µm particle size- - - - - - - - 78

Figure 4.6e: Energy Dispersion Spectroscopy (EDS) spectrum of Point 5 on the SEM image of -180 +125µm particle size -- - - - - - - 79

Figure 4.7: Variation of Agitation on leaching of phosphorus with initial leaching conditions- - - - - - - 81

Figure 4.8: Variation of Temperature with the amount of phosphorus leached with initial Leaching conditions- - - - 82

Figure 4.9: Variation of concentration and time with initial established conditions of temperature and agitation on the leaching of -355 +250µm particle size with Sulphuric acid solution- - - - - - - - - 84

Figure 4.10: Variation of concentration and time with initial established conditions of temperature and agitation on the leaching of -355 +250µm particle size with Hydrochloric acid solution- - - - - - - - 85

Figure 4.11: Variation of concentration and time with initial established conditions of temperature and agitation on the leaching of -355 +250µm particle size with Citric acid Solution- - - - - - - - 86

Figure 4.12: Relationship of concentration, time and leaching rate using sulphuric acid as predicted from factorial design- - - - - - - - 89
Figure 4.13: Relationship of concentration, time and leaching rate using hydrochloric acid as predicted from factorial design - - - - - - - - 90
Figure 4.14: Relationship of concentration, time and leaching rate Using citric acidas predicted from factorial Design- - - - - - - - 90
Figure 4.15: The leaching of -180 +125µm particle size with the Different acids with the optimum conditions defined from the -355 +250µm particle size- - - - 91
Figure 4.16: XRD pattern of -355 +250µm particle size after calcinations at 700^{o}C- - - - - - 94
Figure 4.17: XRD pattern of -355 +250µm particle size after calcinations at 800^{o}C- - - - - - 95
Figure 4.18: XRD pattern of -355 +250µm particle size after calcinations at 900^{o}C- - - - - - 95
Figure 4.19: XRD pattern of -180 +125µm particle size after Calcinations at 700^{o}C- - - - - - 96

Figure 4.20: XRD pattern of -180 +125µm particle size after calcinations at 800^{o}C- - - - - - 97

Figure 4.21: XRD pattern of -180 +125µm particle size after calcinations at 900^{o}C- - - - - - 97

Figure 4.22: Effects of different acids on the leaching of -355 +250µm Particle size with the optimum leaching concentration after calcinations- - - - - - - 99

Figure 4.23: Effects of different acids on the leaching of -180 +125µm particle size with the optimum leaching concentration after calcinations- - - - - - - 100

Figure 4.24: Comparative chat for various optimum leaching conditions with different acids and particle sizes before and after calcination- - - - - - - 101

LIST OF PLATES

PLATE I: Scanning electron microscope (SEM) image and randomly Selected points for energy dispersion spectroscopy (EDS) spectrum of head sample- - - - - - 61

PLATE IIa—IIj: SEM mapping showing distribution of various elements in the micrograph of the head sample- - - - 64

PLATE III: Scanning Electron microscope (SEM) image and selected points for energy dispersion spectroscopy (EDS) spectrum of the -355 +250µm particle size - - - - - - 69

PLATE IVa—IVj: SEM mapping showing distribution of various elements in the micrograph of the -355 +250µm particle size- 72

PLATE V: Scanning Electron microscope (SEM) image and selected points for energy dispersion spectroscopy (EDS) spectrum of the -180 +125µm particle size- - - - 76

LIST OF APPENDIXES

APPENDIX A

Table A1: XRF result for the variation of agitation rate on leaching of

-355 +250µm particle size with Sulphuric acid- - - 139

Table A2: XRF result for the variation of agitation rate on leaching of

-355 +250µm particle size with 0.5M Hydrochloric acid- - 140

Table A3 : XRF result for the variation of agitation rate on leaching of

-355 +250µm particle size with 0.5M Citric acid- - - 141

APPENDIX B

Table B1: XRF result for the variation of Temperature on leaching of

-355 +250µm particle size with 0.3M Sulphuric acid- - 142

Table B2: XRF result for the variation of Temperature on leaching of

-355 +250µm particle size with 0.5M Hydrochloric acid - - 143

Table B3: XRF result for the variation of Temperature on leaching of

-355 +250µm particle size with 0.5M Citric acid- - - 144

APPENDIX C

Table C1: XRF result showing the effect of 0.15M concentration of Sulphuric acid and variation of time on the leaching of -355 +250 µm particle size- - - - - - 145

Table C2: XRF result showing the effect of 0.3M concentration of Sulphuric acid and variation of time on the leaching of -355 +250 µm particle size- - - - - - 146

Table C3: XRF result showing the effect of 0.6M concentration of Sulphuric acid and variation of time on the leaching of -355 +250 µm particle size- - - - - - 147

Table C4: XRF result showing the effect of 0.9M concentration of Sulphuric acid and variation of time on the leaching of -355 +250 µm particle size- - - - - - 148

Table C5: XRF result showing the effect of 1.2M concentration of Sulphuric acid and variation of time on the leaching of -355 +250 µm particle size- - - - - - 149

Table C6: XRF result showing the effect of 0.5M concentration of Hydrochloric acid and variation of time on the leaching of -355 +250 µm particle size- - - - - - 150

Table C7: XRF result showing the effect of 1.0M concentration of Hydrochloricacid and variation of time on the leaching of -355 +250 µm particle size- - - - - - 151

Table C8: XRF result showing the effect of 1.5M concentration of Hydrochloric acid and variation of time on the leaching of -355 +250 µm particle size- - - - - - 152

Table C9: XRF result showing the effect of 2.0M concentration of Hydrochloric acid and variation of time on the leaching of -355 +250 µm particle size-- - - - - 153

Table C10: XRF result showing the effect of 2.5M concentration of Hydrochloric acid and variation of time on the leaching of -355 +250µm particle size- - - - - 154

Table C11: XRF result showing the effect of 0.5M concentration of Citric acid and variation of time on the leaching of -355 +250µm particle size- - - - - - 155

Table C12: XRF result showing the effect of 1.0M concentration of Citric acid and variation of time on the leaching of -355 +250µm particle size- - - - - - 156

Table C13: XRF result showing the effect of 1.5M concentration of Citric acid and variation of time on the leaching of -355 +250µm particle size- - - - - - 157

Table C14: XRF result showing the effect of 2.0M concentration of Citric acid and variation of time on the leaching of -355 +250µm particle size- - - - - - 158

Table C15: XRF result showing the effect of 2.5M concentration of Citric acid and variation of time on the leaching of -355 +250µm particle size - - - - - - 159

APPENDIX D

Table D1: XRF Results for the leaching of of -180 +125 µm particle size under optimum leaching conditions- - - - 160

APPENDIX E

Table E1: XRF result for leaching of -355 +250µm particle size with the optimum leaching conditions after calcinations at 700^{o}C- 161

Table E2: XRF result for leaching of -355 +250µm particle size with the optimum leaching conditions after calcinations at 800^{o}C- 162

Table E3: XRF result for leaching of -355 +250µm particle size with the Optimum leaching conditions after calcinations at 900^{o}C- - 163

Table E4: XRF result for leaching of -180 +125µm particle size with the Optimum leaching conditions after calcinations at 700^{o}C- - 164

Table E5: XRF result for leaching of -180 +125µm particle size with the Optimum leaching conditions after calcinations at 800^{o}C- - 165

Table E6: XRF result for leaching of -180 +125µm particle size with the optimum leaching conditions after calcinations at 900^{o}C- - 166

CHAPTER ONE

1.0 INTRODUCTION.

The acquisition of iron and steel technology forms the main bedrock for the technological foundation of any developing nation. The building of bridges, rail lines and dense traffic motorways, the manufacture of motor vehicles, ships, military hard ware, agricultural and industrial appliances, household utility goods and educational and technical equipment, the construction of towering structures and underground bunkers, channels and tunnels, social and recreational centers, stadia and gymnasia, all these and many more encountered in daily life, are partially or wholly associated with the availability of iron and steel materials (Uwadiale, 1984).

The economic and political consequences of a perpetual dependence on imports of iron and steel raw materials and finished products by any nation are numerous and diverse. Economically, it leads to a drain of the nation's foreign reserves, to the advantage of the supplying nation(s). Politically, the manufacture, supply, construction and erection of portions or entire components of strategic military hardware, communication complexes, oil rigs, pipelines and refineries, airports, seaports or harbors, and even office, dwelling and storage infrastructure leaves the host nation completely exposed to the outside world in terms of security and sovereignty.

1.1 Mineral resources in Nigeria.

Nigeria is abundantly endowed with mineral resources – from asbestos and bauxite, through cassiterite, columbite, diamond, gold, monazite, sapphires and tantalite, to uranium and zircon. Virtually all metalliferous and non-metalliferous, solid and liquid minerals of economic importance abound in differing proportions.

1.2 Nigerian iron ores.

Large deposits of iron ores have been discovered in the country making Nigeria one of the richest countries in the world as far as mineral resources are concerned, with workable iron ore reserve estimate of 2.5 billion tons (Min. and Ind. In Nigeria. 1987). From Table 1.1 it is seen that Agbaja has the largest reserve in Nigeria. In terms of total iron content, it also has some of the highest values. It is closely followed by the Koton-karfe and the Bassa Nge deposit which lie in the same region (Amadi et al., 1983). The Agbaja-Lokoja-Koton-karfe-Bassa Nge ore body is located in the Lokoja confluence ($6^0$45E; $7^0$47N), and covers an expanse of land approximately 400Km^2 in the geographical area of Nigeria now known as Kogi State (BRGM 1983). The confluence divides the deposit into three major areas: (i) The Agbaja-Mount Patti-Lokoja area (approximately 150Km^2), located west of the river Niger; (ii) The Koton-karfe area (approximately 170Km^2), located north of the confluence; and the Bassa Nge area (approximately 80Km^2), located south east of the confluence as shown in Figure 1.1 (Uwadiale, 1984).

From the Nigerian iron ores (Table 1.1) only those found in Itakpe (36.88%Fe, 0.18%P_2O_5) and Ajabanoko hills (37.22%Fe, 0.10%P_2O_5) between Okene and Lokoja in Kogi State are considered suitable for iron and steel making after

beneficiation because of the acceptable level of impurities such as phosphorus, sulphur, arsenics, zinc, and alkali metals, etc (Min. and Ind. In Nigeria. 1987).

Table 1.1: The Nigerian iron ore deposits and their proven reserves (in million tonnes)

S/No	State	Location	Iron content	Proven reserves
1	Kogi	Bassa-Nge	43-49%	400 million tonnes
2		Agbado Okadu	38-48%	60 million tonnes
3		Ajabanoko	40%	60million tonnes
4		Jatti	40%	-
5		Koton Karfe	43-53%	428 million tonnes
6		Itakpe	36-38%	200 million tonnes
7		Chokochoko	30-40%	14 million tonnes
8		Akoina	41-47%	-
9		Tajimi	39-58%	200 million tonnes
10		Ero	Under investigation	-
11		Ebiya	‘’	-
12		Obanaja	‘’	-
13		Agbaja	43-49%	2 billion tonnes
14		Kakun (Kabba)	38-42%	-
15		Ubo-Toso	Under investigation	-
16	Kaduna	Kagara (Kubacha)	58-63%	-
17		Birni Gwari	30-35%	-
18	Ondo	Akunu (Ikare)	Under investigation	-
19	Bauchi	Reshi	10-19%	-
20		Ayiwawa	6-23%	-
21		Gamawa	40-45%	-
22	Plateau	Veketuwo	40-50%	-
23	Nasarawa	Toto Muro	25-38%	3.8 million tonnes
24	Kebbi	Dakingari	37%	-
25	Anambra	Nsude hill	43-50%	40.6 million tonnes
26	Borno	Karfe	34-45%	-

Source: (Uwadiale, 1989; Oloche and Hirse 1995; Oyeyinka, 1997; Thomas, 2002)

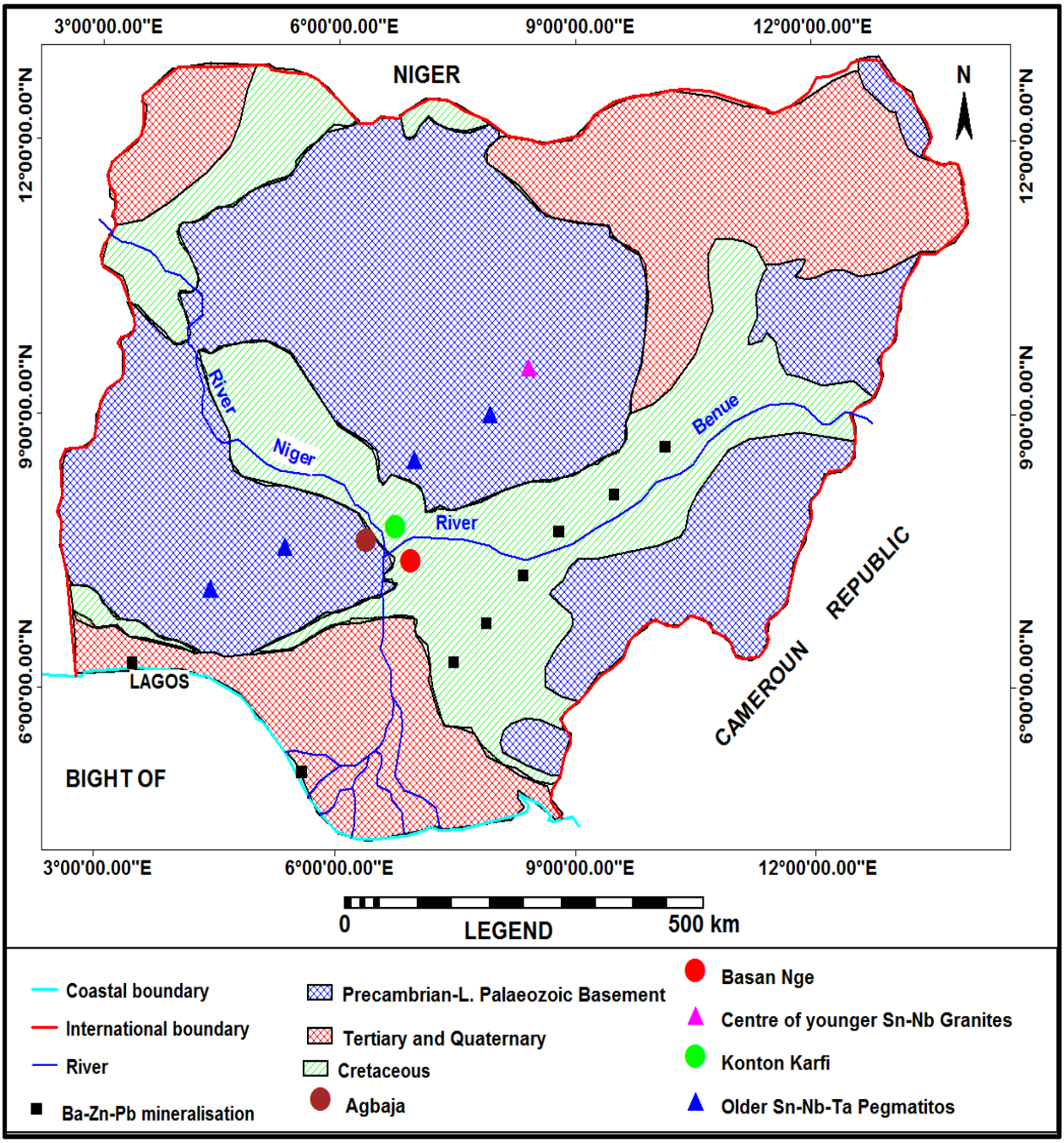


Figure 1.1 : Geological Sketch Map of Nigeria Showing the Location of Koton Karfe Iron Ore Deposit. Source: Uwadiale, 1984

The Itakpe iron ore has been beneficiated and used for iron and steel making using the direct reduction method (Delta Steel Company) and conventional blast furnace (Ajaokuta steel plant). It is estimated at about 200 million tonnes and would only last for about 25 years on the estimate that over 7 million tonnes of the ore (Run-off-Mine Ore) would be mined annually to meet the demand of the Delta Steel Company and the Ajaokuta steel plant respectively (Also and Yakubu 1995). Hence the need to look at the possibility of upgrading other iron ore reserves in order to ensure the continuity of supply of iron concentrate to the steel plants.

Deposits such as Koton-karfe iron ore (48.125%Fe; estimated at 428 million tons) and Agbaja iron ore (47.80%Fe; estimated at 2 Billion tons) containing high proportion of phosphorus (2.14%P_2O_5 for Koton-karfe iron ore and 2.08%P_2O_5 for Agbaja iron ore) and fine grain texture are not suitable for use in iron and steel making (Baba et. al, 2005). Detailed chemical composition of some Nigerian iron ore deposits are given in Table 1.2.

The Koton-karfe iron ore deposit is found in the northern part of Koton-karfe town in Kogi State. The iron ore deposit was discovered by the geological survey of Nigeria and found to contain siderite, magnetite and goethite as the major iron bearing minerals while hematite and other associated minerals are the minor constituents. The ore has low silica content, is oolitic and pisolitic in nature and formed ore of the meta-sedimentary iron ore deposit. (Famuboni, 1990).

Table 1.2: Chemical Composition of some Nigerian Iron Ores

	ITAKPE	**OSHOKO-SHOKO**	**AJABANOKO**	**AGBAJA**	**KOTON-KARFE**	**BASSA-NGE**
%K_2O	0.42	0.53	0.26	0.04	0.02	0.02
%CaO	0.30	0.21	0.15	0.72	0.45	0.17
%TiO_2	0.10	0.61	-	0.37	0.24	0.26
%MnO	0.05	0.08	0.01	0.14	0.56	0.31
%Fe	36.88	34.45	37.22	47.80	48.125	46.9
%MgO	0.20	0.18	0.15	0.38	0.07	0.47
%Al_2O_3	1.00	9.67	3.39	9.60	6.70	10.87
%SiO_2	48.0	51.07	46.50	10.89	5.13	8.28
%P_2O_5	0.18	0.02	0.10	2.08	2.14	1.45
%S	0.05	0.007	0.03	0.12	0.04	0.05

SOURCE (Uwadiale 1984, Garba 1999 and Aondona 2000)

1.3 RESEARCH PROBLEM.

Elements such as phosphorus (P) and sulphur (S) when contained in large amount in iron ores have detrimental effects on the steel produced. The depletion of the richer iron ore deposits as a result of advancing global technologies and civilization necessitated the processing of lower quality iron ores (Jian and Sharma 2004) or complex ores as well as industrial mining wastes. In iron ores, elements such as phosphorus, sulphur, and alkalis increase the cost of steel production. The P and Potassium (K) contained within the lower quality iron ore have a detrimental effect on the smelting and steel making processes (Yusfin et al., 1999). These compounds are deposited on the surface of the coke, where they act as catalyst in the gasification of carbon in the presence of carbon dioxide (CO_2). Another noticeable harmful effect of phosphorus is that it impacts to steel cold shortness. Large quantity of phosphorous reduces the ductility of steel,

thereby increasing the tendency of the steel to crack when cold worked (Serdar,1999). This failure of steels containing high amount of phosphorus is due to the following:

a. Phosphorus widens appreciably the two phase regions between the solidus and the liquidus lines, so that strong primary segregation occurs during solidification of an ingot or casting, and narrows substantially the γ-region which facilitates segregation in the solid state.
b. The rate of diffusion of phosphorus in α and γ-solid solutions is relatively low, thus producing structural inhomogeneities which can only hardly be eliminated by heat treatment. (Kudrin, 1985)

As a result of these effects, the steelmaking companies charge penalties when purchasing iron ores that contain these impurities especially phosphorus and alkalis (Williams and Cloete 2008, Yusfin et al., 1999).

The acceptable limit of phosphorus in iron ore is in the range of 0.07 - 0.075%. Every increase of 0.001% in phosphorous content attracts a penalty of $A 0.80/tonne - $A 1.00/tonne ($A – Australian dollar). This means that for an ore containing 0.080% phosphorous, the penalty would be around $A 4.0/tonne (Cheng et al., 1999). For a company selling millions of tonnes to the smelter it would result in the loss of millions of dollars.

Over the past couple of decades, there have been reports of increasing levels of phosphorus in the raw materials used in steel making (Lenintov et al., 2007; Monaghan et al., 1998), due to a gradual shortage of low – phosphorus iron ores

and coking coals. Thus the steel makers are facing stiffer challenges in achieving the desired phosphorus levels in the finished products and increased cost of production. Several steel plants have adopted the practice of external dephosphorization where a part of the phosphorus is removed before the main steel making process (Somnath 2007).

Various attempts have been made by researchers to make possible the utilization of the high phosphorus iron ore deposits. Among such attempts is the use of Hydrometallurgy. Hence an attempt will be made in this research to reduce the high amount of phosphorus (2.14% P_2O_5) of the Koton-karfe iron ore through chemical leaching using various acids. Even though it has low silicon modulus and contains fine grain texture (Garba, 1999)

1.4 OBJECTIVES.

The major objective of this research is to reduce the phosphorus content of the Koton-karfe iron ore using leaching with acids (Sulphuric acid (H_2SO_4), Hydrochloric acid (HCl), and Citric acid ($C_6H_8O_7$)).

Other objectives are:

- To carry out chemical and mineralogical characterization of Koton-karfe iron ore using X – Ray fluorescence Spectrometer (XRF), X – Ray diffractometer (XRD), Scanning electron microscopy/Energy dispersion spectrum (SEM/EDS).
- To investigate the effect of acid type and leaching parameters (temperature, time, agitation, particle size and concentration of reagent) on the leaching rate.

- To determine the optimum concentration of acid that can be used for the dephosphorization of the iron ore.
- To validate the obtained optimum conditions statistically using analysis of variance
- To investigate the effect of calcination on the ore and the rate of leaching of the phosphorus.
- To study the kinetics of leaching the iron ore.

1.5 JUSTIFICATION

- No previous work has been carried out to reduce the high phosphorus content of the Koton-karfe iron ore by chemical leaching. Hence this work is the first attempt of reducing the high phosphorus content of the ore through Hydrometallurgy.
- A successful reduction in phosphorus of the iron ore to acceptable limits would allow economic exploitation and processing of the Koton-karfe iron ore and other similar ones for use in iron and steel making.
- The technology of the dephosphorization of the Koton-karfe iron ore by Hydrometallurgy would be established.

1.6 SCOPE OF WORK.

This research involved collection of the Koton-karfe iron ore from the deposit site. Crushing, grinding and sieving to various particle size fractions, then chemical and mineralogical characterization of the head sample and the selected particle size followed by leaching. The head sample and the selected particle sizes

were further calcined at 700, 800 and 900^{o}C and then the calcined ore was leached.

1.7 CONTRIBUTION TO KNOWLEDGE.

Based on the analysis of the results obtained, it has been established that:

1). Phosphorus occurs as $AlPO_4$ and in solid solution with Goethite and is almost uniformly distributed within the various particle sizes of the Koton-karfe iron ore.

2). The optimum conditions of leaching the -355 +250 and -180 +250µm particle sizes of the Koton-karfe iron ore with Citric, Hydrochloric and Sulphuric acids have been established.

3). Leaching of the ore yielded up to 45.40, 35.31 and 29.73% phosphorus removal for sulphuric, hydrochloric and citric acids respectively. To enhance leaching, calcinations at 900^{o}C gave phosphorus leaching rate of 35.14, 57.30 and 73.51% for Citric, Hydrochloric and Sulphuric acids respectively.

4). Leaching of the Koton-karfe iron ore with citric acid is a diffusion controlled process, while with sulphuric and hydrochloric acid it is intermediate controlled and the dissolution of iron in the leach solution is minimal within the concentration and acids studied.

5). Sulphuric acid is the best acid for leaching the Koton-karfe iron ore at optimum conditions of 0.9M concentration, 80minutes, 500rpm and 30^{o}C.

CHAPTER TWO

2.0 LITERATURE REVIEW

2.1 Geology of Koton-karfe Iron Ore

Koton-karfe iron ore deposit is mainly of the sedimentary type with uncertain basal bed thickness due to poor exposure. These basal beds are conformable over-lain by a lithology comprising mainly sandstones and subsidiary claystones, fine conglomerates and siltstones. Both beds and the underlying ores are probably about 300m thick. They are known by various local names, Bida sandstone around Bida, and Lokoja basal sandstone around Niger/Benue confluence. Massive appearance and flat beds are most common in the basal area of the sandstones in Bida area, while the upper shows widely developed large scale across stratification (Thomas 2008).

2.2 Previous works on the upgrading of the Koton-karfe iron ore.

Thomas (2012) determined the work index of the Koton-karfe iron ore as received (run-off-mine) and after calcinations at 1200^{o}C, using the Berry and Bruce method. He reported that the work index for the as received was 17.00kwh/tonne, while that for the calcined gave 11.33kwh/tonne. He attributed the difference in the work indexes to the possible presence of moisture and some minerals in the as received sample, while in the calcined sample most of the volatile minerals must have been decomposed or transformed thereby making it easier to grind. He also reported that the Koton-karfe iron ore is a soft texture iron ore of the type B according to the Denver grindability curves, which meant that minimum amount of energy was required to crush or grind the ore.

Thomas(2008) Developed a Process Route for the Beneficiation of the Koton-karfe iron ore to be used as feeds to Ajaokuta and Delta steel plants. The work includes physical separation process employed to concentrate the ore in terms of its iron content and to reduce the contents of the associated gangues. He reported that of the three concentration methods used (gravity, magnetic and froth floatation), magnetic concentration method gave the best results at particle size fraction of -180+125µm. However, the high phosphorus content of the ore undoubtedly affects its suitability and process ability for iron and steel making and thus, must be reduced to a desirable or tolerable level.

2.3 PHOSPHORUS IN IRON ORES.

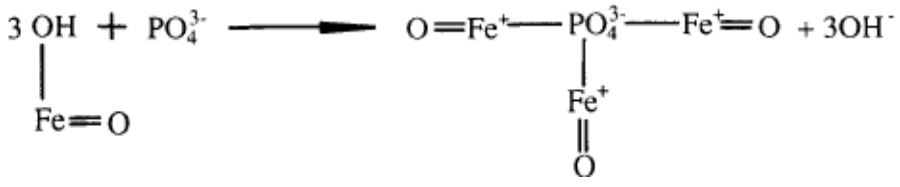
Phosphorus is not free in nature and almost always occurs in the fully oxidized state as phosphates, orthophosphates or as apatite. The element is widely distributed in these forms in soils, rocks, oceans etc. (Corbridge 1980)

Phosphorus is present in iron ores usually in the form of apatite $\{Ca_5F(PO_4)_3\}$, (Dennis 1983) orthophosphates of iron $\{Fe_3(PO_4)_2, FePO_4\}$ and/or double oxides with iron as pent oxide $\{xFe_2O_3.yP_2O_5\}$. If x:y is less than 3 during the reorganization of ionic structure then it exists as $Fe_3(PO_4)_2$ otherwise $xFe_2O_3.yP_2O_5$ (Van Wazer 1988).

2.4 Phosphorus in Goethite.

Various theories have been proposed to explain the existence of phosphorus in goethite. Graham (1973) proposed that elemental phosphorus existed in solid solution with goethite. Dukino (1997) has disputed this theory on the basis that interstitial solid solution is likely only if the substituting cation is of a similar or smaller size than the lattice bound cation and its charge is the same. The size and valence of phosphorus are not suitable for its existence in solid solution with goethite, and it is considered unlikely that elemental phosphorus exists in solid solution with goethite.

A more plausible mechanism has been proposed by Morris (1973) and Barbour (1973) and supported by Dukino (1997). It has been suggested that, prior to the dehydration of ferrihydrate to goethite, a surface hydroxyl group is replaced by a phosphate ligand as shown in the following model:



(2.1)

This theory is considered to be a likely explanation of the existence of phosphorus in goethite.

2.5 Phosphorus in Pig iron.

Phosphorus in the ores passes into the pig iron when the ores are smelted. The amount present in an ore is of critical importance as it dictates to a large extent the

type of steelmaking process to be employed and also the nature of the furnace refractory lining. (Dennis 1983)

Phosphorus is an undesirable element in high carbon steels but up to 0.12%P may be added to aid machinability or stiffen low carbon steel. Maximum permissible phosphorus contents are specified for all grades of steel and as phosphorus can be removed only in basic processes, it is frequently the phosphorus content of the charge to the steel furnace which determines whether an acid or basic process is to be used. (Ward 1982)

To minimize the amount of phosphorus which must be removed in steelmaking, pig iron is normally produced from iron ores or charged materials containing as little phosphorus as possible. Only in pig iron for Thomas steelmaking process is high phosphorus content desirable, as in this case, the oxidation of a minimum amount of phosphorus is necessary to complete the heat requirement of the operation. Cast irons deliberately containing phosphorus are also made because their exceptional fluidity renders them suitable for the manufacture of intricate thin-walled castings (Ward, 1982).

The most important reaction of P_2O_5 is its ability to take up water, that is;

- $P_2O_5 + 3H_2O = 2H_3PO_4$ (2.2)

Forming orthophosphoric acid (H_3PO_4). (Van Wazer 1988)

In addition to that, phosphorus pentoxide will dehydrate acids, forming metaphosphoric acid and the acid anhydrites. (*http://en.m.wikipedia.org)*

2.6 Leaching Process

Leaching is the process of extracting a soluble constituent from a solid by means of a solvent. In extractive metallurgy, it is the process of dissolving a certain mineral(s) from an ore or concentrate or dissolving certain constituents from metallurgical products such as calcines, mattes, scrap alloys, anodic slimes etc., in this respect, either one of the following can be achieved (*Habashi, 1980*):

a. Opening of ores, concentrates, or metallurgical products to recover the metal values.
b. Leaching easily soluble constituents (usually gangue minerals) in an ore or a concentrate in order to have it in a more concentrated form i.e a chemical beneficiation method e.g. the leaching of tungsten floatation concentrate with hydrochloric acid to dissolve away calcite and apatite.

It is necessary that the ore be finely ground in order to expose the minerals of interest. Economic factors usually decide the particle size to which the ore would be ground before leaching (*Burkin, 1986).*

2.6.1 Types of Leaching Processes

There are three main types of leaching processes according to the chemical nature of the leaching media or agent:

a. Acid Leaching in which chemical acid is used as a leaching agent to effect the dissolution.
b. Alkaline Leaching in which an alkaline solution is used as a leaching agent e.g. carbonates, hydroxides etc.

c. Microbial Leaching in which bacteria accelerate leaching reaction involving the oxidation of sulfide minerals and of ferrous ions. Several types of bacteria such as ferrobacillus ferrooxidans, thiobacillus ferrooxidans, etc. are capable of growing on pure inorganic media obtaining their energy requirements by oxidizing inorganic substances like sulphur, thiosulphates, ferrous ions etc (*Habashi, 1980*).

2.6.2 Choice of Leaching Agents

The choice of a leaching agent depends on many factors:

a. Chemical and physical character of the material to be leached.
b. Cost of the reagent: An expensive reagent is undesirable because any traces lost during handling will represent a large economic loss.
c. Corroding action of the reagent and consequently the materials of construction or handling equipment. If the leaching agent is corrosive a material that will be able to resist the corrosive action should be used as this will reduce the cost.
d. Selectivity for the desired constituent to be leached: An ideal reagent will extract only the desired component.
e. Ability to be regenerated: Ability of regenerating the reagent for recycle is also an important criteria, e.g. in the leaching of ZnO by H_2SO_4, the acid is regenerated during electrolysis. (*Burkin, 1986)*

The selectivity of a leaching agent towards a particular mineral in an ore depends on:

a. Concentration of the leaching agent.
b. Temperature.

c. Contact time or time of dwell. (*Burkin, 1986)*

Water is an ideal leaching agent because it is cheap and noncorrosive, but its action is only limited to few minerals. Leaching agents commonly used fall in the following categories: Acids, bases, and acqueous salt solution; chlorine water is used to a minor extent. Table 2.1 gives a summary of the commonly used leaching agents and some of their application. Leaching agents may be used either alone or in combination with oxidizing agents. In few cases they are used in combination with reducing agents (Habashi, 1993).

Table 2.1: A summary of the commonly used leaching agents and their applications.

GROUP	REAGENT	EXAMPLES
Water	H_2O	Sulfates, chlorides, borates
Acids	H_2SO_4 (conc.)	Sulfide concentrate, laterites, monazite, titanium slag.
	H_2SO_4 (dil.)+oxidant	Uranium ores, sulfides.
	HCl	Chemical beneficiation of ilmenite.
	HNO_3	Uranium concentrate.
	HF	Niobium and tantalum ores.
	Aqua regia	Refining of gold bullion and platinum metals.
	H_2SO_3	Manganese ores
	H_2SiF_6	Clay (for alumina recovery)
Bases	NaOH	Bauxite
	NH_4OH	Laterites after reduction, nickel sulfide concentrate.
Aqueous salt solutions	Na_2CO_3	Tungsten ores (scheelite).
	Na_2CO_3 + oxidant	Uranium ores.
	NaCN	Gold and silver ores

Source (Habashi, 1993)

The acids used in this research are sulphuric, hydrochloric and citric acids.

2.7 SULFURIC ACID.

Sulfuric acid is a highly corrosive strong mineral acid with the molecular formula H_2SO_4. It is a colorless to slightly yellow viscous liquid which is soluble in water at all concentrations. Sometimes, it may be dark brown as dyed during industrial production process in order to alert people's awareness to its hazards. It is a diprotic acid which may show different properties depending upon its concentration. Its corrosiveness on metals, stones, skin, eyes and flesh or other materials can be mainly ascribed to its strong acidic nature and if concentrated strong dehydrating property and strong oxidizing property. Moreover, it is hygroscopic which readily absorbs water vapour in air. (http://en.wikipedia.org/Sulfuric_acid)

Sulfuric acid is widely produced with different method, such as from sulfur, oxygen and water via the conventional contact process (DCDA) or the wet sulfuric acid process (WSA) and some other methods. (Davenport and King, 2006).

World production of sulphuric acid in 2004 was about 180 million tonnes, with the following geographic distribution: Asia 35%, North America (including Mexico) 24%, Africa 11%, Western Europe 10%, Eastern Europe and Russia 10%, Australia and Oceania 7%, South America 7% (Davenport and King 2006). Most of this amount (~60%) is consumed for mineral processing, fertilizers, particularly superphosphates, ammonium phosphate and ammonium sulfates. This is seen in the "wet method" for the production of phosphoric acid, used for

manufacture of phosphate fertilizers. In this method, phosphate rock is used, and more than 100 million tonnes are processed annually. This raw material is fluorapatite, though the exact composition may vary. (http://en.wikipedia.org/Sulfuric_acid). About 20% is used in chemical industry for production of detergents, synthetic resins, dyestuffs, pharmaceuticals, petroleum catalysts, insecticides and antifreeze, as well as in various processes such as oil well acidicizing, paper sizing, water treatment. About 6% of uses are related to pigments and include paints, enamels, printing inks, coated fabrics and paper, and the rest is dispersed into a multitude of applications such as production of explosives, cellophane, acetate and viscose textiles, lubricants, non-ferrous metals and batteries (Greenwood and Earnshaw 1997).

Sulfuric acid is used in large quantities by the iron and steelmaking industry to remove oxidation rust and scaling from rolled sheet and billets prior to sale to the automobile and major appliances industry (http://en.wikipedia.org/Sulfuric_acid). Used acid is often recycled using a spent acid regeneration (SAR) plant. These plants combust spent acid with natural gas, refinery gas, fuel oil or other fuel sources. This combustion process produces gaseous sulfur dioxide (SO_2) and sulfur trioxide (SO_3) which are then used to manufacture "new" sulfuric acid. SAR plants are common additions to metal smelting plants, oil refineries, and other industries where sulfuric acid is consumed in bulk, as operating a SAR plant is much cheaper than the recurring costs of spent acid disposal and new acid purchases. (http://en.wikipedia.org/Sulfuric_acid)

2.8 HYDROCHLORIC ACID.

Hydrochloric acid is a clear, colourless solution of hydrogen chloride (HCl) in water. It is a highly corrosive, strong mineral acid. Hydrochloric acid is found naturally in gastric acid. (http://en.wikipedia.org/Hhdrochloric_acid)

Hydrochloric acid is prepared by dissolving hydrogen chloride in water. Hydrogen chloride can be generated in many ways, and thus several precursors to hydrochloric acid exist. The large-scale production of hydrochloric acid is almost always integrated with the industrial scale production of other chemicals. (http://en.wikipedia.org/Hydrochloricric_acid)

Physical properties of hydrochloric acid, such as boiling and melting points, density, and pH, depend on the concentration or molarity of HCl in the aqueous solution. They range from those of water at very low concentrations approaching 0% HCl to values for fuming hydrochloric acid at over 40% HCl. (Perry et. al., 1984)

Hydrochloric acid is produced in solutions up to 38% HCl (concentrated grade). Higher concentrations up to just over 40% are chemically possible, but the evaporation rate is then so high that storage and handling need extra precautions, such as pressure and low temperature. Bulk industrial-grade is therefore 30% to 34%, optimized for effective transport and limited product loss by HCl vapors. (Norton 2008)

One of the most important applications of hydrochloric acid is in the pickling of steel, to remove rust or iron oxide scale from iron or steel before subsequent processing, such as extrusion, rolling, galvanizing, and other techniques. (Norton, 2008 and Greenwood and Earnshaw, 1997) Technical quality HCl at typically 18% concentration is the most commonly used pickling agent for the pickling of carbon steel grades.

Another major use of hydrochloric acid is in the production of organic compounds, such as vinyl chloride and dichloroethane for PVC (Greenwood and Earnshaw, 1997). Numerous products can be produced with hydrochloric acid in normal acid-base reactions, resulting in inorganic compounds. These include water treatment chemicals such as iron (III) chloride and polyaluminium chloride (PAC).

In industry demanding purity (food, pharmaceutical, drinking water), high-quality hydrochloric acid is used to control the pH of process water streams. In less-demanding industry, technical quality hydrochloric acid suffices for neutralizing waste streams and swimming pool treatment (Greenwood and Earnshaw, 1997).

Hydrochloric acid is used for a large number of small-scale applications, such as leather processing, purification of common salt, household cleaning (Maton et. al, 1993), and building construction (Greenwood and Earnshaw, 1997). Oil production may be stimulated by injecting hydrochloric acid into the rock formation of an oil well, dissolving a portion of the rock, and creating a large-pore

structure. Oil well acidizing is a common process in the North Sea oil production industry. (Norton 2008).

Many chemical reactions involving hydrochloric acid are applied in the production of food, food ingredients, and food additives. Typical products include aspartame, fructose, lysine, hydrolyzed vegetable protein as food enhancer, and in gelatin production (Norton 2008 and Greenwood and Earnshaw, 1997).

2.9 CITRIC ACID.

Citric acid (2-hydroxy-1,2,3 propanetricarboxylic acid, $C_6H_8O_7$) is widely distributed in plant and animals tissue and fluids (Sanchez-Reira 1999) Citric acid is a weak organic acid. It is a natural preservative/conservative and is also used to add an acidic, or sour, taste to foods and soft drinks. In biochemistry, the conjugate base of citric acid, citrate, is important as an intermediate in the citric acid cycle, and therefore occurs in the metabolism of virtually all living things. (Frank 2005)

Citric acid exists in greater than trace amounts in a variety of fruits and vegetables, most notably citrus fruits. Lemons and limes have particularly high concentrations of the acid; it can constitute as much as 8% of the dry weight of these fruits (about 47 g/L in the juices). The concentrations of citric acid in citrus fruits range from 0.005 mol/L for oranges and grape fruits to 0.30 mol/L in lemons and limes. Within species, these values vary depending on the cultivar and the circumstances in which the fruit was grown. Industrial-scale citric acid

production began in 1890 based on the Italian citrus fruit industry. (Penniston et al.,2008).

At room temperature, citric acid is a white crystalline powder. In chemical structure, citric acid shares the properties of other carboxylic acids. Molar mass 192.124g/mol (anhydrous) and 210.14g/mol (monohydrate), density 1.665g/cm^3, melting point 153 °C, when heated above 175 °C it decomposes through the loss of carbon dioxide and water. (Frank 2005)

Citric acid is a slightly stronger acid than typical carboxylic acids because the anion can be stabilized by intramolecular hydrogen-bonding from other protic groups on citric acid. In 2007, worldwide annual production stood at approximately 1,600,000 tonnes. More than 50% of this volume was produced in China. More than 50% was used as acidulent in beverages, some 20% in other food applications (Penniston et al.,2008, Frank 2005), 20% for detergent applications and 10% for related applications other than food, such as cosmetics, pharmaceutics and in the chemical industry. (Wang and Liu 1996, Ates et al., 2002 and Penniston et al., 2008)

Citric acid has three important properties. First is its acid capacity, second is giving taste and the last is making chelate with metal ions, (Feyza and Soner 2005), as such it has found application in foods, cleaning and chelating agents, cosmetics and pharmaceuticals, dyeing, photography (Frank 2005), in agriculture it is used to fix soil phosphorous (Drouillon and Merckx 2003, and Braithwaite et. al. 1990).

2.10 Leaching Techniques

There are various techniques through which leaching of metallic ores is carried out. In all the metal or substance intended to be obtained in solution is removed by a solvent or left in the residual solid. These include:

a. **Leaching "In situ"**

In this technique, the ore deposit is exposed to the leaching solvent in its naturally occurring place. The solvent percolates through the ore and dissolves the solute. This technique is employed in leaching of some copper ores.(*Ghosh and Ray, 1991)*

b. Heap or Dump Leaching

This technique also involves the exposure of large heaps of an ore placed above the ground to a leaching reagent, so that the solution percolates through the ore. An extraction carried out in this manner may require longer time and the loss of metal in solution that seeps into the ground represents an inherent inefficiency. *(Ghosh and Ray, 1991)*

c. Percolation or Vat Leaching

This involves leaching in a tank or vat through sand or by either percolation or agitation done mechanically or with compressed air in the case of leaching slime. (Ghosh and Ray, 1991).

d. Pressure Leaching

This is carried out in autoclave at higher pressure and temperatures than are feasible in open tanks. The advantages of this technique are that gaseous reagents such as oxygen, hydrogen, etc. can be used and the high pressure enhances the solubility of the gas in the leaching solution (Ghosh and Ray, 1991).

2.11 Mechanism of Leaching.

Leaching is basically a heterogeneous process which takes place in several steps:

1. Diffusion of the reactants through the diffusion layer
2. Adsorption of the reactant on the solid
3. Chemical reaction between the reactant and the solid
4. Desorption of the product from the solid
5. Diffusion of the leaching product through the diffusion layer.

From the above, leaching process may be diffusion controlled, reaction controlled or intermediate controlled (i.e. both chemical and diffusion controlled) depending on the activation energy for the process. (Habashi 1999)

2.12 Factors influencing leaching kinetics.

Depending on the leaching mechanism, i.e if the leaching process is reaction or diffusion controlled the leaching kinetics are influenced differently by variation of these parameters. (Habashi 1999)

Particle size: The kinetics is affected in different ways by the particle size during chemical reaction controlled and diffusion controlled leaching respectively. Generally smaller particle size yields faster leaching kinetics.

- For chemically controlled leaching the dependence is proportional to $\frac{1}{r}$
- For diffusion-controlled leaching the dependence is proportional to $\frac{1}{r^2}$

Temperature: Temperature is a factor of great importance for the leaching kinetics and in general a higher temperature yields faster leaching kinetics.

- For chemically controlled leaching the rate constant increases exponentially with increased temperature in accordance with Arrhenius' Equation:

$$\boldsymbol{k = Ae^{-\frac{E}{RT}}} \qquad (2.3)$$

- For diffusion controlled leaching, however, the diffusion constant increases linearly with increasing temperature in accordance with Stokes-Einstein's equation:

$$\boldsymbol{D = \frac{R.T}{6.\pi.r.\eta.N}} \qquad (2.4)$$

In this equation R is the general gas constant, r is the radius of the diffusing molecule (assumed to be a sphere), η the viscosity of the medium and N is Avogadro's number.

The rate of diffusion in a solution is governed by Fick's Law

$$\boldsymbol{J = \frac{dn}{dt} = -A.D.\frac{dC}{dx}} \qquad (2.5)$$

J = the amount of substance that diffuse through a surface per time unit

A = the area of the reacting particle

D= the diffusion constant

$$\frac{dC}{dx} = \textbf{the concentration gradient}$$

The leaching rate is thus dependent on the area of the leaching body, the diffusion coefficient and the concentration gradient. (Habashi 1999)

Agitation rate: increased stirring may reduce the thickness of the diffusion layer and it has the following effect on the two leaching mechanisms.

- Chemically controlled leaching is not affected, or is affected to a limited extent by the agitation rate, as the chemical reaction is much slower than the diffusion through the diffusion layer

- With diffusion controlled leaching the leach rate increases with increased agitation as the diffusion layer diminishes. The diffusion layer cannot be completely eliminated, which results in variation of the dependence of the leaching rate on the stirring speed.

The dependence of the diffusion layer on the agitation during leaching in a tank is described by the formula:

$$\Delta x = L.N_{Re}^{-0.9}.N_{Sc}^{-\frac{1}{3}} \qquad (2.6)$$

Where Δx is the thickness of the diffusion layer and L is the characteristic length. N_{RE} and N_{SC} are Reynold's number and Schmidt's number as defined below:

$$N_{Re} = \frac{\rho.N.(2.r)^2}{\mu} \quad (2.7)$$

Here μ is the dynamic viscosity, ρ is the pulp density, N is the rotation speed of the stirrer and R is the radius of the stirrer.

$$N_{Sc} = \frac{\mu}{\rho.D} \quad (2.8)$$

In Schmidt's number D is the diffusion constant.

Reagent concentration: In general, leaching rate increases with increased concentration of reagent, but only up to a certain maximum level. The leaching mechanism may be changed as a result of changes in the concentration of reagent.

2.13 Determination of leaching rate.

The reaction rate of a heterogeneous reaction, for example that of a mineral with an acid, may, provided that the acid concentration is constant, may be expressed through the formula: (Habashi ,1999)

$$-\frac{dW}{dt} = k.A.C \quad (2.9)$$

Where W= the weight of the leached particle at time t

W_O= initial weight of the particle

k= the rate constant

A= the surface area of the leached partice

C= the concentration of reactant

Depending on the geometry of the solid leached, different kinetic expressions can be derived.

2.14 Kinetic equation expressed as fraction leached,(α)

Fraction leached (α) is defined as

$$\boldsymbol{\alpha = \frac{W_O - W}{W_O}} \qquad (2.10)$$

Where W= the weight of the leached particle at time t

W_O= initial weight of the particle

Fraction leached for a spherical particle will then be

$$\boldsymbol{\alpha = 1 - \frac{r^3}{r_o^3}}$$

$$\boldsymbol{r = r_0[1 - \alpha]^{1/3}} \qquad (2.11)$$

Chemically controlled leaching of spherical particle is often described as the "shrinking particle" model whose expression is written as

$$\boldsymbol{1 - [1 - \alpha]^{1/3} = \frac{k.C}{r_o.p}.t} \qquad (2.12)$$

Where k= the rate constant, C= the concentration of reactant, and ρ= density

As is evident from equation (2.11), the leaching rate is inversely proportional to the radius of the particle (r_o). Provided that the concentration of the leach solution can be assumed to be constant and that the density is known, the rate constant (k) may be determined by plotting the left hand side against time (t) (Habashi, 1999).

Diffusion controlled leaching of a spherical particle is often described as the "shrinking core" model whose equation is written as

$$\boldsymbol{1 - \frac{2}{3}.\alpha - [1 - \alpha]^{2/3} = \frac{2.M.D.C}{\beta.\rho.r_o^2}.t} \qquad (2.13)$$

Where β, ρ and M are stoichiometric factor, density and molecular weight respectively.

As is evident from equation (2.12) the leaching rate is inversely proportional to the square of the radius of the particle. Assuming that the concentration (C) is constant, everything except the diffusion constant (D) are constant in the left hand side of the equation. The diffusion constant can be determined by plotting the left hand side against time. (Habashi, 1999)

2.15 Determination of Activation Energy.

To obtain the activation energy, the values of K (the rate constant) at two different temperatures will be used in equation (2.13) (Moore 1981)

$$lnk = lnA - \frac{E_A}{RT} \qquad (2.14)$$

Where A = Pre-exponential or frequency factor

E_A= Activation energy

R = Gas constant

T = temperature in Kelvin

Plotting ln K versus 1/T (the Arrhenius plot) a straight line of slope $-E_A/R$ is produced.

From the values of activation energy obtained the rate controlling step will be determined. When the chemical reaction is the rate controlling step, the activation energy is usually in the range 40 – 100KJ/mole. When diffusion is the rate

controlling step th activation energy is usually 21KJ/mole or less. For intermediate controlled leaching the activation energy fall in the range of 21 - 40KJ/mole (Habashi, 1999).

2.16 METHODS FOR REMOVAL OF PHOSPHOROUS FROM IRON ORES.

Phosphorous (P) level in iron ores are reduced using one of the following techniques:

1. Physical separation
2. Chemical leaching.
3. Before, during or after steel making.

2.16.1 Physical separation

For physical separation crushed ores should be fine ground until the phosphorous minerals dissociates from iron minerals, and then dephosphorize with flotation or magnetic separation (Zhang and Muhammed 1989) low P extraction, high grinding cost and iron loss are the major disadvantages of this method. Sometimes lower quality iron ore are blended with high quality ore to "dilute" the P concentration in the final iron ore. Such as the work of Dukino et al.,(2000) where low phosphorus ore (0.005% P) is blended with high phosphorous ore (0.10% P) the former being the major component of the blend. However the ratio of low quality iron ore to high quality iron ore is increasing.

2.16.2 Chemical leaching.

Chemical leaching to reduce P from iron ores involves the selective leaching of phosphorus from iron ores by any acid or base of choice depending on the nature of combination of phosphorus in the matrix of the iron ore, it involves crushing and grinding the ore to increase the surface area for enhanced acid attack. In the course of leaching the concentration of acid should be kept within the range that the loss of iron ore is minimal and P leaching is maximized.

2.16.3 Phosphorus reduction before, during and after steel making.

2.16.3.1 Reduction of phosphorus during Iron making.

Phosphorus in iron and steel comes from iron bearing materials (iron ores, scraps, e.t.c), coke, and flux in the form of P_2O_5, $3(CaO)\ P_2O_5$. , $3(FeO)\ P_2O_5$.

The main phosphorus reaction in the blast furnace are as follows:

$$P_2O_5 + 5C \rightarrow 2P + 5CO \quad (-990.66KJ) \qquad (2.15)$$

$$2(3(CaO)\ P_2O_5) + 3SiO_2 + 10C \rightarrow 3(2(CaO).SiO_2) + 4P + 10CO \quad (-2836KJ) \qquad (2.16)$$

$$P_2O_5 + 5Fe \rightarrow 2P + 5FeO \quad (-196.46KJ) \qquad (2.17)$$

$$3Fe + P \rightarrow Fe3P \quad (+181.24KJ) \qquad (2.18)$$

Phosphorus recovery is nearly 100% to pig iron, i.e nearly all phosphorus enters the pig iron (Babich et al, 2008). Phosphorus can be removed both under oxidizing as well as reducing conditions. But removal of phosphorus under reducing condition is not practical since its removal is highly hazardous. Thus

phosphorus removal is practiced mostly under oxidizing conditions. But the blast furnace is mainly a reducing process.

2.16.3.2 Dephosphorization during steelmaking.

Research on the removal of phosphorus during steel making started with the Bessemer and open hearth processes, during the last years of the 19^{th} century (Somnath 2007). Snelus (1879) was among the earliest workers to study the reaction of phosphorus during the Bessemer process of steelmaking. He patented the use of basic lining, based on lime and magnesia, for the removal of phosphorus from high phosphorus pig irons. Thomas and Gilchrist (1879) independently investigated the influence of the lining materials and the fluxes on the elimination of phosphorus during blowing of a high phosphorus pig iron. Following experiments and trials spanning close to three years, they concluded that the presence of a basic lining and the addition of basic fluxes were essential for production of low phosphorus steel from phosphorus-bearing hot metal. Snelus as well as Thomas and Gilchrist, successfully demonstrated the benefits of using a basic lining and basic slag on an industrial scale and their findings led to the adoption of basic lining in Bessemer steelmaking converters. This technique was gradually adopted in several countries and gained fame as the "Thomas process". Around the same time, Harmet (1879) proposed the idea of repouring to produce low phosphorus steel using a Bessemer converter, He suggested a two stage blowing, where silicon was first oxidized in a vessel with acidic lining and the desiliconised metal was then transferred to a second vessel with a basic lining for oxidation of phosphorus and carbon. Adoption of the two stage process

sharply reduced the consumption of basic fluxes since no basic flux was necessary during the first part of the blow. This concept has become popular with several steel makers, particularly those using pig iron and/or hot metal with high [P]/[Si] ratio, and has been adopted in some of the recent steelmaking techniques as well (Naito and Wakoh (2005), Jiang et al, (2007)), these basic principles have been modified and forms the basis of dephosphorization in the most common methods of steel making (basic oxygen converters and electric arc furnaces) even today.

The principal conditions essential for dephosphorization in steel making are (Kudrin, 1985):

1. Formation of oxidizing furnace atmosphere and respectively of oxidizing slag with a high activity of iron oxide in it. (FeO)

2. High basicity of the slag and high activity of CaO in it (the slag must be high in CaO and low in SiO_2).

3. Quick formation of ferruginous-limy slag.

4. A relatively low temperature (especially at moderate and high concentrations of carbon).

5. Low activity (concentration) of phosphorus in the slag.

In order to remove phosphorus (P) from the molten metal and retain it in slag, the activity of P_2O_5 in the slag must be decreased. This can be achieved by forming a

basic slag by adding lime (or limestone). The main component of lime, CaO, reacts with P_2O_5 in to stable compounds by the following (Somnath 2007):

$$2[P] + 5(FeO) + 4(CaO) \rightarrow (CaO)_4(P_2O_5) + 5[Fe] \qquad (2.19)$$

And/or

$$2[P] + 5(FeO) + 3(CaO) \rightarrow (CaO)_3(P_2O_5) + 5[Fe] \qquad (2.20)$$

The extent of dephosphorization is often characterized by the index $(CaO)_4(P_2O_5)/[P]^2$, or simpler ratios $(P_2O_5)/[P]$ or $(P)/[P]$. An increase of these ratios is an indicative of an increasing dephosphorizing ability of the slag (Kudrin, 1985, Somnath 2007).

The demand for the activity of P to be low and avoid the return of P to the molten metal known as Rephosphorization lead to the development of the multiple slag refining process so that the P already contained in slag is retained and the dephosphorization ability of the new slag is harnessed.

The intensity of formation of slag of the desired composition has strong effect on the rate of phosphorus oxidation; this led to the development of treatment in the ladle that involved the use of synthetic slag. By this treatment steel with an elevated phosphorus content was mixed in the ladle with fluid ferruginous limy slag; this treatment decreased the phosphorus content in the metal by 60 – 80% (depending on its initial concentration) (Kudrin 1985). Depending on the technology adopted in the steel making shop dephosphorization may be before or after steel making.

Haroyushi and Masayuki (2003) reported that the hot metal pre-treatment method, where the hot metal is dephosphorize prior to refining in a converter was actively put into practice in the 1980's by the major steel makers of Japan in order to meet customers' requirements for lower phosphorus content in steel products, while reducing slag generation and increasing the iron yield. However, dephosphorization by this method is still insufficient, and a more effective process was desired. A thorough investigation by NKK steel production company on the dephosphorization mechanism revealed that lowering the silicon content in the hot metal to an ultimate level leads to a dramatic improvement in the efficiency of lime for dephosphorization. Based on this finding, a first in the world, open ladle type desiliconization station was installed at Fukuyama works in March 1998. The silicon content of the hot metal was minimized before dephosphorization, improving the efficiency of lime for dephosphorization. Moreover, slag generation through the entire steelmaking process was successfully lowered to an ultimate level. This technology was named the ZSP (zero slag process).

Dephosphorization in the Electric Arc furnace follows the basic principles earmarked above, depending on the practice in the shop and requirements of the final steel produced, one or more methods can be combined (Ghosh and Chartterjee 2008, Jian-ping et al., 2009). Smelting process is effective for dephosphorization but with very high cost and still under research (Jin yong-shi et al., 2006).

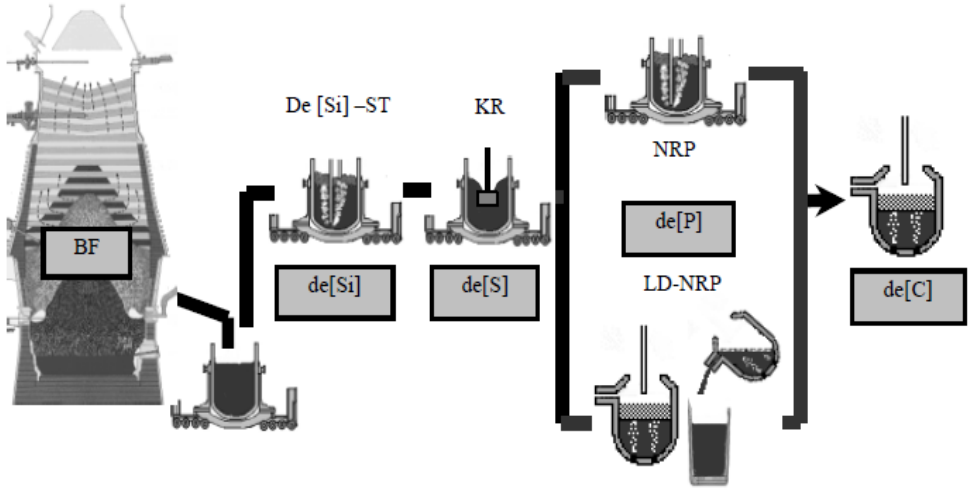


Figure 2.1: The Zero Slag Process (ZSP) process flow at the NKK's Fukuyama's works. Hot metal is transferred through the desiliconization station, desulfurization process called KR, a ladle type dephosphorization station called the NRP (New Refining Process), or an LD-converter-type dephosphorization process called LD-NRP, before finally being charged into a converter.

Chemical approach in which the ore is leached with a suitable solution is a relatively simple and cheap process (Jin yong-shi et al., 2006). Acid leaching is a kind of more effective dephosphorization method (Forssberg and Asolfsson 1981; Zhang and Muhammed 1990.)

2.17 Previous studies on the leaching of iron ores.

Various attempts have been made by researchers towards the possibility of utilizing the high phosphorus-containing iron ore deposits largely found in most countries. Among these, is an attempt to investigate the most effective acids to remove phosphorus and potassium from Sishen iron ore concentrates by chemical leaching using a range of acids and oxidative chemicals, the acids used are, acetic acid, citric acid, ferric sulphate, hydrochloric acid, lactic acid, oxalic acid, propanoic acid and sulphuric acid. 1molar concentrations of all leaching acids

were used for five days at room temperature. They reported that citric acid proved to be best leaching agent for removing potassium from the ore, while sulphuric acid was detected to be the most effective to remove phosphorus and most corrosive on iron. (Williams and Cloete 2008)

During the period 1964 – 1973, some processes were operated in Sweden where the iron ore was leached with nitric acid. In those processes, the phosphorus content was in the ore was reduced from 0.2% to less than 0.05%. the leached ore was then used for production of pellets. However, no scheme was incorporated in those processes for the recovery or recycling of the leach acid, which thus resulted in a high nitric acid consumption cost. The leaching processes were finally taken out of operation and were replaced by flotation processes (Zhang and Muhammed 1989). In recent years, however, the acid-leach approach has been reconsidered as a possible alternative to the current flotation route (Zhang and Muhammed 1988(a); 1988(b); 1989; 1990). Technologically, the leaching process is simpler, as it can directly treat the sinter fines without strict requirements for the particle size as compared to flotation. The cost of the acid consumption was reduced by incorporating in the process a suitable scheme for recovery of the leach acid, as well as the phosphorus (Muhammed and Zhang 1989). Zhang and Muhammed (1989) reported that phosphorus exists mainly as fluorapatite in the ore and can be acidulated by a strong mineral acid. Nitric acid is preferred because of its low reactivity with magnetite (Weast, 1981) which is the main constituent of the iron ore under consideration. A sample of the sinter fines was leached with 6.0M nitric acid solution, the phosphorus content in the ore was decreased to a level below

the set limit as phosphorus removal was 95%. The relative content of iron in the ore slightly increased due to the dissolution of apatite and other constituents. The actual iron loss was less than 0.5%. However, nitric acid had the disadvantage that the nitrate irons tend to be reduced to various nitrogen compounds due to its concentration e.g. NO_2 or NH_4 (Zhang and Muhammed 1989).

Xia Weng et al.,(2011) studied the removal of phosphorus from high phosphorus iron ores by selective hydrochloric acid leaching. The ore used in their research is from Wushan, Chongquing, China. They reported that hydrochloric acid concentration is a very important parameter for dephosphorization. On the condition of high concentration of hydrochloric acid, the phosphate can convert into soluble phosphate salts easily, quickly and completely. But if the concentration of hydrochloric acid was too high it could lead to loss of iron, and the selectivity of the leaching process would be reduced. Their optimum experimental parameter were reaction time 30 – 45 minutes, particle size <0.147mm, hydrochloric acid concentration 2.5 mol/liter, reaction temperature 25^0C and stirring strength 5.02 – 12.76 s^{-1} , with these conditions the hydroxyapatite was converted into soluble phosphate during the process of HCl leaching. The feasibility of dephosphorization of Changde (China) phosphorus containing iron ore (1.12%P) was investigated using alkali and acid leaching. Sulphuric acid, hydrochloric acid, nitric acid and sodium hydroxide were used for the leaching. They reported that Alkali-leaching is ineffective to remove phosphorus from the iron ore. With 0.2 mol/L and 1.0 mol/L sodium hydroxide, only 24.41% and 27.96% phosphorus was removed respectively. A prolonged

alkali-leaching would go against dephosphorization because of the reprecipitation of phosphorus with other metal ions released during the leaching. Acid-leaching is an effective method to remove phosphorus from Changde iron ore. Sulfuric acid is more effective to dephosphorization than hydrochloric acid and nitric acid. 91.61% phosphorus is extracted with 1.0% sulfuric acid after leaching for 20min at room temperature. The optimum stirring speed is 620 revolution per minute. The suitable leaching time for sulfuric-acid-leaching is 20 minutes. Iron loss during the acid-leaching can be negligible, which is less than 0.25%, making the process quite economical Jin Yong-shi et. al., (2006). Rawling (2007), worked on the chemical leaching of Iron ore using a range of oxidants, and concluded that Citric acid proved to be the best leaching agent for the removal of potassium from the iron ore, while sulphuric acid reduced the amount of phosphorus from the ore.

Forssberg and Adolfsson (1981) investigated the economic feasibility of acid leaching of iron ore in which apatite, $Ca_5(PO_4)_3(F, Cl, OH)$, was the phosphorous containing mineral. Nitric and hydrochloric acid leaching agents were used. They reported that the economy of leaching with hydrochloric or nitric acid depend very much on the extent to which the phosphorus can be recovered as phosphoric acid.

The dephosphorization of iron ore using acid leaching was also investigated by Matsuo et al., (1980). The iron ore contained phosphorus in the form of apatite, $Ca_5(PO_4)_3F$. The acids tested were hydrochloric, nitric and sulphuric acid. The optimum acid concentration was determined to be between 2 – 7%. The optimum leaching time was found to exceed 10 hours. Without the use of heat treatment, a

20% reduction in the phosphorous content was achieved. With heat treatment a reduction of phosphorus of up to 40% was obtained.

Graham, (1973) reported that phosphorous in Western Australia iron ores exists within goethite, FeOOH, in the form of solid solution. The dephosphorization of the high phosphorus ore from the Pilbara region of Western Australia was investigated by Gooden et al., (1979), physical beneficiation methods failed as the phosphorus was in solid solution in goethite. Chemical dephosphorization methods for iron ore were reviewed and tested on the ore samples. Leaching without thermal treatment was found to be quite ineffective. The effect of heat treatment with and without the addition of salt, was investigated. Experiments demonstrated that in a fairly elevated temperature range, salt was not required for solubilization, and it actually hindered the dephosphorization process. The effect of roasting temperature on dephosphorization was investigated using a roasting time of 0.5 hours. With heat treatment and leaching with hydrochloric, nitric and sulphuric acid and sodium hydroxide solutions, the phosphorus content in the ore was reduced to acceptable limits. Sulphuric acid was extensively tested as this was the most economical acid. Using sulphuric acid, it was found that the quantity of iron leached was dependent on the solution concentration. The minimum sulphuric acid concentration required to dissolve phosphorus was found to be 0.2M. The optimum leaching time was found to between 0.1 and 0.5 hours. Increasing the leaching temperature above 50^0C or 60^0C did not improve the leaching of phosphorus. Sodium hydroxide was found to be equally effective as

sulphuric acid at concentrations around 0.2M. However, the process was not as cost effective as sulphuric acid.

Cheng et al., (1999) reported that iron ore from Western Australia contains 0.15% phosphorus, the sample used in his studies contained 0.126% phosphorus, after roasting at 1250^{o}C, lump ore (P_{80} 5.6mm), pellet 1 (grinding to 100% - 1.5mm before pelletisation) and pellet 2 (grinding to 100% - 0.15mm before pelletisation) were leached in solutions with different sulphuric acid concentrations. After leaching for 5 hours at 60^{o}C in 0.1M sulphuric acid solution, 67.2%, 69.0% and 68.7% of the phosphorus was leached from the above three samples respectively. The phosphorus content was reduced from 0.126% to 0.044%, 0.55% and 0.042% respectively, the highest phosphorus dissolution with pellet 2 was attributed to the high porosity of the pellets, which increased by 26.9% after roasting. The iron loss for the 3 samples was 0.20%, 0.018% and 0.022% respectively, indicating that the iron loss in the lump are was about ten times of that in the pellet samples. The iron loss in the lump ore was about ten times of that in the pellet sample and was attributed to the amount of fines in the sample, the iron loss in the two pellet samples was negligible. The optimum sulphuric acid concentration was 0.1M.

Belikov et al., (2003) reported that in 2001 they tested a dephosphorization technology for Lisakovsk brown iron ore concentrates containing 48 – 49% Fe and 0.6 – 0.8% P. The technology includes roasting of the concentrate at 900^{0}C, sulphuric acid leaching of the phosphorus, drying of the dephosphorized commercial concentrates containing 57 – 58% Fe and 0.12 – 0.25% P, and

neutralization of the acidic solution. Research show that maximum phosphorus extraction requires heat treatment of the Lisakovsk concentrate. The effectiveness of heat treatment depends considerably on atmosphere and temperature in the course of roasting. It is found that leaching whether acidic or alkaline is most effective after roasting at 650 – 950^0C, hence the concentrate was subjected to cyclic thermochemical treatment (roasting and leaching), after each cycle, the pulp is filtered and the resulting cake is sent to the next treatment cycle. In all five cycles are undertaken at 700, 800, and 900^0C. It was found that the degree of oolite dephosphorization depends on the equilibrium phosphorus concentration in the interboundry region, which increases with increase in the temperature but hardly depends on the roasting time. Cyclic roasting and leaching yields a phosphorus content of less than 0.12%, on account of decrease in the equilibrium concentration after the removal of some of the phosphorus in each cycle (Levintov et al.,2007).

Peixoto (1991) investigated the effect of heat treatment on the acid leaching of iron ore. When the iron ore contained phosphorus in solid solution in the goethite phase, it was found that thermal treatment of the ore at 1200^0C caused a structural re-arrangement of goethite which converted to hematite and facilitated the dissolution of phosphorus in the mineral acids. Without thermal treatment of the ore, hydrochloric acid was not effective. After pelletisation, the leaching with hydrochloric acid achieved 34% reduction in phosphorus. No loss of iron was observed. Phosphorous is less soluble in hematite than in goethite. Goethite can be converted to hematite by roasting, which will cause the ore to be more

amenable to leaching. The degree of conversion of goethite to hematite is expected to increase with the roasting temperature and time (Cheng et al., 1999).

Biological processes for phosphorus removal have also been evaluated based on the use of several fungi, some being oxalic acid producing. Anyakwo and Obot (2008) worked on the use of Aspergillus niger and their cultural filtrates for removing phosphorus from Agbaja iron ore, and concluded that phosphorus removal efficiency at the end of the 49days of the leaching are 81, 63, and 68% for 5, 100, and 250 mesh grain size respectively. William and Cloete (2008) worked on the production and use of citric acid for the removal of phosphorous and potassium from the iron ore concentrates of the Sishen iron ore mine, South Africa. In their studies submerged fermentation of Aspergillus niger for the production of citric acid was used, and the citric acid produced used for the leaching of the iron ore. They reported that 1 molar citric acid leaching solution at 60^0C proved to be the most efficient, removing 35.29% phosphorous and 23.53% Potassium contained within the iron ore concentrate.

Sun and Yang (1997) indicated that after leaching of a high phosphorus iron ore with Thiobacillus followed by a chemical treatment using a solution containing tannin, the phosphorus content dropped to as less than 0.2%. However, the original phosphorus content was not mentioned in the patent abstract. Another researcher in china performed dephosphorization using bacteria leaching with chemical treatment and nitric acid leaching (Wang, 1997). In the bacteria leaching with Thiobacillus the phosphorus dropped from 0.36% to 0.18%, and with

chemical leaching In nitric acid the phosphorus content was reduced to less than 0.05%.

A real scientific interest in hydrometallurgical processing of high phosphorus iron ores was noticed when several papers and patents were published (Gooden et al., 1974; Muhammed and Zhang, 1989; Kokal, 1990; Cheng et al., 1999; Dukino et al., 2000). Ever since, traditionally low price of iron ore products have impeded the large scale industrial application of chemical dephosphorization. In the last ten years, the situation of iron ore markets have changed dramatically due to an increase on the world steel consumption, pushed up mainly by the economic growth of China and other Asian emerging markets. Currently, prices of iron ore are increasing in real terms and the production of this commodity is increasing as well (Poveromo, 2005). This new scenario for the iron mining industry has revived the interest in upgrading the quality of phosphorus bearing iron ores by hydrometallurgical routes and for example at least one beneficiation plant to leach phosphorus from iron ores has been recently installed in kazakhstan (Kokal et al., 2003).

Based on these backgrounds, little or no work has been done on the leaching of Koton-karfe iron ore with acids. It is for this reason that a chemical process of reducing the phosphorus content was considered. Therefore this study is to determine which acid would be considered for the removal of phosphorus from the Koton-karfe iron ore, To contribute to the efforts of a number of researches on the possibility of removing phosphorus from iron ores prior to iron and steel making by the most economical process, an investigation will be carried out on

Koton-karfe iron ore in this work using a hydrometallurgical approach. The research will be essentially based on acid-chemical leaching process involving the use of a range of dilute, inexpensive and readily available acids. The effectiveness of each of the acid in terms of the amount of phosphorus being removed and percent iron dissolved/loss will be investigated and compared.

2.18 Statistical Design and Development of Mathematical Model

Factorial design and linear regression techniques have been widely used in engineering analysis. These techniques consist of plan of experiment with objective of acquiring data in a controlled way, executing the experiment in order to obtain information about the behavior of the given process. Nwoye (2008) derived a model for predicting the time for dissolution of pre-quantified concentration of phosphorus during leaching of Agbaja iron ore in oxalic acid as:

$$\tau = Log\left[\frac{\left[\frac{P^{1/4}}{1.8}\right]}{LogT}\right] \qquad (2.21)$$

Where

T = Leaching temperature (^{O}C) in the experinment

N= 1.8 (Dissolution coefficient of phosphorous in oxalic acid solution).

P= Concentration of dissolved phosphorous (mg/kg)

τ= Leaching time (secs)

The model was found to depend on a range of specified leaching temperatures (45 – 70^{0}C) for its validity. They also reported that the time for dissolution of any

given concentration of phosphorus decreases with increase in the temperature (up to70^0C), at initial pH 5.5 and average grain size of 150µm.

Nwoye et, al. (2008) derived a model for predicting the concentration of dissolved iron during leaching of Agbaja iron ore in sulphuric acid as:

$$\%Fe = Z\left[\alpha/T\right]^3 \qquad (2.22)$$

Where

T= Solution temperature (^{O}C) at the time t, when the concentration of dissolved iron is evaluate

Z= pH coefficient for iron dissolution in sulphuric acid solution during the leaching

α= final pH of the leaching solution at the time t,

The model was formulated at leaching temperature of 25 ^{O}C, initial solution pH 5.0 and average grain size 150µm, is dependent on the final pH and temperature of the leaching solution. The model shows that the concentration of iron dissolved during the leaching process is directly proportional to the third power of the ratio of final leaching pH and temperature.

CHAPTER THREE

3.0 MATERIALS AND METHODS.

3.1 Equipment

The equipments that were used in the course of this research include:

Denver pulverizing machine, Denver jaw crushing machine, Denver sieve shaking machine, X – Ray fluorescence Spectrometer (XRF), X – Ray diffractometer (XRD), Scanning emission microscopy/Energy dispersion spectrum (SEM/EDS), Inductively Coupled plasma optical emission spectroscopy(ICP-OES), Electric furnace, Conical Flasks and Beakers, Digital Weight Scale, Drier, magnetic stirrer and a pH meter

3.2 Materials

The materials used include; Koton-karfe Iron ore sample, sulphuric acid, hydrochloric acid, citric acid, and Filter Papers.

3.2.1 Material Collection and Preparation:

The sample of the iron ore used for this research work was obtained from the Koton-karfe Iron ore deposit in Kogi State, Nigeria. 80kg of the Samples were collected from different points on the deposit by simple random sampling. The ore was crushed and ground using the Denver crusher (JC - 300) and ball milling machine (GMO85) respectively. The ground ore was sieved to produce different particle size fractions:+355µm, -355 +250µm, -250 +180µm, -180 +125µm, -125 +90µm, -90 +50µm, and -50µm.

3.3 Chemical characterization of the head sample.

The chemical composition of the head sample was determined using XRF.

3.3.1 Determination of the chemical composition of the head Sample.

The XRF was done in the Faculty of Natural and Agricultural Science, Geology Department, University of Pretoria, Pretoria South Africa. Thermo fisher ARL9400 XP+ Sequential XRF and uniquant software was used for the XRF analysis. Before the analysis, the ore was first milled to -75µm, the samples were prepared as pressed powder briquettes as required by the machine standard for proper mineral count and analysis. Each sample was placed in the machine for one hour thirty minutes (thirty minutes for major elements and one hour for trace elements). The software used analyzed for all elements in the periodic table between Sodium (Na) and Uranium (U), but only elements found above the detection limits were reported. All major elements were expressed as oxides and analyzed in percentage (%) composition.

For trace element analyses the samples were mixed with polyvinyl alcohol (PVA) binder and pressed into a pellet using a 10ton press. The sequentialXRF with WinXRF software was used for the analysis. A blank and certified reference material were analyzed with the sample to ascertain accuracy of the result. The result is reported in parts per million (ppm).

3.4 Mineralogical characterization of the head sample.

Mineralogical characterization of the head sample of the Koton-karfe iron ore was carried out using XRD and SEM.

3.4.1 X – Ray diffractometer (XRD) Characterization.

The XRD analysis was carried out at the Faculty of Natural and Agricultural Science, Geology Department, University of Pretoria, Pretoria South Africa. The samples were prepared for XRD analysis using a back loading preparation method.

The backloading sample preparation method involved, cleaning the holder ring and back piece with acetone, placing the ring in the spring-loaded holder, transfer enough sample material to fill the ring just above level, using the blade to tap the powder into place, making sure no gaps were left near the edge of the ring. Pressing the pug down and clearing away of powder that fell on the outer ring, while holding the dye in place, the pug was then removed and the back piece was placed over the ring, then the ring was released from the spring loader holder. Care was taken to avoid crack or collapse of material. The rings were marked with a permanent marker and then put in the machine sample holder and then place in the machine.

The sample was analysed using a PANalytical X'Pert Pro powder diffractometer with X'Celerator detector and variable divergence- and receiving slits each set at 10mm, with Fe filtered Co-Kα radiation. The samples were scanned at the required 2Θ angle. The phases were identified using X'Pert Highscore plus software. The relative phase amounts (weight%) were estimated using the Rietveld method (Autoquan Program). Errors are on the 3 sigma.

3.4.2 Scanning Emission Microscopy/Energy Dispersion Spectrum (SEM/EDS).

The SEM-EDS was carried out in the Centre for Scientific and Industrial research (CSIR), Building 19, Centre for Nano studies. Pretoria Republic of South Africa, using the Field Emission Scanning Electron Microscope equipped with Energy Dispersive spectrometer (FESEM - EDS) model number JEOL JSM-7500F and a sparter coating machine (Emiteck K950X) for gold plating of particles. During the observation EDS mapping and EDS point analysis were also carried out and back scatter images generated.

In SEM analysis a small amount of powder sample was taken and placed on the sample holder which was then placed inside the machine. A vacuum was then built in the sample chamber, then the sample was irradiated to generate emissions from which micrographs of the sample was generated after which back scatter images of the sample were captured.

3.5 The Leaching process.

3.5.1 Leaching reagents used.

The acids used for this research are Sulphuric acid (H_2SO_4), Hydrochloric acid (HCl) and Citric acid ($C_6H_8O_7$). All leach solutions were prepared from analytical grade of acids by dissolution of calculated amount in deionised water. Sulphuric acid (H_2SO_4) used had 98% concentration and density 1.84g/cm^3 (batch no 350313) Hydrochloric acid (HCl) used had 32% concentration and density 1.159g/cm^3 (batch no 350418), and the Citric acid ($C_6H_8O_7.H_2O$) assay 99.7%, density 1.5g/cm^3 (batch no 322400).

3.5.2 Leaching Procedures:

The leaching was carried out in five stages:

Stage I: 40g of -355 +250µm particle size was weighed, and then transferred into 500ml conical flask containing 200ml of 0.3M sulphuric acid at temperature of 30^0. The mixture was covered with glass lid and agitated with the aid of magnetic stirrer at an initial rate of 100rpm. The mixture was leached for a constant time of 1hr after which the solution was filtered, the residue washed thoroughly and taken for analyses. The process was repeated varying agitation speed from 200 – 500rpm at an interval of 100rpm. The above procedure was repeated for citric acid and hydrochloric acid at concentration of 0.5M each.

Stage II: From stage I the best agitation was determined for the different acids and used in this stage. The leaching in this stage was carried out at constant time (1hr), acid concentration (0.3M) for sulphuric acid, agitation of 500rpm and an initial temperature of 30^0C after which the solution was filtered, the residue washed thoroughly and taken for analyses. The stage II process was repeated with varying temperature of 40 - 80^0C at an interval of 10^0C. This process was repeated for citric acid at 0.5M and 400rpm while for hydrochloric acid 0.5M concentration was used at 300rpm.

Stage III: With the optimum parameters developed from stages one and two for agitation and temperature respectively, the effect of the variation of concentration and time were studied at this stage. For sulphuric acid, an initial concentration of 0.15M was used with varying time from 0 – 120minutes at an interval of

20minutes (at 500rpm and 30^0C), after every 20minutes of leaching, samples were taken, filtered and the residue washed thoroughly with distilled water, dried and analyzed and the leach liquor kept for further analysis. This process was repeated with sulphuric acid but varying concentration from 0.3 – 1.2M at an interval of 0.3M; at each concentration varying time as stated above. The whole process as described is repeated with hydrochloric and citric acid but with variation of acid concentration from 0.5 – 2.5M at an interval of 0.5M, varying time from 0 – 120 minutes for every concentration, at constant temperature (30^0C) and agitation of 400rpm and 300rpm for hydrochloric and citric acid respectively.

From the above procedures the best leaching parameters were attained.

Stage IV: In this stage the effect of the variation of particle size was investigated. The optimum conditions developed from stages I - III above were used to leach another particle size (-180 +125µm size fraction).

Stage V: The iron ore was calcined at varying temperatures from 700 – 900^0C at an interval of 100^0C and the two particle sizes (-355 +250µm and -180 +125µm) used for the research were leached with the optimum conditions generated from stages I – IV.

3.6 Determination of phosphorus content before and after leaching of the ore.

The phosphorus content of the ore before and after leaching was determined using XRF analysis. The samples were prepared using the same method as for the head sample.

3.7 Determination of the Amounts of Phosphorus removed during Leaching with Acids.

Reduction in the contents of phosphorus, as a result of the acid-leaching process was calculated using the results from the XRF analysis using equation (3.1);

$$\boldsymbol{R_P} = \frac{\%\boldsymbol{P_B} - \%\boldsymbol{P_A}}{\%\boldsymbol{P_B}} \boldsymbol{X}\ 100 \qquad (3.1)$$

Where R_P = Reduction in Phosphorus Content (%)

P_A= phosphorus content after leaching (%)

P_B= phosphorus content before leaching (%)

3.8 Analysis of the acids before leaching and the leached liquor.

3.8.1 Determination of acid content before leaching and in the leached solution.

The acid before leaching and the leach liquor were analyzed using Inductively coupled plasma optical emission spectrometry (ICP-OES), while the pH was measured using a hand held pH/ORP meter.

3.8.2 Analysis using Inductively coupled plasma optical emission spectrometry (ICP-OES).

The inductively coupled plasma optical emission spectrometry (ICP-OES) Thermo scientific (Thermo flex900) was used for the analysis of the leach liquor, at the Department of Chemistry, Tshwane University of Technology, Pretoria South Africa. The analyses were carried out for the acid before leaching and the leach liquor. The ICP-OES instrument was started, brought to operation

conditions and allowed to stabilize. Standard samples were prepared and run on the machine to ascertain calibration of the machine and these standards were then used for the sample analysis. The sample for analysis was then put in the machine through the sample introduction system; the sample was then converted to aerosols via a nebulizer. The aerosols were transported to the inductively coupled plasma which is a high temperature zone (8,000–10,000ºC). The analytes were heated (excited) to different (atomic and/or ionic) states and produce characteristic optical emissions (lights). These emissions were separated based on their respective wavelengths and their intensities were measured (spectrometry). The intensities were proportional to the concentrations of analytes in the aqueous sample. The quantification is *an* external multipoint linear standardization by comparing the emission intensity of an unknown sample with that of a standard sample. This was carried out only for the concentrations that gave the best leaching parameters.

3.9 pH Measurement

The pH of the leach solution before and after leaching was measured. This was carried out using the hand held pH/ORP meter (Model No. 8651). The pH meter was calibrated before use and the probe was always rinsed in fresh de-ionized water before use in order to remove any impurity adhering to the probe.

3.10 Determination of the Amounts of Iron dissolved in acid during Leaching.

The amount of iron, aluminium and silicon lost to the leaching process was calculated using the results obtained from the ICP-OES analysis by the equation (3.2);

$$\boldsymbol{R_{Fe}} = \frac{\%\boldsymbol{Fe_B} - \%\boldsymbol{Fe_A}}{\%\boldsymbol{Fe_B}} \qquad (3.2)$$

R_{Fe} = dissolved iron content (%)

Fe_B = iron content before leaching(%)

Fe_A = iron content after leaching(%)

The principle applied in equation 3.2 was also used to determine the amount of aluminium, silicon, manganese, cobalt and nickel dissolved in the various acids after leaching.

3.11 Determination of leaching rate constant (k).

The modified versions of the initial shrinking core models mentioned in equations (2.11) and (2.12) as modified elsewhere (Olanipekun 2000 and Sultana 2012) were used:

$$\mathbf{1} - [\mathbf{1} - \boldsymbol{\alpha}]^{\mathbf{1/3}} = \boldsymbol{k_1}.\boldsymbol{t} \qquad (3.3)$$

$$\mathbf{1} - \frac{\mathbf{2}}{\mathbf{3}}.\boldsymbol{\alpha} - [\mathbf{1} - \boldsymbol{\alpha}]^{\mathbf{2/3}} = \boldsymbol{k_2}.\boldsymbol{t} \qquad (3.4)$$

Where $\boldsymbol{\alpha}$ is the fraction of P dissolved at time t, $\boldsymbol{k_1}$ *and* $\boldsymbol{k_2}$ are the overall rate constants. Equation (3.3) assumes that the step controlling the leaching rate is the chemical reaction taking place on the surface of the mineral, and equation (3.4)

assumes that the controlling step is the diffusion through the product layer. From the above kinetic equations a plot of the left hand side as a function of time should give a straight line with slope k.

3.12 Determination of Activation Energy.

To obtain the activation energy, the values of K (the rate constant) at two different temperatures were used in equation (2.13) (Moore 1981)

$$lnk = lnA - \frac{E_A}{RT} \qquad (3.5)$$

Where A = Pre-exponential or frequency factor

E_A= Activation energy

R = Gas constant

T = temperature in Kelvin

Plotting ln K versus 1/T (the Arrhenius plot) a straight line of slope $-E_A/R$ is produced.

From the values of activation energy obtained the rate controlling step was verified. When the chemical reaction is the rate controlling step, the activation energy is usually in the range 40 – 100KJ/mole, when diffusion is the rate controlling step the activation energy is usually 21KJ/mole or less. For intermediate controlled leaching the activation energy falls in the range of 21 - 40KJ/mole (Habashi, 1999).

3.13 Statistical validation of the optimum Leaching condition.

A full factorial design of experiments of the type P^n (Sahin,2005) was used in the study of the leaching rate, where n corresponds to the number of factors and P represents the number of levels. n = 2 (concentration and time) and P =2 (upper and lower level) for each variable. The leaching rates were analyzed using the commercial soft ware Design-Expert 6.0 (stat. Eas Inc USA).

The levels for the two factors are as entered in Table 3.1 and the treatment combination as shown in Table 3.2.

Table 3.1: Level of factors for the Leaching process

Factors	Low level	High level
Concentration (x)	-1	+1
Time (Z)	-1	+1

Table 3.2: Design layout and response data for the various acids used as a leachant.

Standard order	A (Time mins)	B (Conc Molar)	Response (Leaching rate %)
1	Low	Low	
2	High	Low	
3	High	High	
4	low	High	

The analysis of variance (ANOVA) will be used to investigate which design parameters significantly affect the leaching process.

With the results obtained from the research the effect of particle size, stirring rate, time, acid concentration, and temperature variation on the leaching by various acids will be determined.

CHAPTER FOUR

4.0 RESULTS

4.1 CHARACTERIZATION OF THE HEAD SAMPLE.

Table 4.1, Figure 4.1 and Plate I show the result of the XRF analysis, XRD pattern and SEM image respectively. While Table 4.2, Figure 4.2a—4.2e and

Table 4.1: XRF analysis of head sample showing constituent oxides and percentage composition.

Constituent oxides	Percentage Composition
SiO_2	15.49
TiO_2	0.20
Al_2O_3	13.76
Fe_2O_3	67.02
MnO	0.41
MgO	0.41
CaO	0.26
Na_2O	*<0.01*
K_2O	0.07
P_2O_5	1.81
Cr_2O_3	0.02
NiO	0.02
V_2O_5	0.07
ZrO_2	0.01
SO_3	0.17
WO_3	0.04
BaO	0.06
Cl	0.04
CuO	*<0.01*
ZnO	0.05
Co_3O_4	0.06
SrO	0.03
MoO_3	0.01
RuO_4	*<0.01*
Rh_2O_3	*<0.01*

Plate IIa—IIj and Table 4.3 show the results of reitveld analysis, Energy dispersion spectroscopy (EDS) point analysis, SEM mapping and a summary of the count for the individual element of the head sample using SEM images.

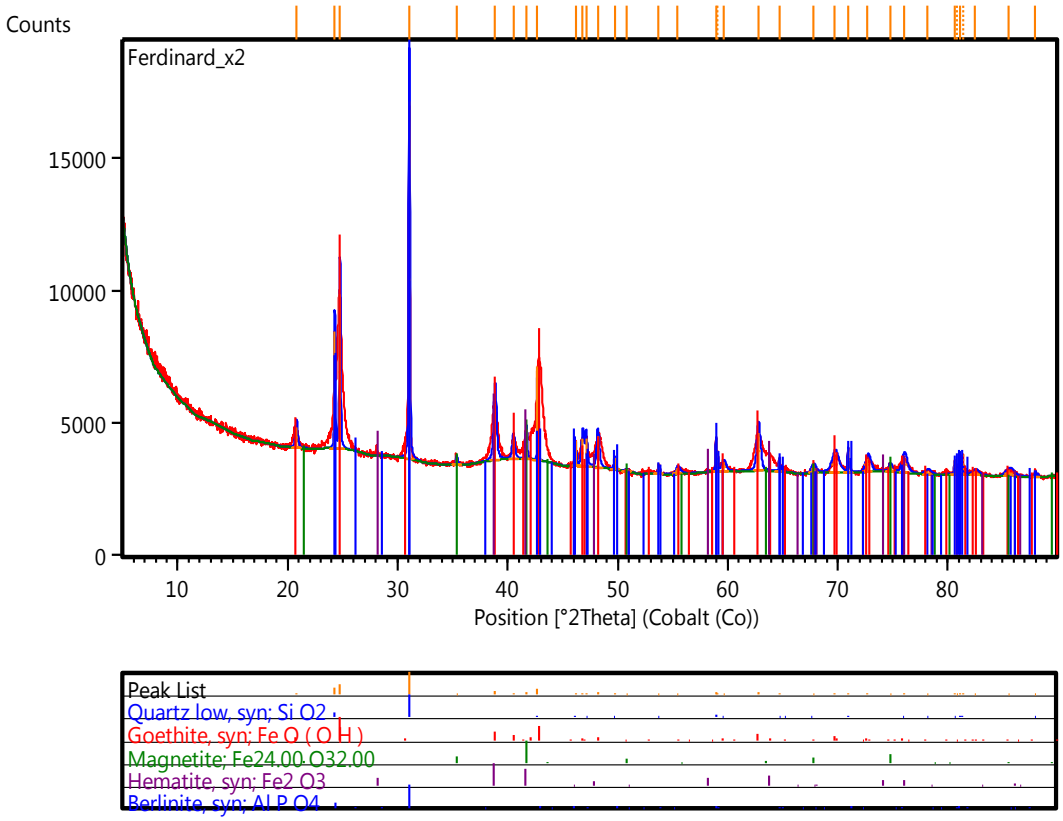


Figure 4.1 : The X- ray Diffraction (XRD) pattern of the Head sample, indicating the form in which some of the minerals appear.

Table 4.2: The relative phase amounts (weight %) as estimated by the Rietveld method.

Mineral	Weight (%)	3σ error
Goethite_	81.54	0.81
Hematite	2.8	0.3
Magnetite	0.76	0.28
Quartz	13.78	0.54
Berlinite_	1.13	0.63

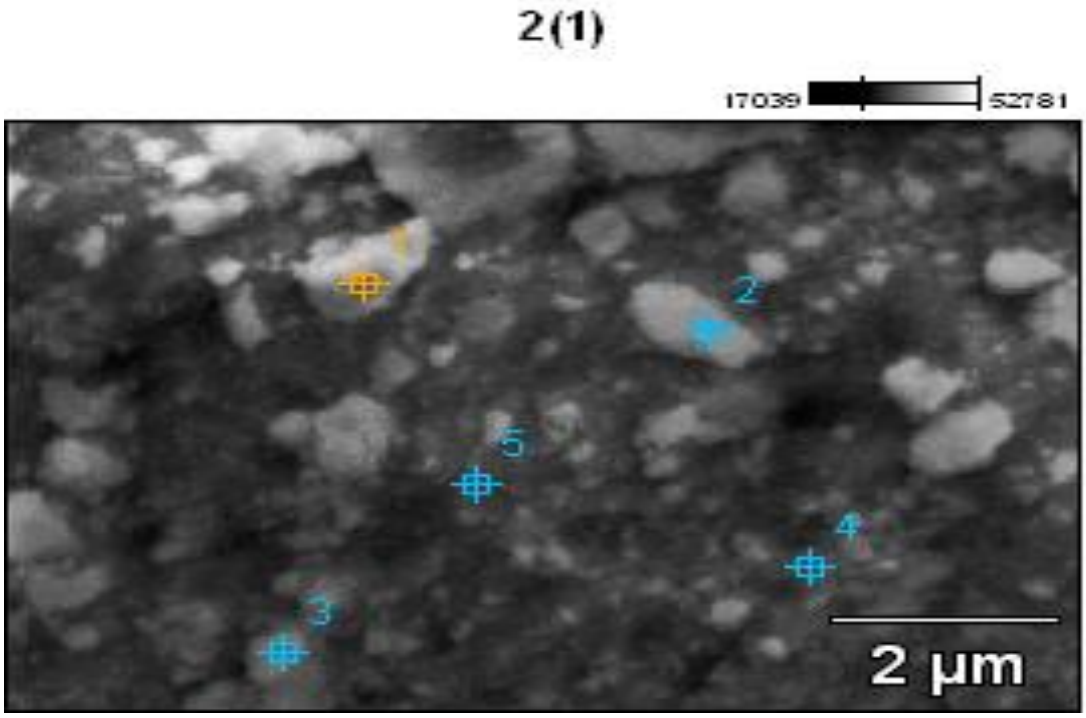


PLATE I: Scanning electron microscope (SEM) image and randomly selected points for energy dispersion spectroscopy (EDS) spectrum of head sample at accelerating voltage: 15.0 kV, Showing Geothite and Quartz (dark background) and hematite and magnetite (whitish patch) X3000.

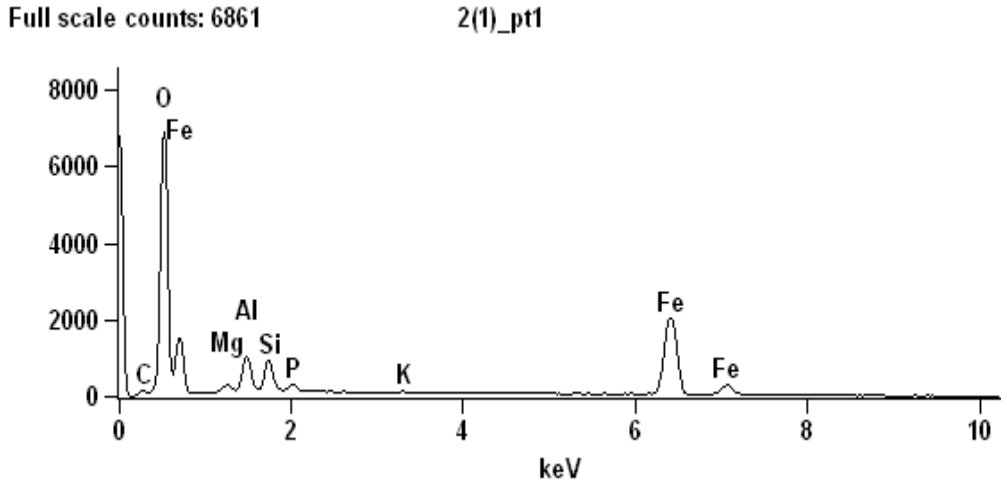


Figure 4.2a: Energy Dispersion Spectroscopy (EDS) spectrum of Point 1 on the head sample in the SEM micrograph.

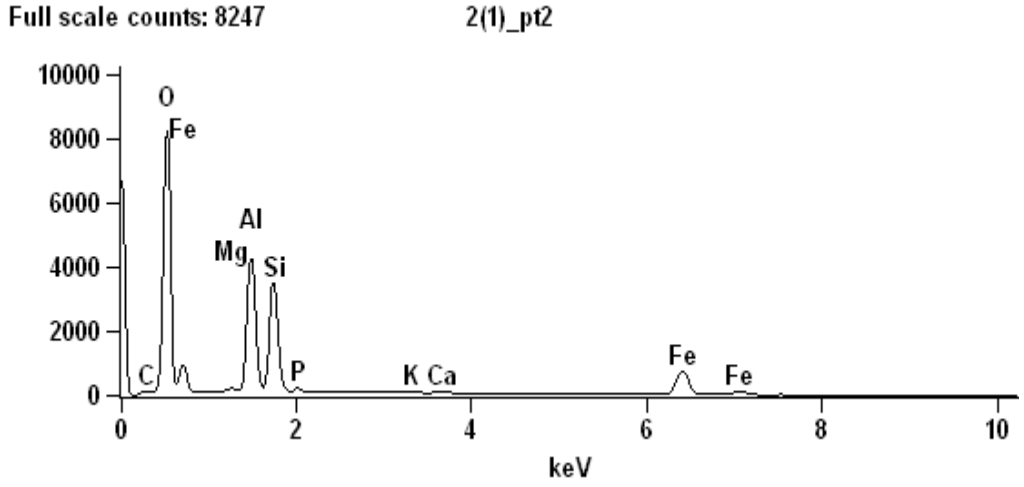


Figure 4.2b: Energy Dispersion Spectroscopy (EDS) spectrum of Point 2 on the head sample in the SEM micrograph.

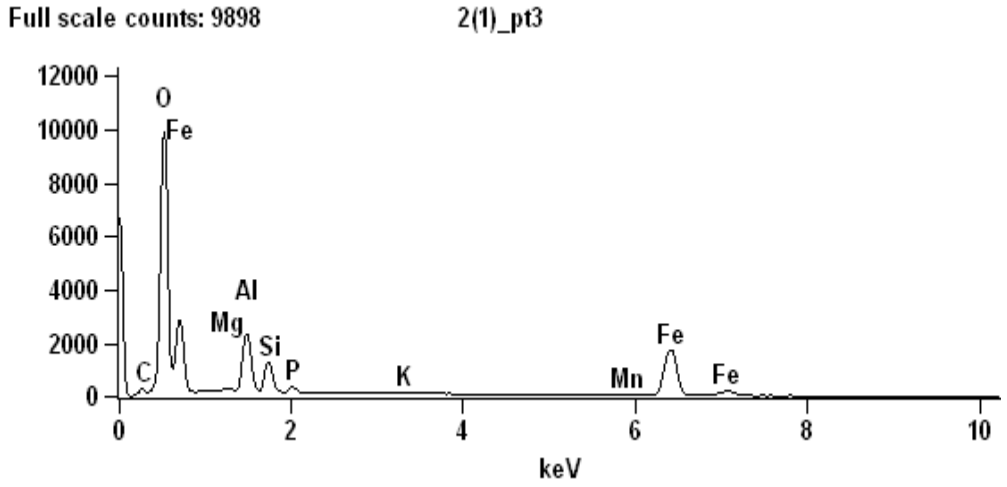


Figure 4.2c: Energy Dispersion Spectroscopy (EDS) spectrum of Point 3 on the head sample in the SEM micrograph.

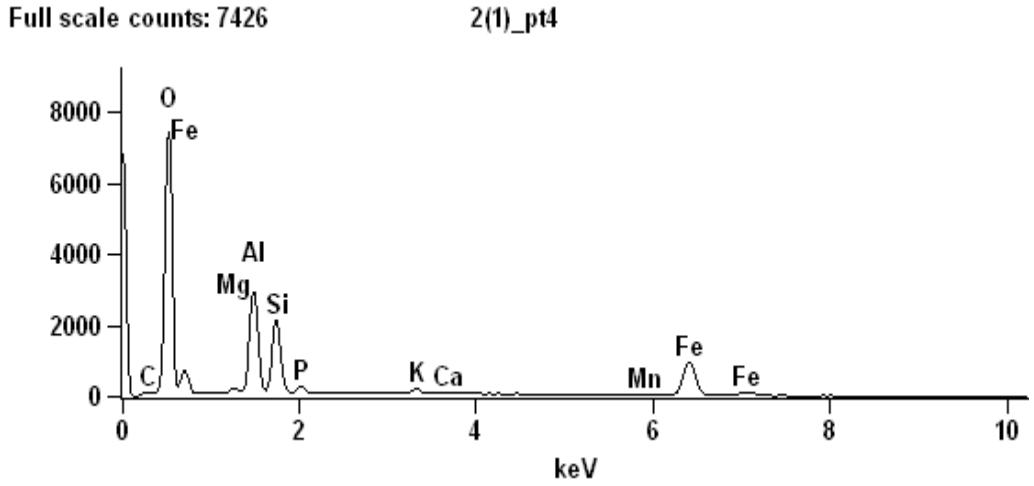


Figure 4.2d: Energy Dispersion Spectroscopy (EDS) spectrum of Point 4 on the head sample in the SEM micrograph.

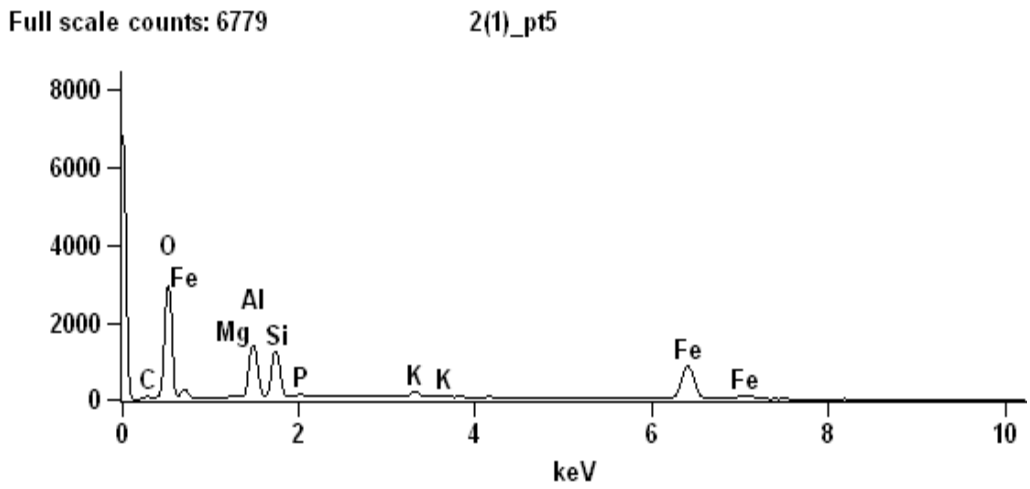


Figure 4.2e: Energy Dispersion Spectroscopy (EDS) spectrum of Point 5 on the head sample in the SEM micrograph.

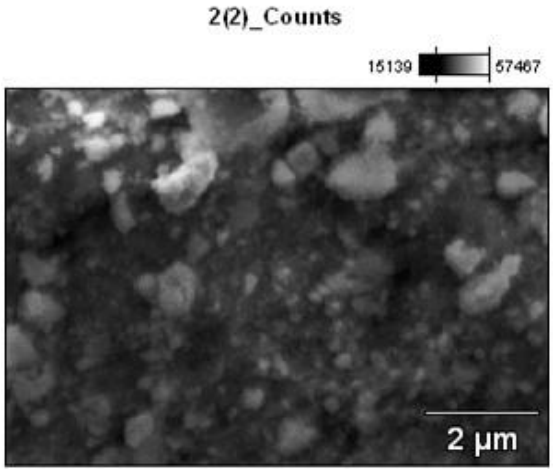


PLATE: IIa

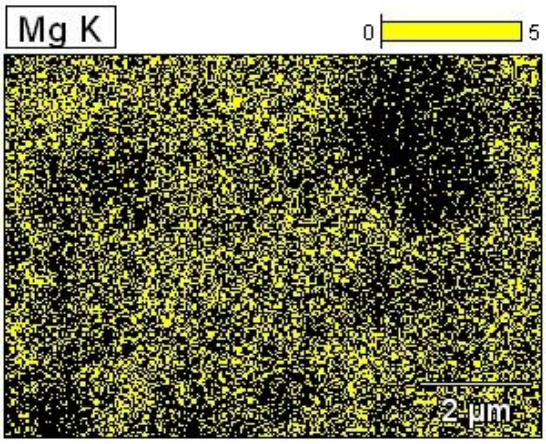


PLATE: IIb

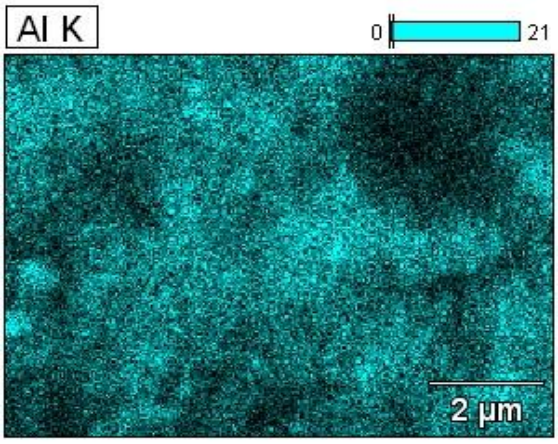


PLATE: IIc

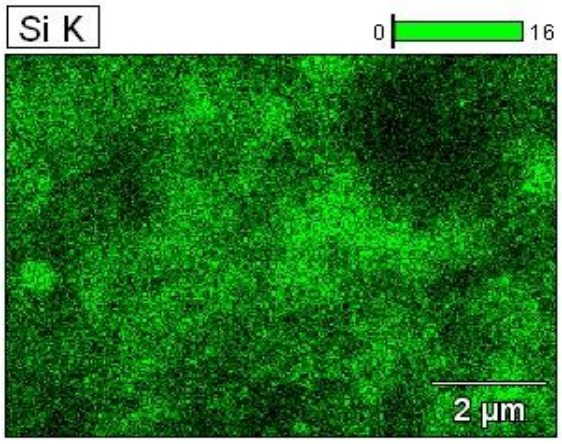


PLATE: IId

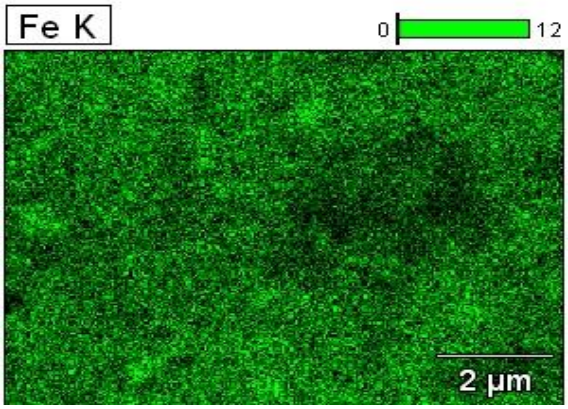


PLATE: IIe

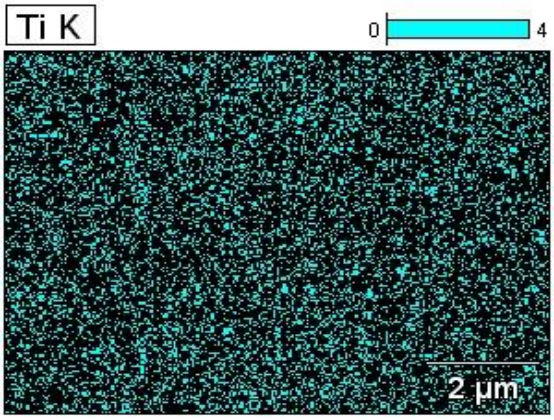


PLATE: IIf

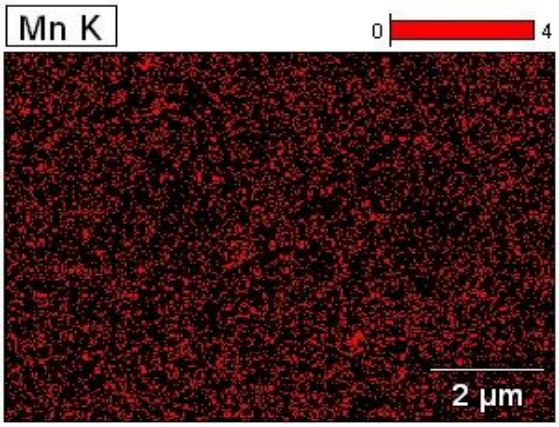


PLATE: IIg

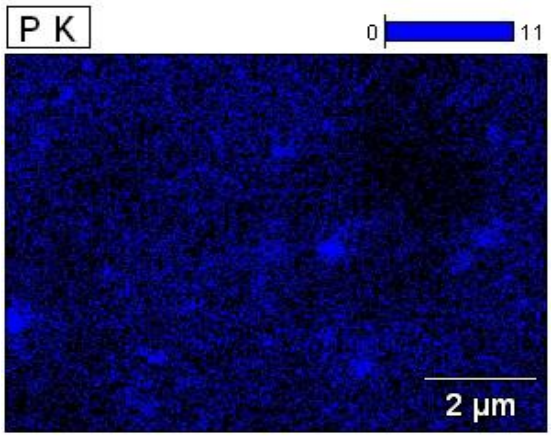


PLATE: IIh

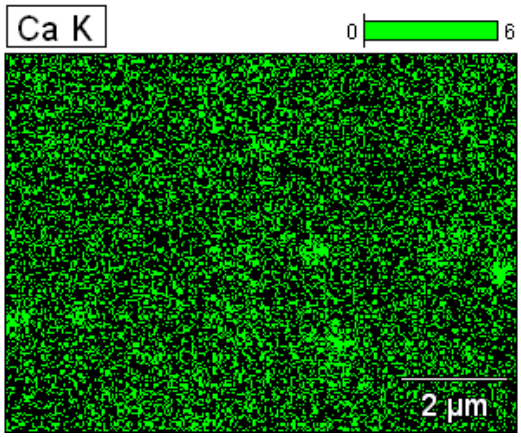


PLATE: IIi

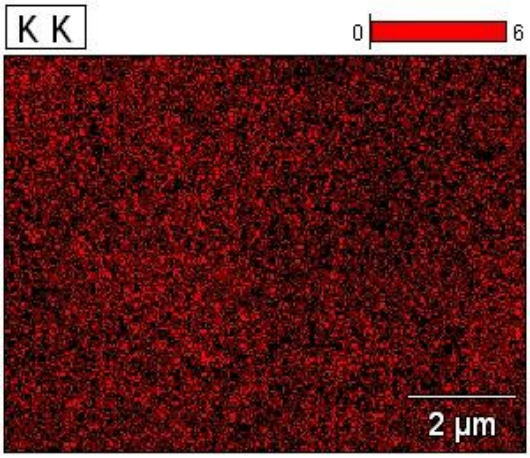


PLATE: IIj

PLATE IIa—IIj: SEM mapping showing distribution of various elements in the micrograph of the head sample.

Table 4.3: Summary of the count of the individual elements on the head sample.

Element Line	*Weight %*	*Weight % Error*	*Atom %*	*Atom % Error*
C K	15.31	+/- 0.29	38.13	+/- 0.72
O K	0.00	---	0.00	+/- 0.00
Mg K	0.14	+/- 0.05	0.18	+/- 0.06
Al K	15.93	+/- 0.15	17.66	+/- 0.16
Si K	12.57	+/- 0.15	13.38	+/- 0.16
P K	1.24	+/- 0.11	1.20	+/- 0.10
Ca K	0.51	+/- 0.09	0.38	+/- 0.07
Fe K	54.29	+/- 0.53	29.08	+/- 0.28
Total	100.00		100.00	

4.1 Distribution of minerals in the various particle sizes of the iron ore.

Table 4.4 shows the XRF analysis of the various particle sizes.

Table 4.4. XRF Analysis of the various particle sizes

	Percentage Composition							
Constituent oxides	**Head Sample**	**+355**	**-355 +250**	**-250 +180**	**-180 +125**	**-125 +90**	**-90 +50**	**-50**
SiO_2	15.49	16.49	15.81	17.33	14.06	13.66	15.99	14.91
TiO_2	0.20	0.22	0.24	0.24	0.22	0.28	0.31	0.33
Al_2O_3	13.76	11.76	12.20	12.68	12.25	14.37	18.80	18.44
Fe_2O_3	67.02	67.52	67.73	65.99	69.81	67.72	60.67	61.97
MnO	0.41	0.43	0.45	0.42	0.43	0.47	0.45	0.50
MgO	0.41	0.41	0.47	0.36	0.39	0.35	0.20	0.26
CaO	0.26	0.31	0.35	0.38	0.22	0.42	0.62	0.66
Na_2O	*<0.01*	*<0.01*	*<0.01*	*<0.01*	*<0.01*	*<0.01*	*<0.01*	*<0.01*
K_2O	0.07	0.07	0.08	0.08	0.08	0.09	0.13	0.13
P_2O_5	1.81	1.84	1.98	1.66	1.85	1.75	1.88	1.85
Cr_2O_3	0.02	0.02	0.02	0.02	0.02	0.02	0.03	0.02
NiO	0.02	0.02	0.02	0.02	0.02	0.02	0.01	0.01
V_2O_5	0.07	0.07	0.07	0.06	0.07	0.07	0.07	0.07
ZrO_2	0.01	0.01	0.01	0.01	0.01	0.02	0.02	0.02
SO_3	0.17	0.17	0.15	0.17	0.17	0.15	0.13	0.13
WO_3	0.04	0.04	0.07	0.05	0.05	0.04	*<0.01*	*<0.01*
BaO	0.06	0.06	0.07	0.07	0.07	0.09	0.10	0.11
Cl	0.04	0.04	0.06	0.04	0.05	0.04	0.09	0.08
CuO	*<0.01*	*<0.01*	*<0.01*	0.01	0.01	0.01	0.01	0.03
ZnO	0.05	0.05	0.05	0.05	0.05	0.06	0.05	0.07
Co_3O_4	0.06	0.06	0.07	0.06	0.07	0.06	0.05	0.05
SrO	0.03	0.03	0.05	0.05	0.05	0.07	0.07	0.08
MoO3	0.01	0.01	0.02	0.02	0.02	0.01	0.01	*<0.01*
RuO4	*<0.01*	*<0.01*	*<0.01*	*<0.01*	*<0.01*	*<0.01*	*<0.01*	*<0.01*
Rh2O3	*<0.01*	*<0.01*	0.01	*<0.01*	0.01	*<0.01*	*<0.01*	*<0.01*

Note: All particle sizes are in µm.

From the XRF analysis two sample sizes (- 355 +250 and -180 +125µm) were selected for leaching for further investigation

4.3 Further analysis of -355 +250µm particle size.

Figure 4.3, Table 4.5 and Plate III show the result of the XRD pattern, reitveld analysis and SEM image respectively, while Figure 4.4a—4.4e, Plate IVa—IVj and Table 4.6 show the EDS point analysis, mapping and a summary of the count of individual element respectively on the SEM for - 355 +250µm particle size.

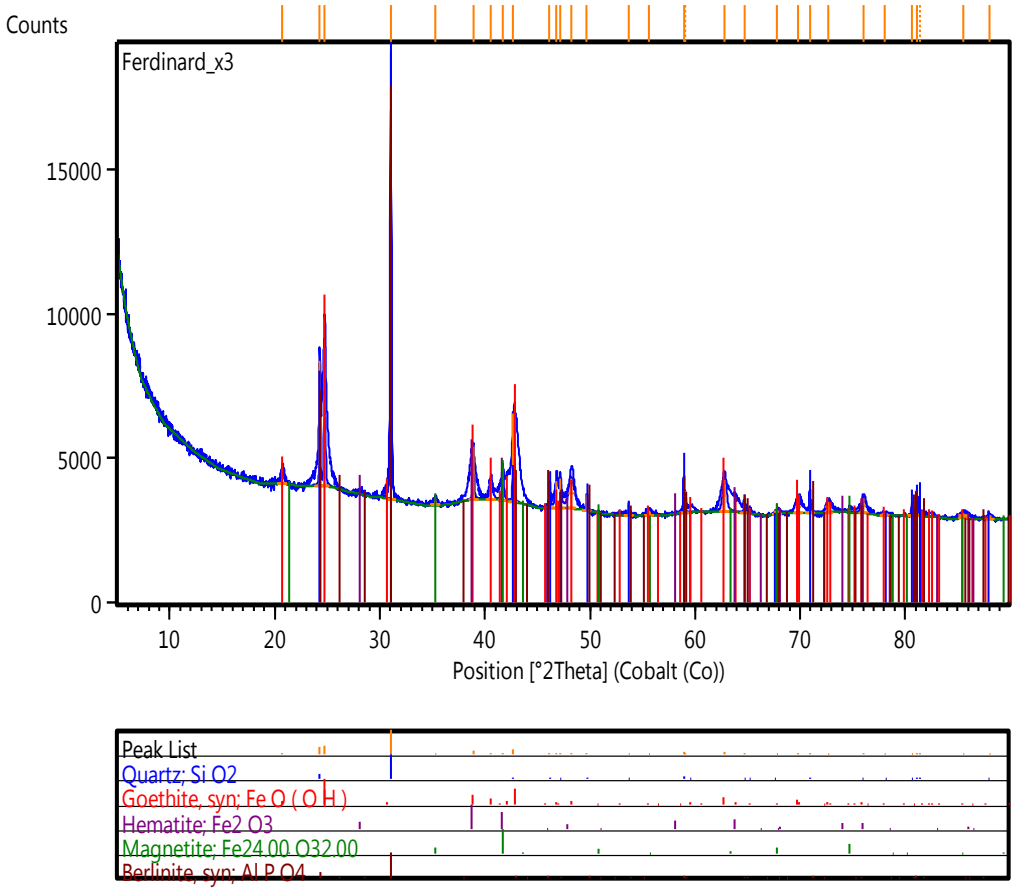


Figure 4.3: The X- ray Diffraction (XRD) pattern of the -355 +250µm particle size, showing the form in which some of the minerals appear.

Table 4.5: The relative phase amounts (weight %) of the -355 +250µm particle size, as estimated by the Rietveld method.

Mineral	Weight (%)	3σ error
Goethite_	81.01	1.08
Hematite	3.17	0.33
Magnetite_	0.72	0.33
Quartz	13.87	0.57
Berlinite_	1.25	0.96

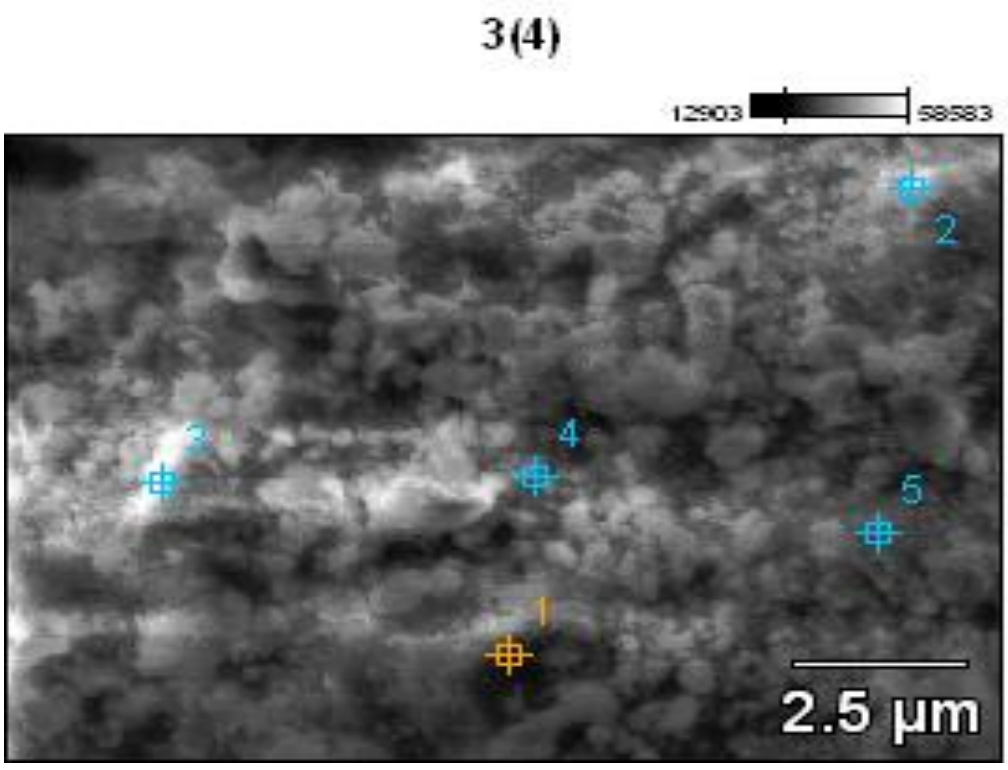


PLATE III: Scanning Electron microscope (SEM) image and selected points for energy dispersion spectroscopy (EDS) spectrum of the -355 +250µm particle size at Accelerating Voltage: 15.0 kV. Showing Goethite and Quartz (dark background) and whitish patch of hematite and magnetite. , X3000

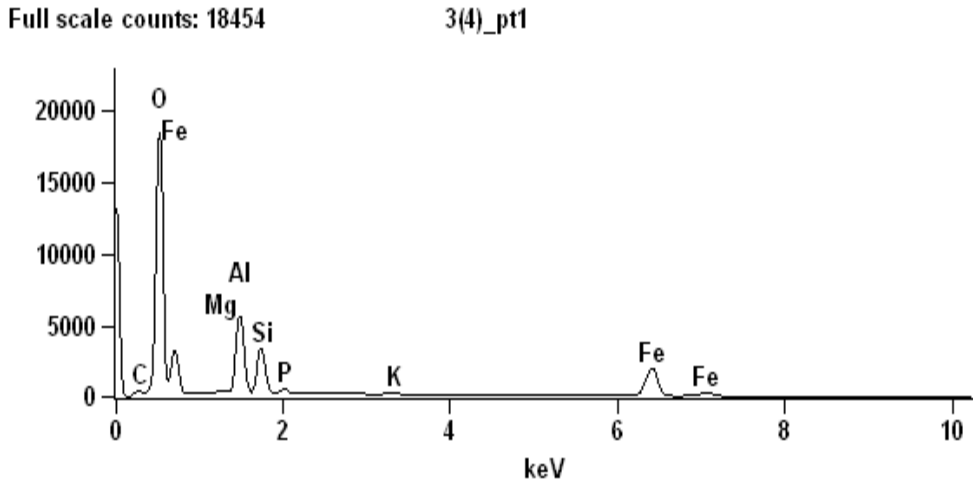


Figure 4.4a: Energy Dispersion Spectroscopy (EDS) spectrum of Point 1 on the SEM image of the -355 +250µm particle size.

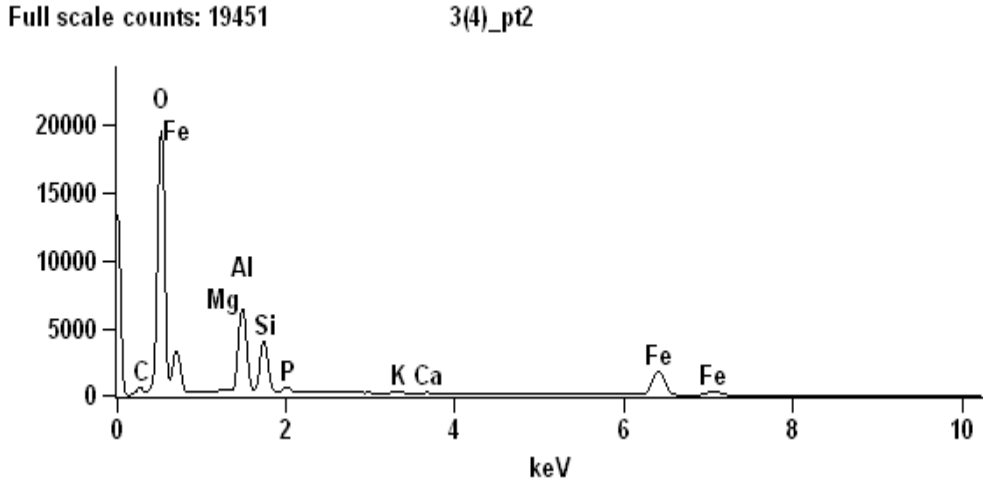


Figure 4.4b: Energy Dispersion Spectroscopy (EDS) spectrum of Point 2 on the SEM image of the -355 +250µm particle size.

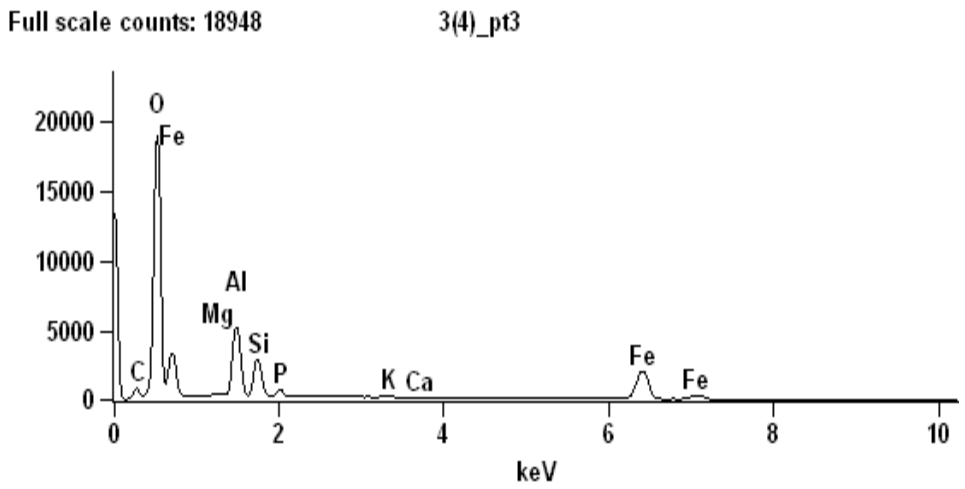


Figure 4.4c: Energy Dispersion Spectroscopy (EDS) spectrum of Point 3 on the SEM image of the -355 +250µm particle size.

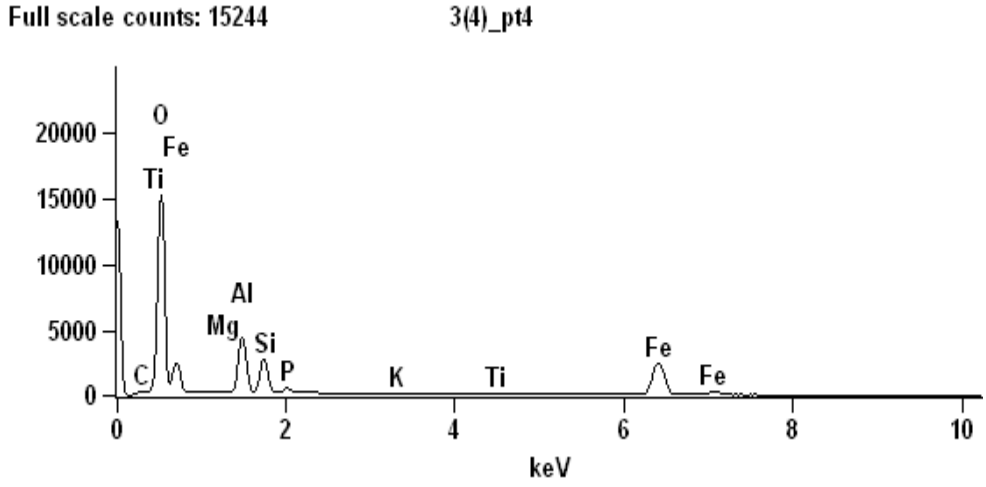


Figure 4.4d: Energy Dispersion Spectroscopy (EDS) spectrum of Point 4 on the SEM image of the -355 +250µm particle size.

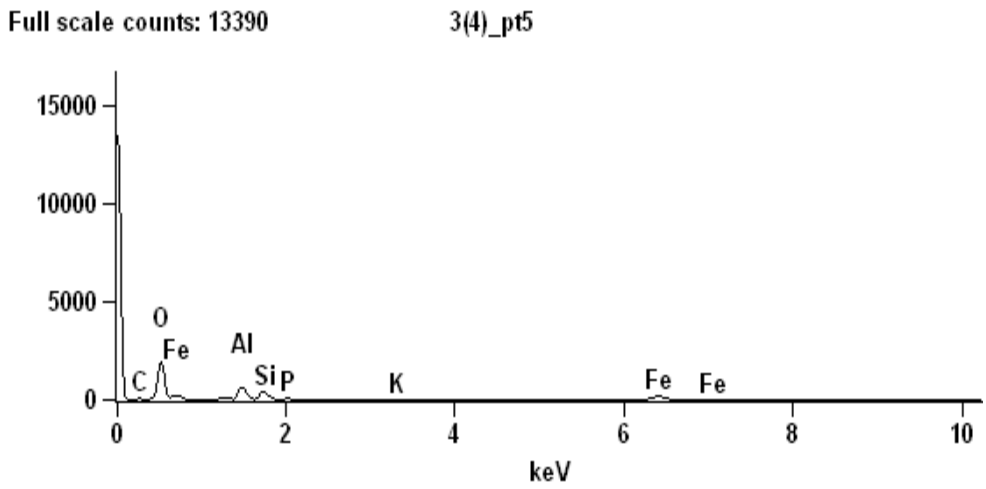


Figure 4.4e: Energy Dispersion Spectroscopy (EDS) spectrum of Point 5 on the SEM image of the -355 +250µm particle size.

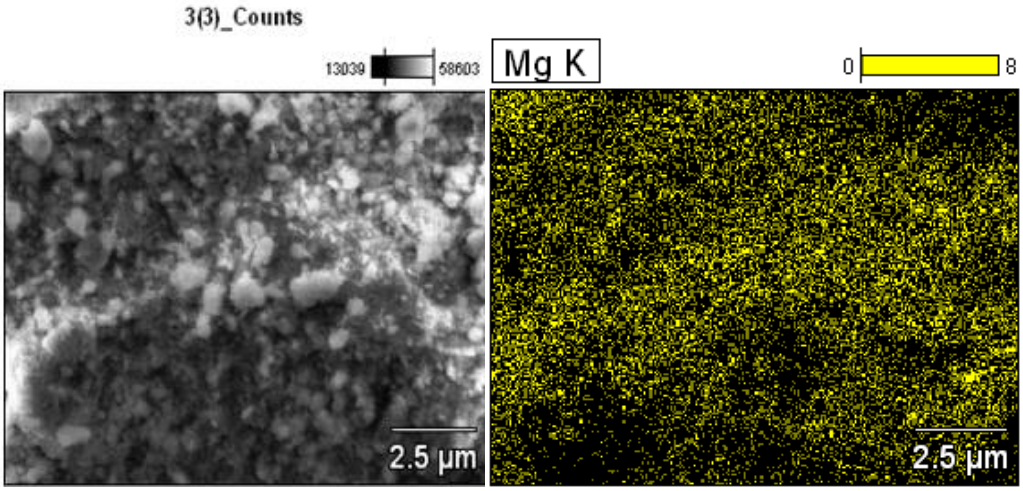


PLATE: IVa PLATE: IVb

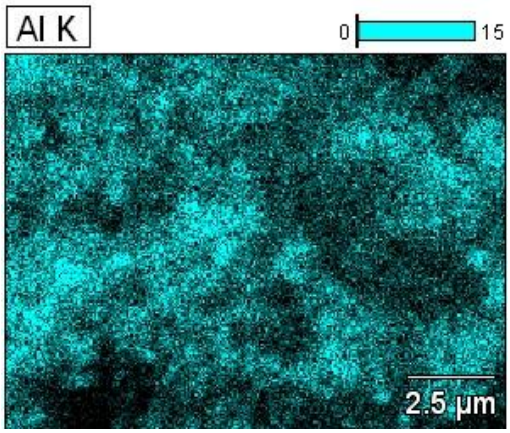


PLATE: IVc

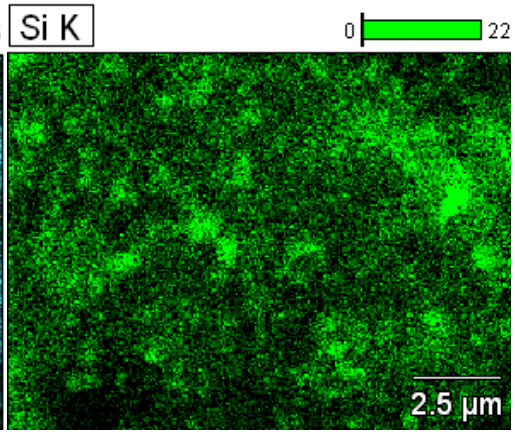


PLATE: IVd

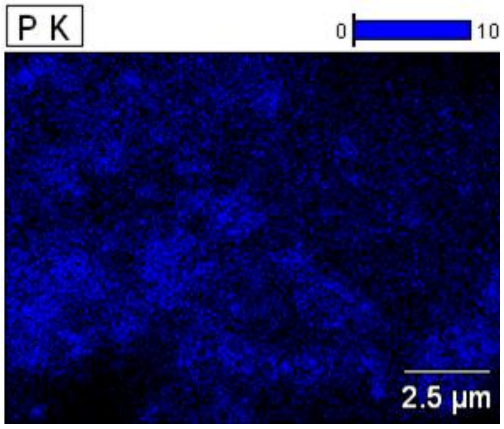


PLATE: IVe

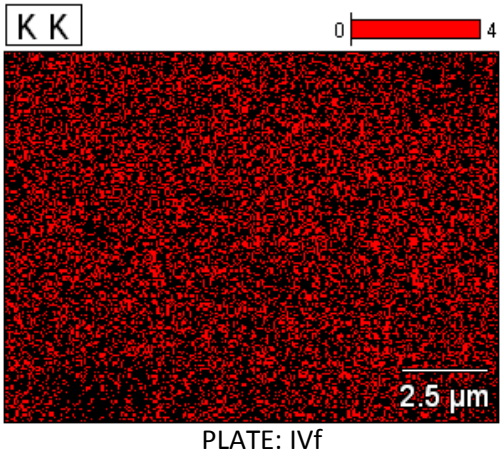


PLATE: IVf

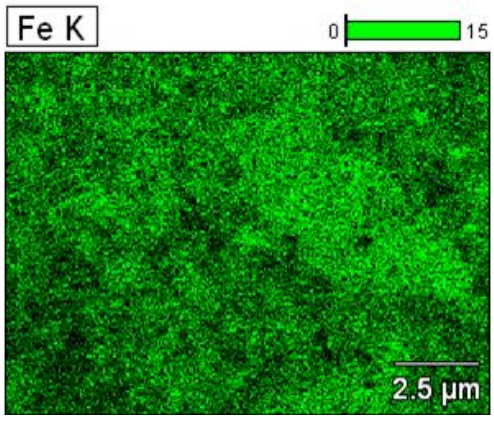


PLATE: IVg

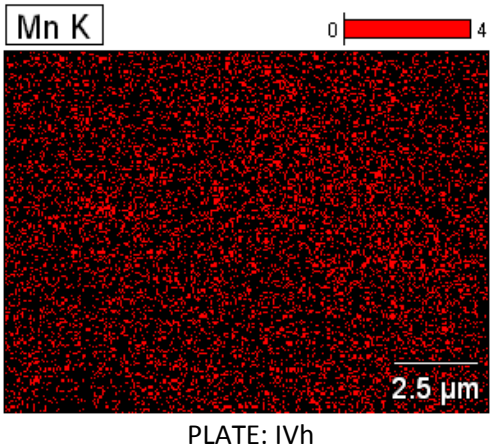


PLATE: IVh

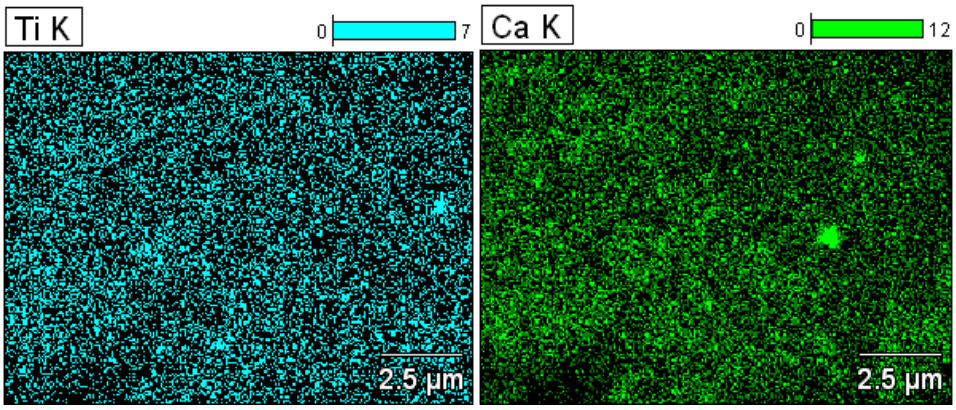


PLATE: IVi PLATE: IVj

PLATE IVa—IVj: SEM mapping showing distribution of various elements in the micrograph of the -355 +250µm particle size.

Table 4.6: Summary of the count of the individual elements on the SEM of the -355 +250µm particle size.

Element Line	*Weight %*	*Weight % Error*	*Atom %*	*Atom % Error*
C K	0.00	---	0.00	+/- 0.00
O K	0.00	---	0.00	+/- 0.00
Mg K	0.24	+/- 0.06	0.42	+/- 0.10
Al K	18.76	+/- 0.17	23.67	+/- 0.28
Si K	14.78	+/- 0.18	15.07	+/- 0.28
P K	3.83	+/- 0.14	5.35	+/- 0.20
K K	0.33	+/- 0.05	0.37	+/- 0.06
Ca K	1.60	+/- 0.13	1.73	+/- 0.14
Ti K	0.61	+/- 0.10	0.55	+/- 0.09
Fe K	59.70	+/- 0.67	52.47	+/- 0.52
Ba L	1.15	+/- 0.24	0.36	+/- 0.08
Total	100.00		100.00	

4.4 Further analysis of -180 +125µm particle size.

Figure 4.5, Table 4.7 and Plate V show the result of the XRD pattern, reitveld analysis and SEM image respectively, while Figure 4.6a—4.6e, and Table 4.8 show the EDS point analysis, and a summary of the count of individual element respectively on the SEM for -180 +125µm particle size.

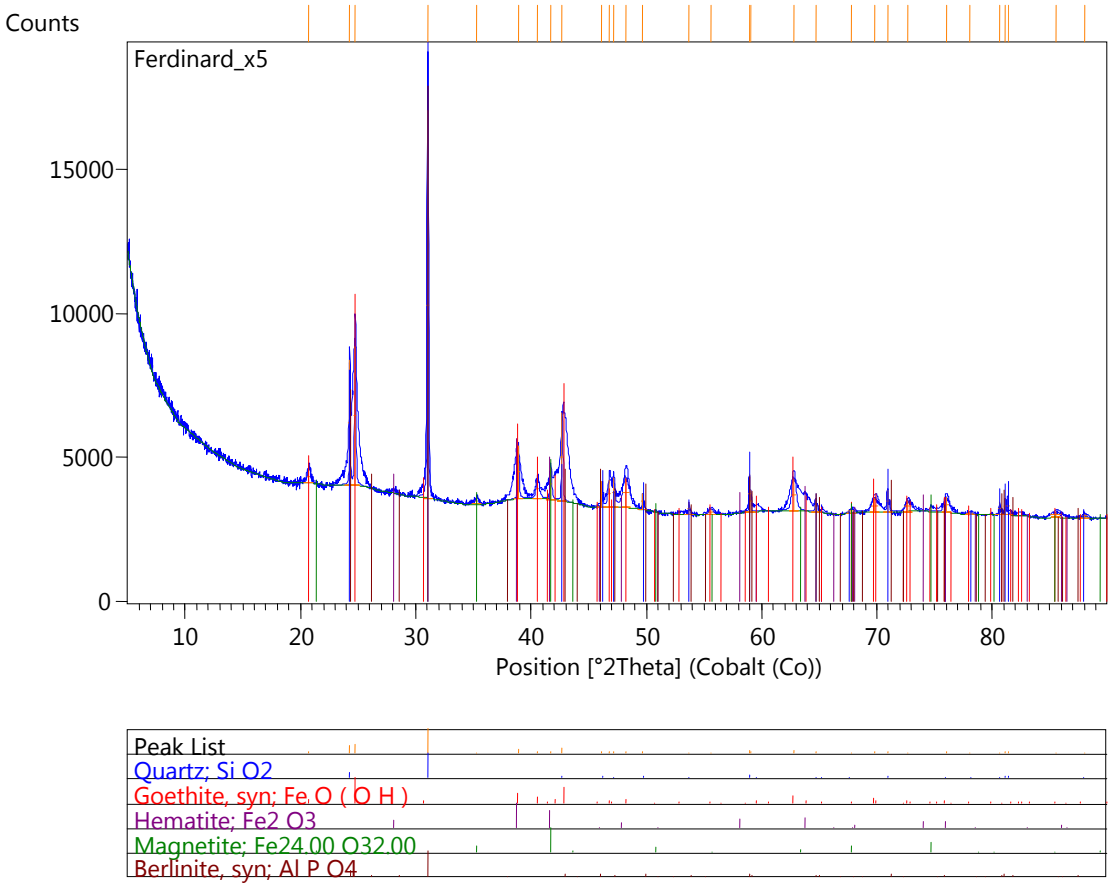


Figure 4.5: The X- ray Diffraction (XRD) pattern of the -180 +125µm particle size, indicating the form in which some of the minerals appear.

Table 4.7: The relative phase amounts (weight %) of the -180 +125µm particle size, as estimated by the Rietveld method.

Mineral	Weight (%)	3σ error
Goethite_	82.19	1.08
Hematite	3.32	0.33
Magnetite_	0.72	0.33
Quartz	12.61	0.57
Berlinite_	1.18	0.96

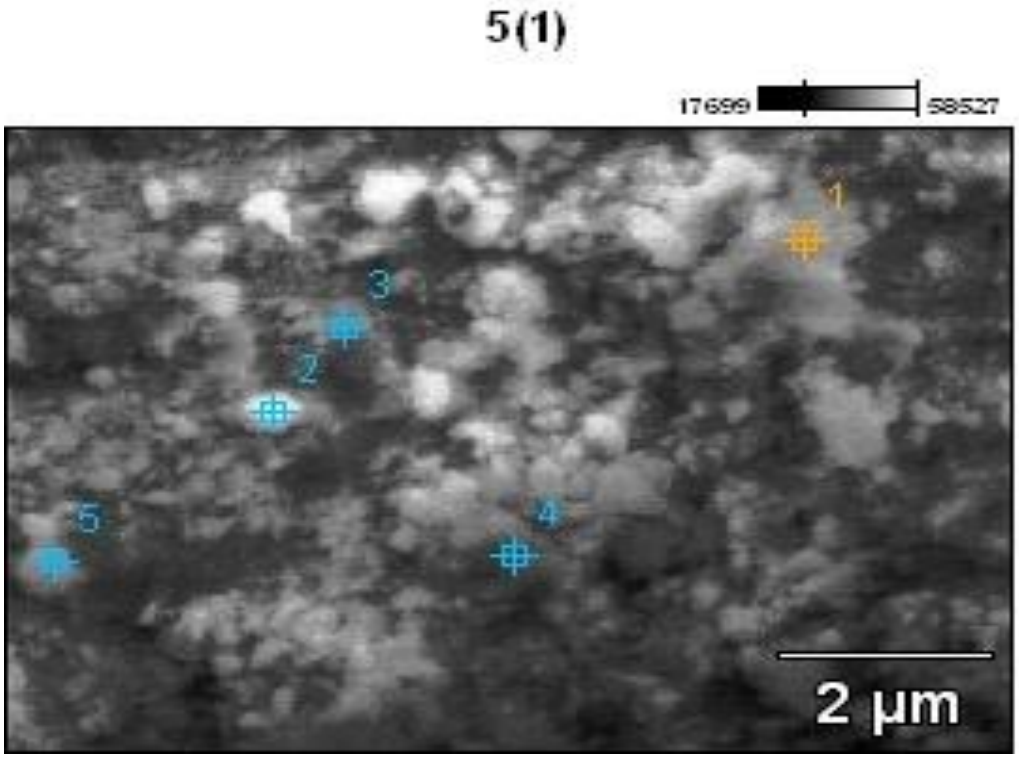


PLATE V: Scanning Electron microscope (SEM) image and selected points for energy dispersion spectroscopy (EDS) spectrum of the -180 +125µm particle size at accelerating Voltage: 15.0 kV, showing Geothite and Quartz (dark background) and whitish patch of hematite and magnetite X3000.

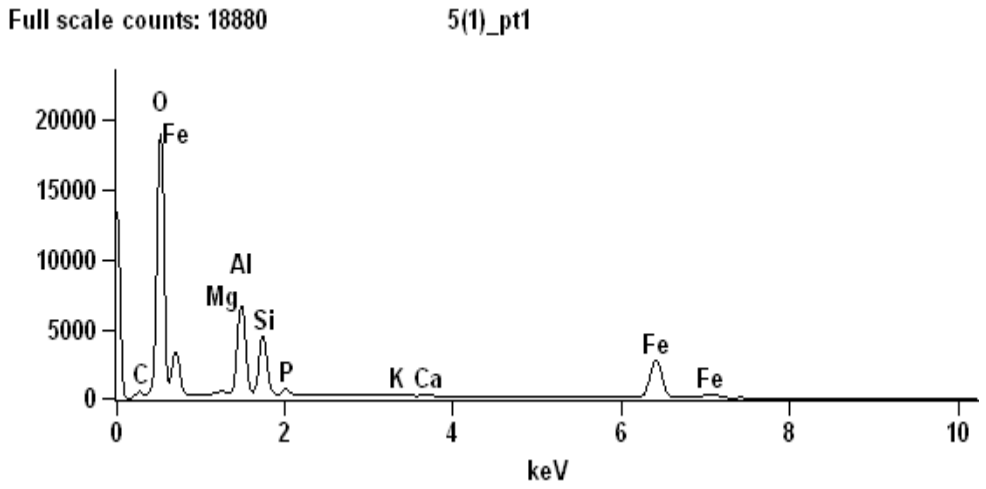


Figure 4.6a: Energy Dispersion Spectroscopy (EDS) spectrum of Point 1 on the SEM image of the -180 +125µm particle size.

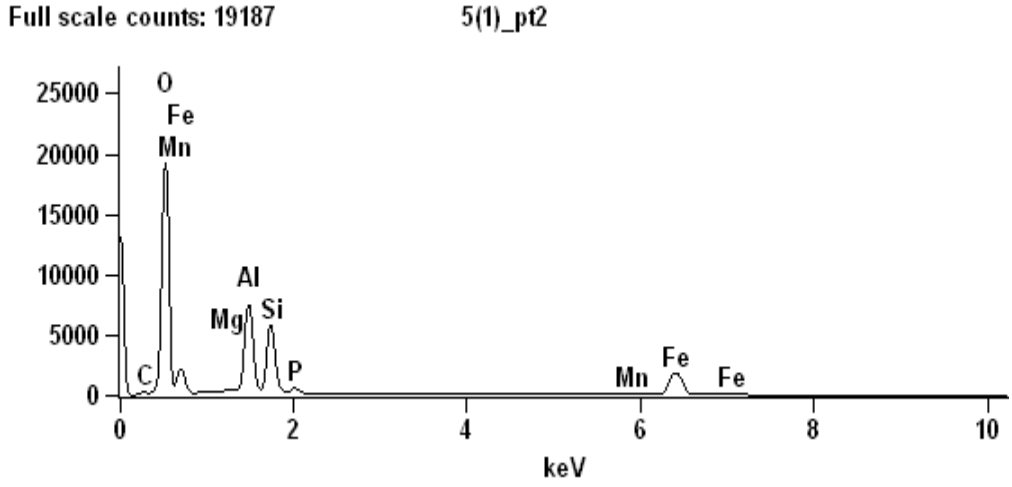


Figure 4.6b: Energy Dispersion Spectroscopy (EDS) spectrum of Point 2 on the SEM image of the -180 +125µm particle size.

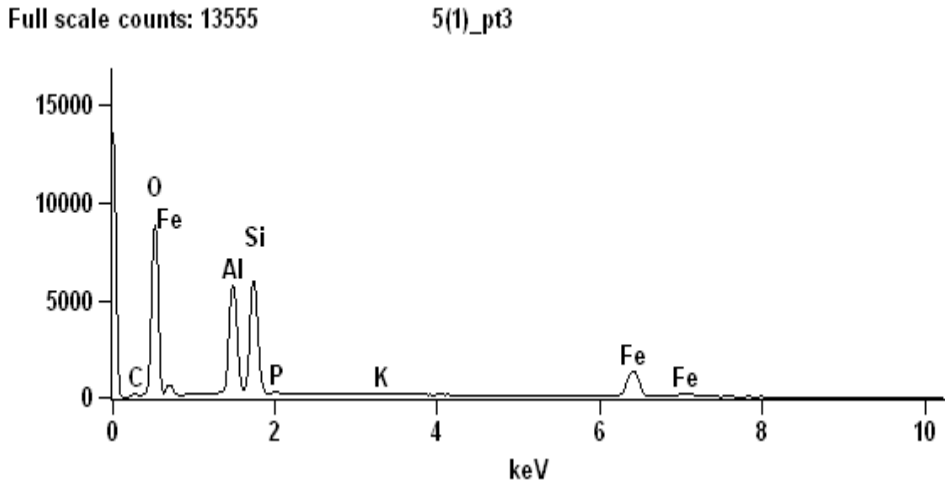


Figure 4.6c: Energy Dispersion Spectroscopy (EDS) spectrum of Point 3 on the SEM image of the -180 +125µm particle size.

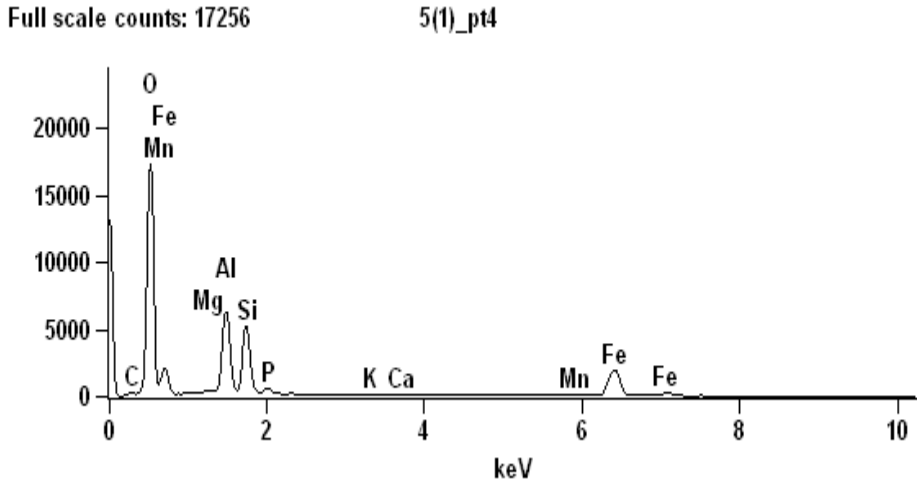


Figure 4.6d: Energy Dispersion Spectroscopy (EDS) spectrum of Point 4 on the SEM image of the -180 +125µm µm particle size.

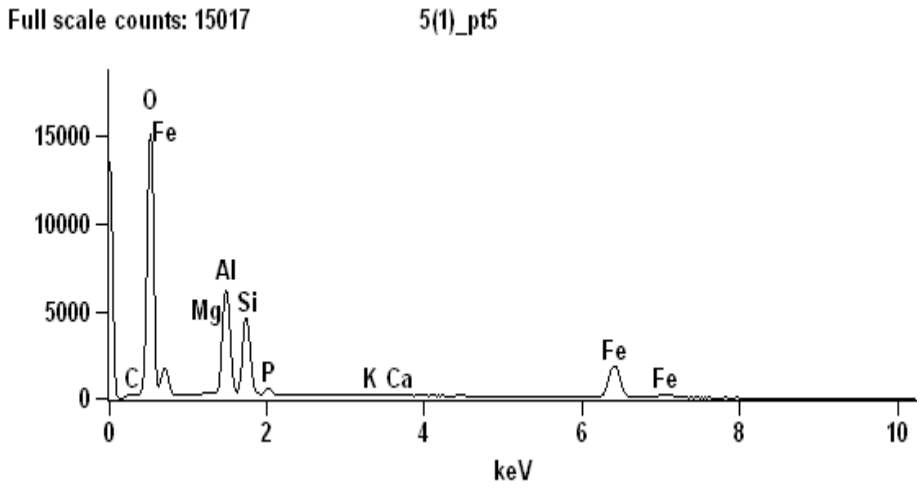


Figure 4.6e: Energy Dispersion Spectroscopy (EDS) spectrum of Point 5 on the SEM image of the -180 +125µm particle size.

Table 4.8: Summary of the count of the individual elements on the SEM of the -180 +125µm particle size.

Element Line	*Weight %*	*Weight % Error*	*Atom %*	*Atom % Error*
C K	0.00	---	0.00	+/- 0.00
O K	0.00	---	0.00	+/- 0.00
Mg K	0.32	+/- 0.06	0.54	+/- 0.10
Al K	18.80	+/- 0.18	28.24	+/- 0.26
Si K	15.46	+/- 0.19	22.31	+/- 0.28
P K	1.95	+/- 0.07	2.55	+/- 0.09
K K	0.29	+/- 0.05	0.30	+/- 0.05
Ca K	0.70	+/- 0.05	0.70	+/- 0.06
Mn K	0.72	+/- 0.13	0.53	+/- 0.09
Fe K	61.76	+/- 0.59	44.82	+/- 0.43
Total	100.00		100.00	

4.5 RESULTS FOR LEACHING OF -355 +250µm PARTICLE SIZE.

4.5.1 Effect of the variation of agitation on the leaching of -355 +250µm particle size.

The result of the effect of Agitation on the leaching of -355 +250µm particle size with sulphuric, hydrochloric and citric acid is reported in Table 4.9. The agitation was varied from 100 – 500rpm at constant time of one (1) hour, temperature of 30^{o}C, and 0.3M acid concentration for sulphuric acid while 0.5M concentration was used for Citric and Hydrochloric acid. The detailed XRF result is given in Appendix A (Table A1 – A3).

Table 4.9: The effect of agitation on the leaching of -355 +250µm particle size with the different acids used.

	AGITATION (rpm)/ PHOSPHORUS LEACHED(%)				
ACID	100	200	300	400	500
H_2SO_4	10.10	21.71	11.11	22.73	23.74
HCl	8.08	20.2	20.7	7.07	20.7
CITRIC	7.57	6.57	6.06	19.7	19.19

Note: 0.3M was used for H_2SO_4, while 0.5M was used for HCl and Citric acid.

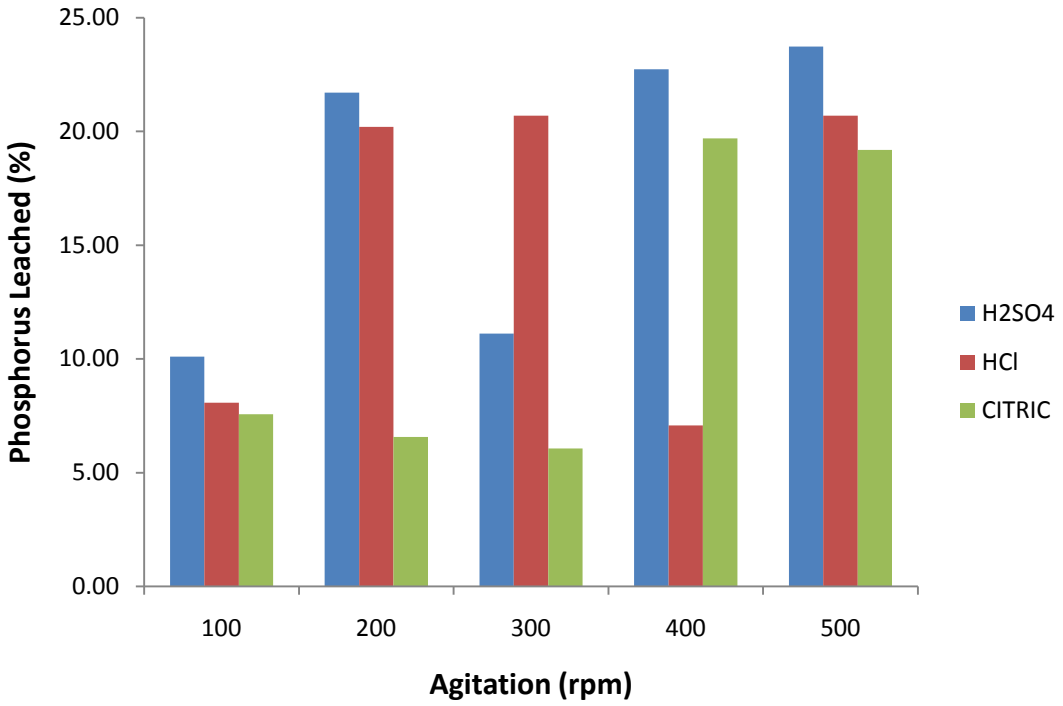


Figure 4.7: Variation of Agitation on the leaching of Phosphorus with initial leaching conditions.

4.5.2 Effect of the variation of temperature on the leaching of -355 +250µm particle size.

The result of the effect of variation of temperature on the amount of phosphorus leached with sulphuric, hydrochloric and citric acid is reported in Table 4.10. The temperature was varied from 30 - 80^{o}C, while the optimum agitation was used for each acid, time kept constant for one (1) hour and concentration of 0.3M for sulphuric acid, and 0.5M used for hydrochloric and citric acid. Detailed XRF results are given on Appendix B (Table B1 – B3).

Table 4.10: Variation of temperature with the amount of phosphorus leached with the different acids used.

	TEMPT (^oC)/ PHOSPHORUS LEACHED (%)					
ACID	30	40	50	60	70	80
H_2SO_4	23.74	17.68	12.12	11.11	5.55	8.08
HCl	20.71	3.03	14.65	2.53	2.53	1.01
CITRIC	19.7	17.68	4.04	3.03	5.56	2.53

Note: 0.3M was used for H_2SO_4, while 0.5M was used for HCl and Citric acid

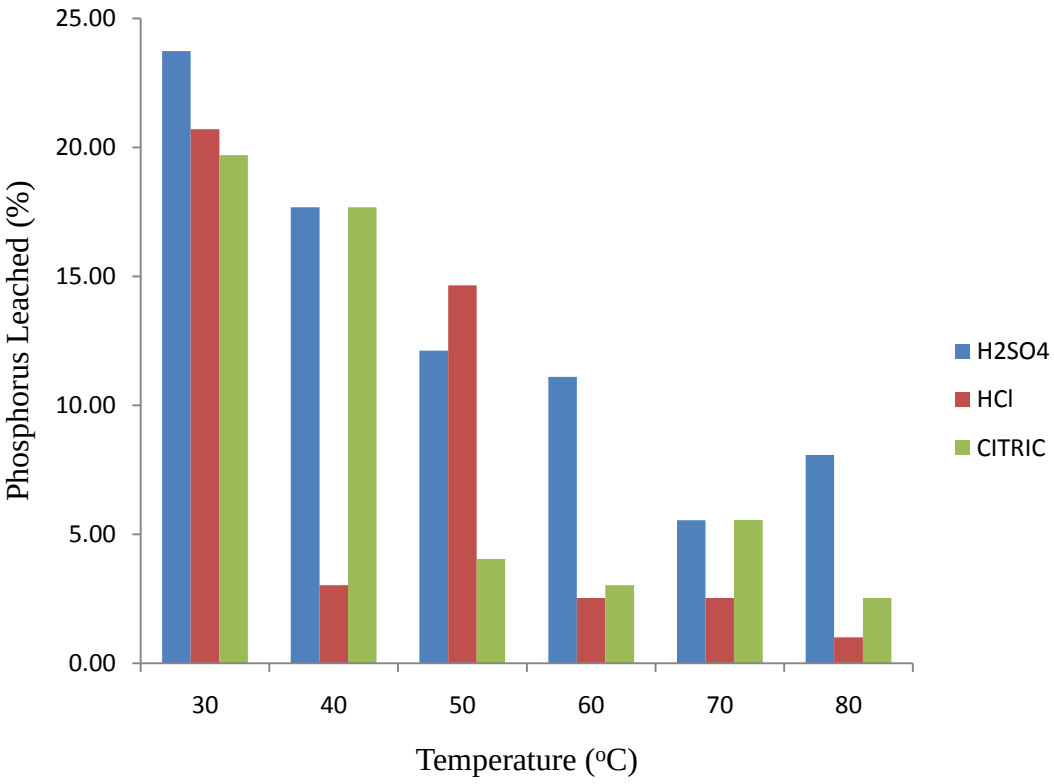


Figure 4.8: Variation of Temperature with the amount of phosphorus leached with initial Leaching conditions.

4.5.3 Effect of the variation of Concentration and time on the leaching of -355 +250µm particle size.

Using the optimum parameters obtained for agitation and temperature variation (Tables 4.9 and 4.10). The result of variation of Concentration and time on the phosphorus leaching rate using sulphuric, hydrochloric and citric acid at -355 +250µm particle size is summarized in Tables 4.11 – 4.13. The XRF results are presented on Appendix C (Table C1 – C15).

Table 4.11: Variation of sulphuric acid concentration and time on the leaching of Phosphorus in the -355 +250µm particle size.

CONC.	TIME(Mins)/LEACHING RATE (%)					
(M)	20	40	60	80	100	120
0.15	7.58	20.71	9.6	7.58	19.7	18.69
0.30	6.57	7.07	23.74	22.73	8.08	20.71
0.60	20.71	7.58	6.06	7.07	21.21	7.58
0.90	9.6	25.76	33.84	41.41	32.83	19.7
1.20	10.61	10.1	11.11	25.76	10.1	21.21

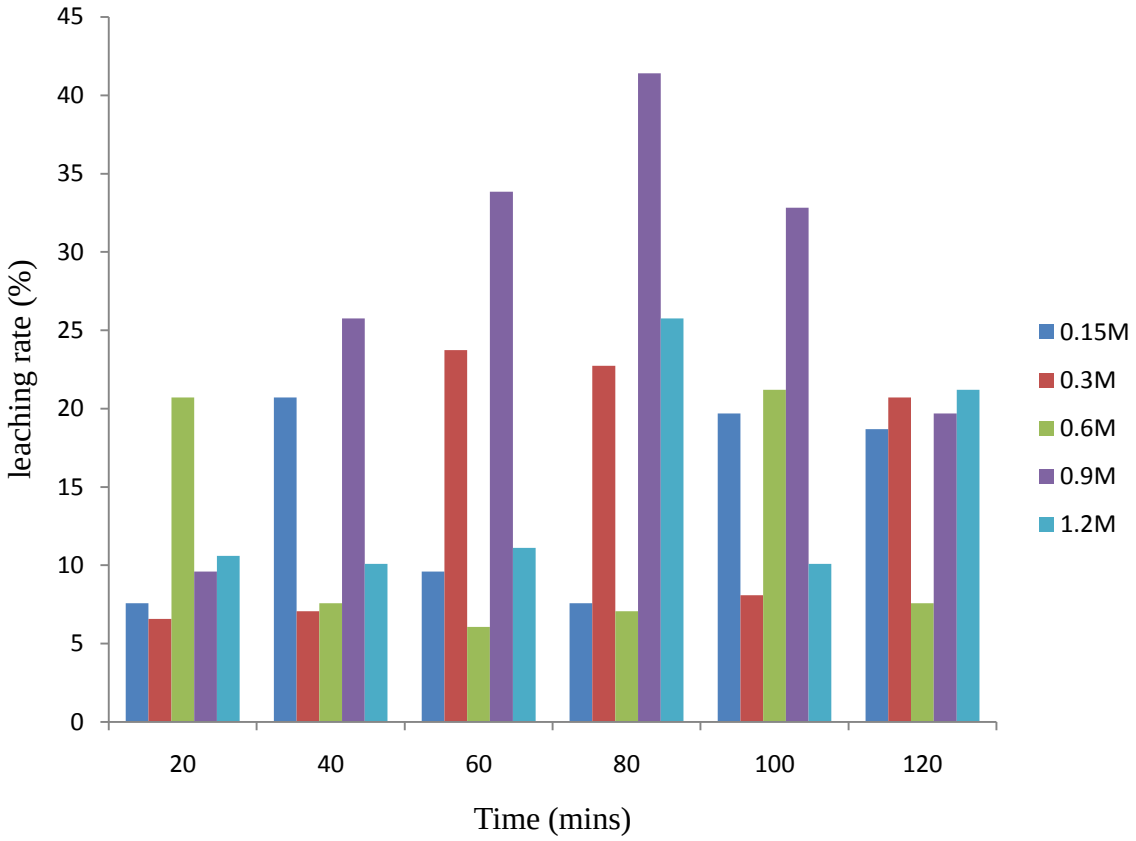


Figure 4.9: Variation of concentration and time with initial established conditions of temperature and agitation on the leaching of -355 +250µm particle size with Sulphuric acid solution

Table 4.12: Variation of Hydrochloric acid concentration and time on the leaching of Phosphorus in the -355 +250µm particle size.

CONC.	TIME(Mins)/LEACHING RATE (%)					
(M)	20	40	60	80	100	120
0.50	6.57	20.71	20.71	22.73	18.69	3.54
1.00	8.59	21.72	7.07	21.72	6.06	3.54
1.50	22.22	7.58	7.07	19.19	21.21	4.54
2.00	8.58	7.57	21.72	22.73	23.23	33.84
2.50	22.22	8.08	7.07	7.58	21.72	19.67

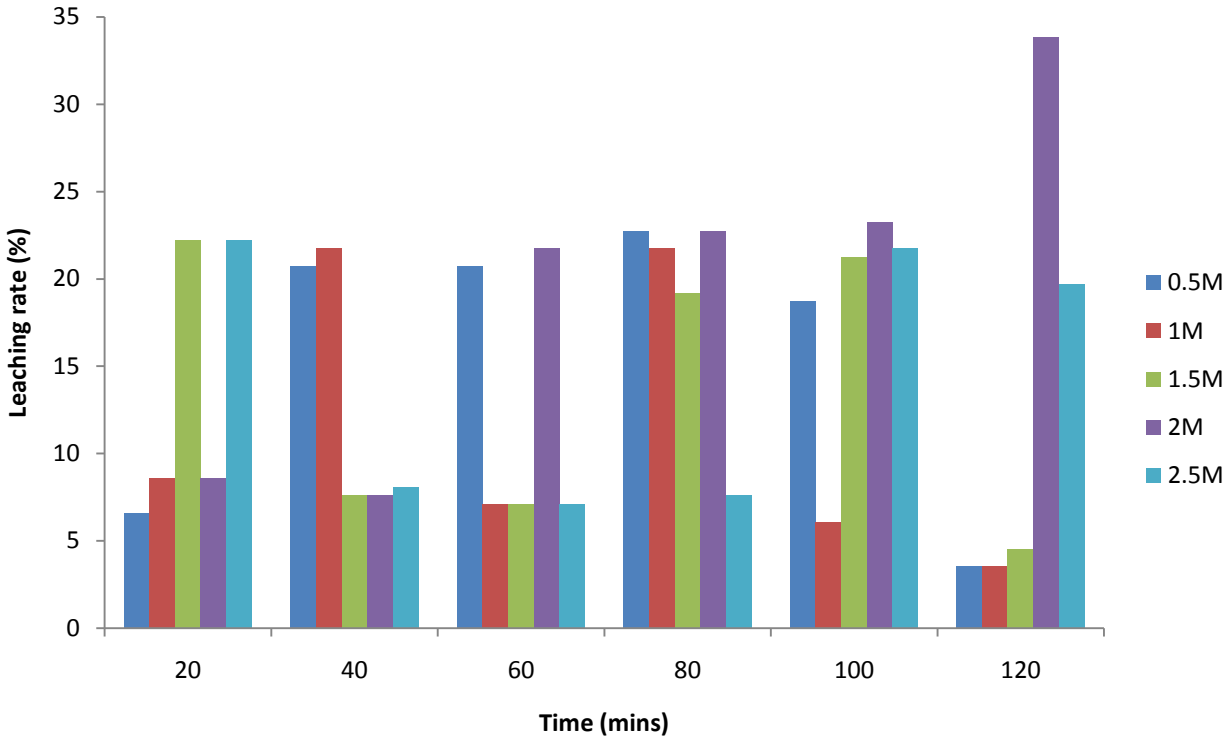


Figure 4.10: Variation of concentration and time with initial established conditions of temperature and agitation on the leaching of -355 +250µm particle size with Hydrochloric acid solution

Table 4.13: Variation of Citric acid concentration and time on the leaching of Phosphorus in the -355 +250µm particle size.

CONC.	**TIME(Mins)/LEACHING RATE (%)**					
(M)	20	40	60	80	100	120
0.50	27.27	25.25	19.67	6.06	17.68	3.54
1.00	7.07	6.57	6.06	18.69	5.56	4.55
1.50	7.58	24.74	6.06	5.56	4.55	15.66
2.00	10.61	18.18	22.73	23.23	11.62	7.07
2.50	8.59	9.09	10.1	8.59	21.21	6.06

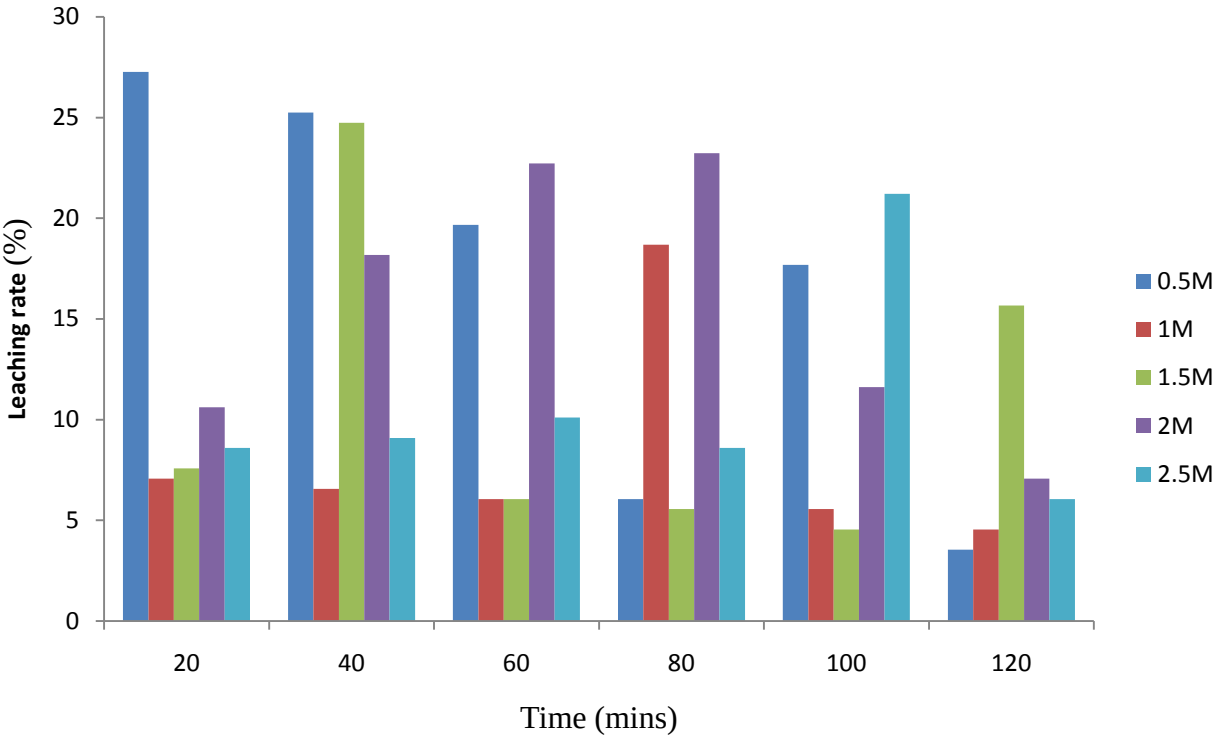


Figure 4.11: Variation of concentration and time with initial established conditions of temperature and agitation on the leaching of -355 +250µm particle size with Citric acid solution.

4.6 FACTORIAL DESIGN FOR DEVELOPED LEACHING CONDITIONS WITH -355 +250 PARTICLE SIZE.

A factorial design of experinment was used in the study of the leaching rate for -355 +250µm particle size and the various acids used. The leaching rates were analysed using the commercial soft ware Design-Expert 6.0 (stat. Eas Inc USA). Tables 4.14 – 4.16 show the experinmental design layout and response data for the leaching rate.

Table 4.14: Design layout and response data for Sulphuric acid as a leachant.

Standard order	A (Time mins)	B (Conc Molar)	Response (Leaching rate %)
1	20	0.15	7.58
2	120	0.15	18.69
3	120	1.2	21.21
4	20	1.2	10.61

Table 4.15: Design layout and response data for Hydrochloric acid as a leachant

Standard order	A (Time mins)	B (Conc Molar)	Response (Leaching rate %)
1	120	2.5	19.67
2	20	0.5	6.57
3	20	2.5	22.22
4	120	0.5	3.54

Table 4.16: Design layout and response data for Citric acid as a leachant.

Standard order	A (Time mins)	B (Conc Molar)	Response (Leaching rate %)
1	120	0.5	3.54
2	20	2.5	8.59
3	120	2.5	6.06
4	20	0.5	27.27

Analysis of variance (ANOVA) was used to determine the design parameter which significantly affect the leaching rate (response). Tables 4.17 – 4.19 show the result of ANOVA for the process. This analysis was evaluated using 95% significance level and $\alpha = 0.05$.

Table 4.17: ANOVA design of leaching rate of Sulphuric acid at boundary conditions of concentration and time

Source	Sum of squares	DF	Mean Square	F Values	P Values
Model	125.53	2	62.77	965.26	0.0228
A	117.83	1	117.83	1812.09	0.015
B	7.7	1	7.7	118.43	0.0583
Residual	0.065	1	0.065		
Cor Total	125.6	3			

Table 4.18:ANOVA design of leaching rate with Hydrochloric acid at boundary conditions of concentration and time

Source	Sum of squares	DF	Mean Square	F Values	P Values
Model	260.28	2	130.14	2259.34	0.0149
A	7.78	1	7.78	135.14	0.0546
B	252.49	1	252.49	4838.54	0.0096
Residual	0.058	1	0.058		
Cor Total	260.33	3			

Table 4.19:ANOVA design of leaching rate with Citric acid at boundary conditions of concentration and time

Source	Sum of squares	DF	Mean Square	F Values	P Values
Model	237.68	2	118.84	1.06	0.5666
A	172.4	1	172.4	1.53	0.4324
B	65.29	1	65.29	0.58	0.5854
Residual	112.36	1	112.36		
Cor Total	350.04	3			

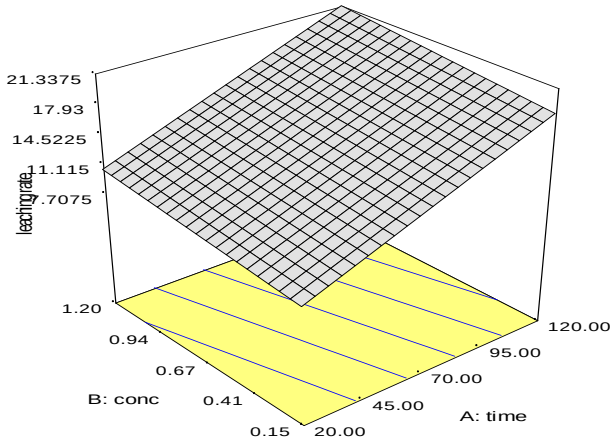


Figure 4.12: Relationship of concentration, time and leaching rate using sulphuric acid as predicted from factorial design.

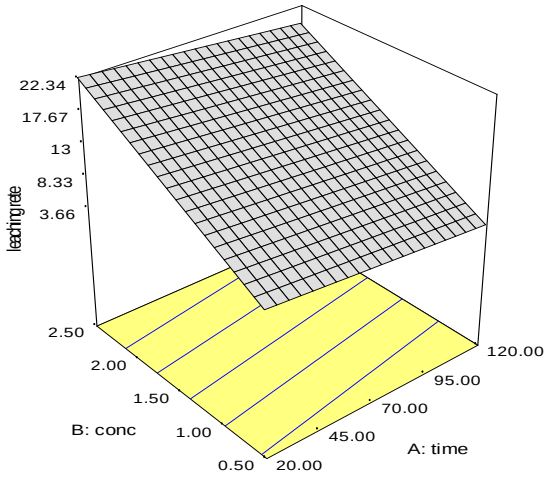


Figure 4.13: Relationship of concentration, time and leaching rate using hydrochloric acid as predicted from factorial design.

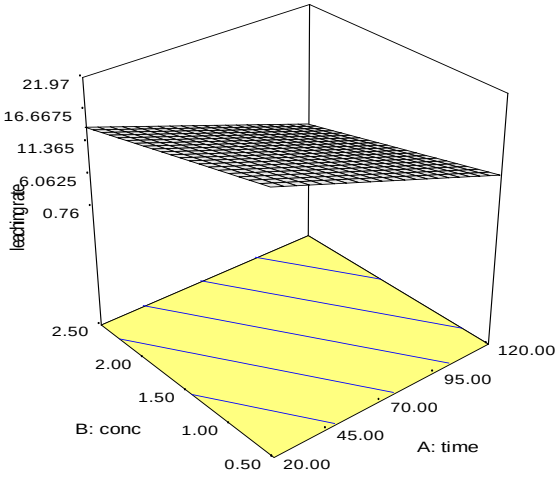


Figure 4.14: Relationship of concentration, time and leaching rate using citric acid as predicted from factorial design.

4.7 Leaching of -180 +125µm particle size.

From the optimum leaching conditions obtained from leaching -355 +250µm particle size with different acids, the leaching of -180 +125µm particle size was performed. The result obtained is given in Table 4.20. See XRF result in Appendix D.

Table 4.20: Result of leaching of -180 +125µm particle size with optimum leaching conditions generated for the different acids.

Acid	Phosphorus Leached (%).
Sulphuric	45.40
Hydrochloric	35.13
Citric	29.73

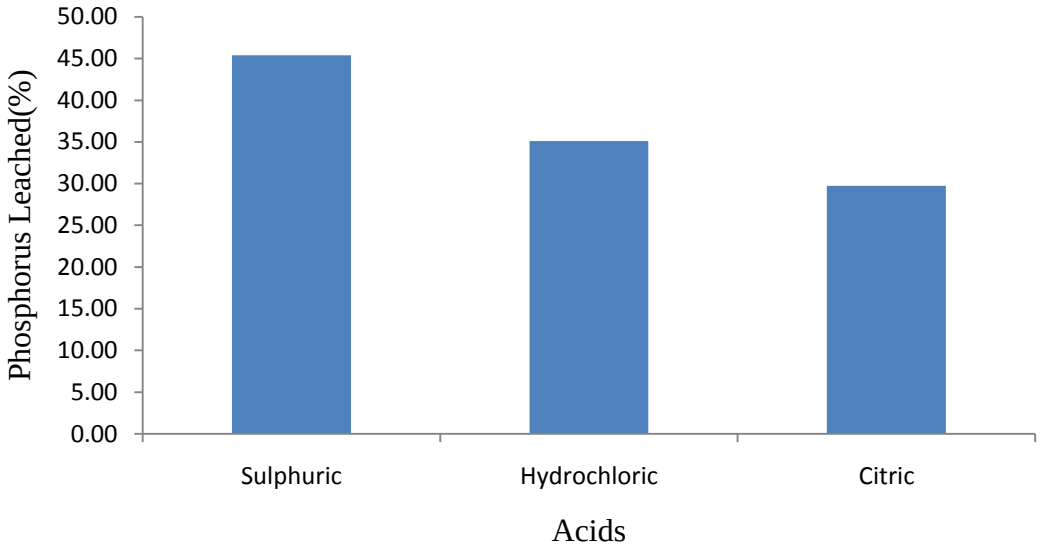


Figure 4.15: The leaching of -180 +125µm particle size with the different acids with the optimum conditions defined from the -355 +250µm particle size.

4.8 Calcination of Iron ore.

Tables 4.21 and 4.22 show the XRF results of iron ore after calcination.

Table 4.21: XRF results obtained after calcination of -355 +250µm particle size of Iron ore at 700, 800 and 900^{o}C.

Constituents	**700^{o}C**	**800^{o}C**	**900^{o}C**
SiO_2	16.61	17.56	17.38
TiO_2	0.22	0.22	0.23
Al_2O_3	13.29	12.64	12.85
Fe_2O_3	66.11	65.91	65.81
MnO	0.42	0.40	0.43
MgO	0.40	0.37	0.41
CaO	0.32	0.29	0.34
Na_2O	*<0.01*	*<0.01*	*<0.01*
K_2O	0.08	0.09	0.08
P_2O_5	1.96	1.95	1.95
Cr_2O_3	0.02	0.02	0.02
NiO	0.02	0.02	0.02
V_2O_5	0.06	0.07	0.07
ZrO_2	0.01	0.01	0.01
SO_3	0.07	0.06	0.05
WO_3	0.04	0.05	0.04
BaO	0.06	0.06	0.06
Cl	0.01	0.01	*<0.01*
CuO	0.01	0.01	0.01
ZnO	0.05	0.05	0.05
Co_3O_4	0.05	0.05	0.06
CeO_2	0.01	0.02	*<0.01*
SrO	0.04	0.04	0.05
MoO_3	0.01	0.01	0.01

Table 4.22: XRF results obtained after Calcination of -180 +125µm particle size of Iron ore at 700, 800 and 900^{o}C.

Constituents	700^{o}C	800^{o}C	900^{o}C
SiO_2	18.20	16.78	16.31
TiO_2	0.22	0.22	0.22
Al_2O_3	13.66	13.20	13.12
Fe_2O_3	64.62	66.33	67.01
MnO	0.38	0.42	0.41
MgO	0.27	0.34	0.32
CaO	0.21	0.21	0.22
Na_2O	*<0.01*	*<0.01*	*<0.01*
K_2O	0.10	0.08	0.09
P_2O_5	1.85	1.85	1.85
Cr_2O_3	0.02	0.02	0.02
NiO	0.02	0.02	0.01
V_2O_5	0.07	0.07	0.07
ZrO_2	0.02	0.01	0.02
SO_3	0.07	0.08	0.04
WO_3	0.04	0.03	0.02
BaO	0.06	0.06	0.06
Cl	0.02	0.01	0.01
CuO	0.01	0.01	0.01
ZnO	0.04	0.05	0.04
Co_3O_4	0.06	0.06	0.05
CeO_2	0.01	0.01	*<0.01*
SrO	0.04	0.04	0.04
MoO_3	*<0.01*	0.02	0.02

4.9 XRD Results after Calcination at different temperatures.

Figures 4.16 – 4.21 show the XRD pattern at the different condition of calcinations and leaching particle sizes and Tables 4.23 and 4.24 give their reitveld analysis.

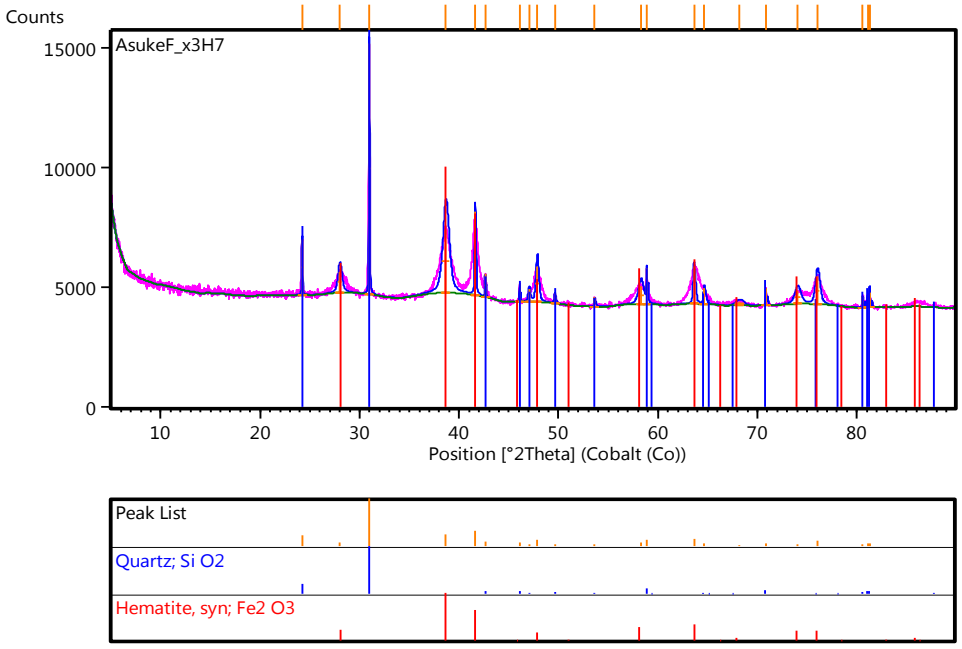


Figure 4.16: XRD pattern of -355 +250µm particle size after calcinations at 700^{o}C.

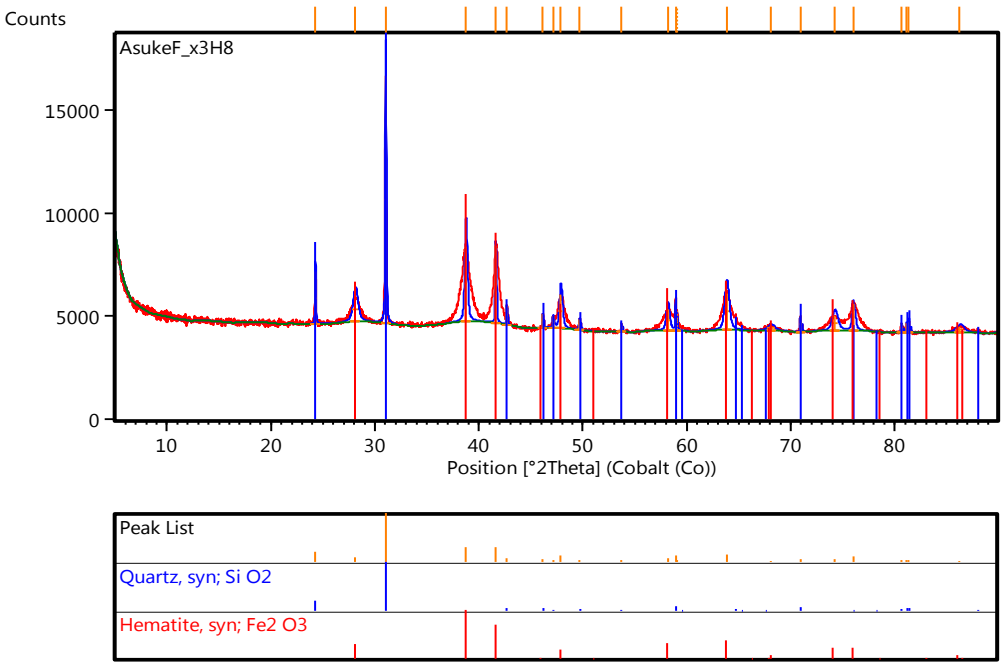


Figure 4.17: XRD pattern of -355 +250µm particle size after calcinations at 800^{o}C.

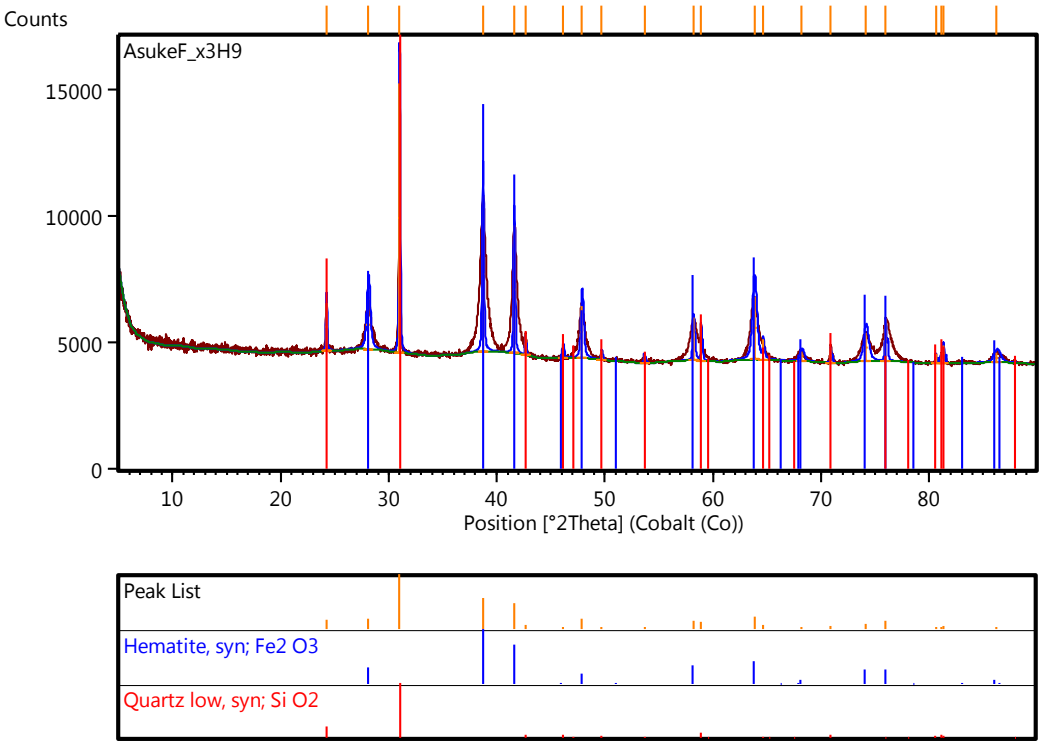


Figure 4.18: XRD pattern of -355 +250µm particle size after calcinations at 900^{o}C.

Table 4.23: The relative phase amounts (weight %) of the -355 +250µm particle size, as estimated by the Rietveld method after calcination.

	700°C		**800°C**		**900°C**	
	weight%	3 σ error	weight%	3 σ error	weight%	3 σ error
Hematite_	84.33	0.93	84.3	0.78	86.73	0.63
Quartz_	15.67	0.93	15.7	0.78	13.27	0.63

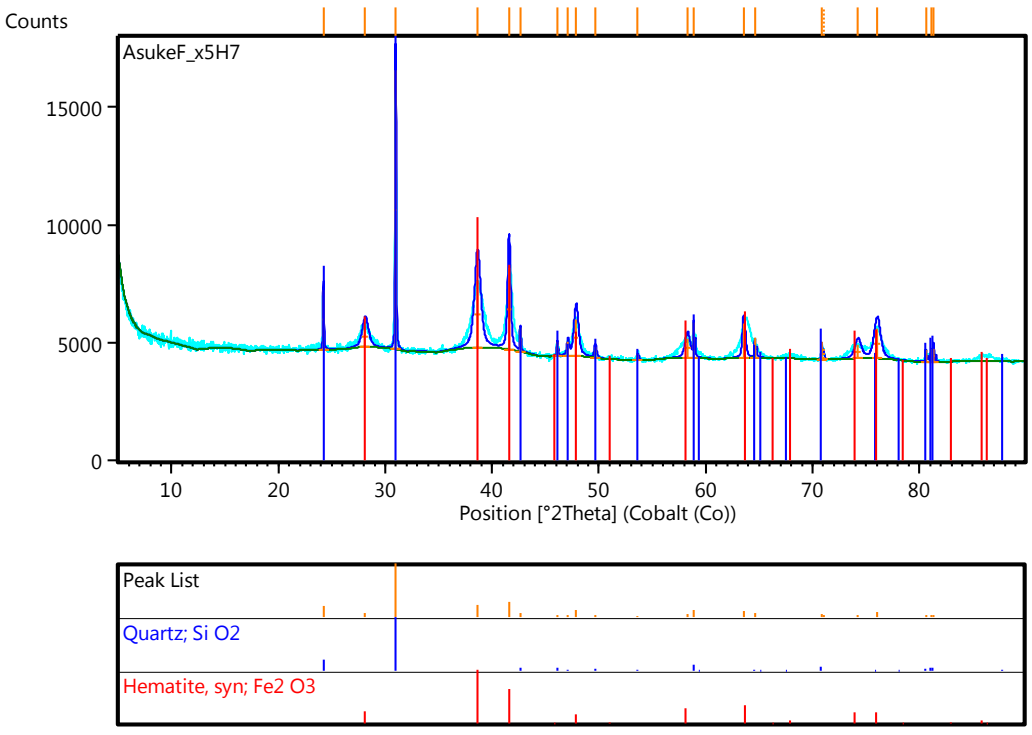


Figure 4.19: XRD pattern of -180 +125µm particle size after calcinations at 700°C.

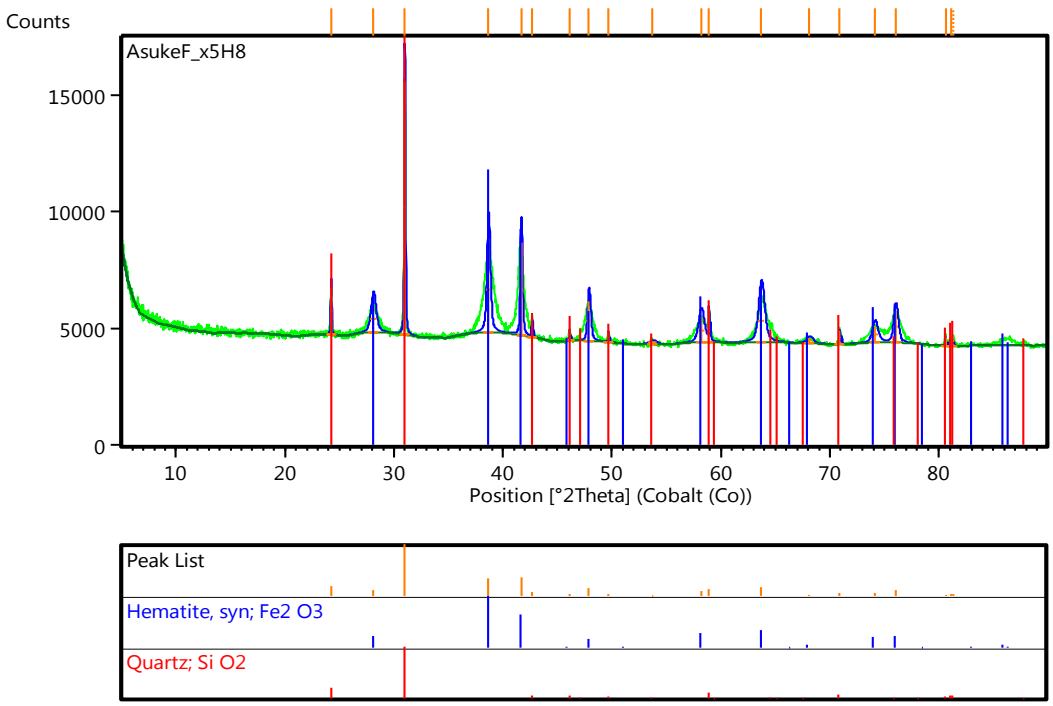


Figure 4.20: XRD pattern of -180 +125µm particle size after calcinations at 800°C.

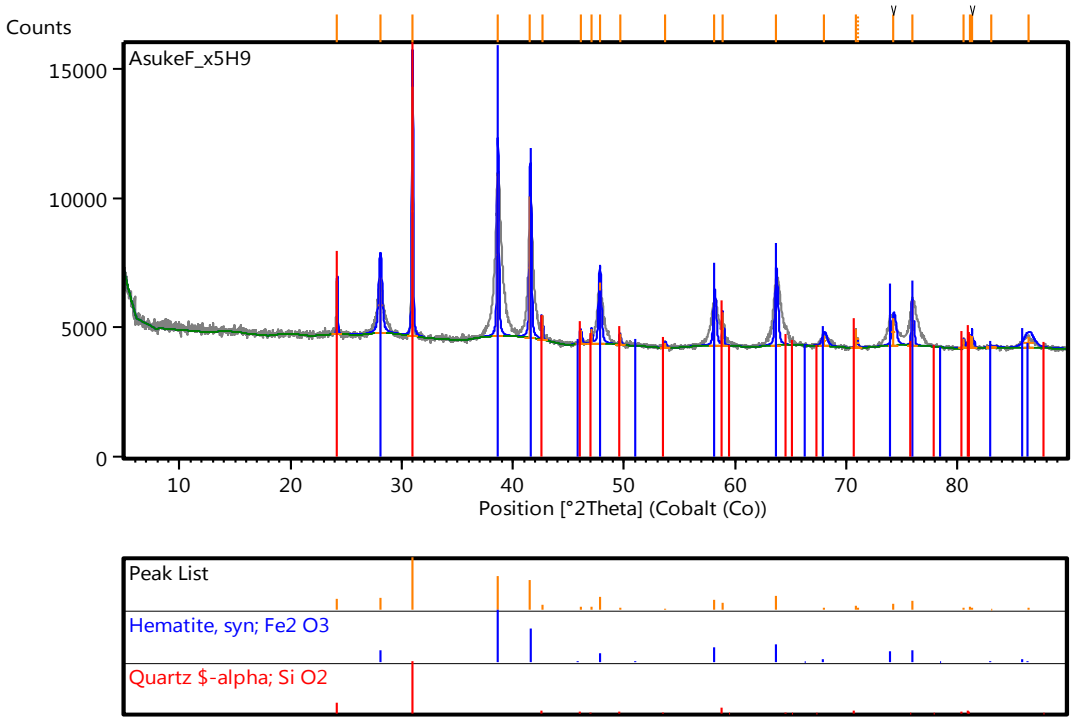


Figure 4.21: XRD pattern of -180 +125µm particle size after calcinations at 900°C.

Table 4,24: The relative phase amounts (weight %) of the -180 +125µm particle size, as estimated by the Rietveld method after calcination.

	700°C		800°C		900°C	
	weight%	3 σ error	weight%	3 σ error	weight%	3 σ error
Hematite_	84.9	0.9	87.49	0.78	88.39	0.63
Quartz_	15.1	0.9	12.51	0.78	11.61	0.63

4.10 Leaching of the calcined Iron ore

The result of leaching after calcination at 700°C, 800°C and 900°C with sulphuric, hydrochloric and citric acid is reported in Tables 4.25 and 4.26 and shown in Figures 4.22 and 4.23. The leaching was carried out with the optimum leaching conditions initially established. Detailed XRF results are given on Appendix E (Table E1 – E6).

Table 4.25: Results of leaching the -355 +250µm particle size with optimum leaching conditions after calcination.

	Citric	**HCL**	**H_2SO_4**
700°C	30.10	35.20	44.90
800°C	32.31	44.62	49.74
900°C	33.85	50.26	61.03

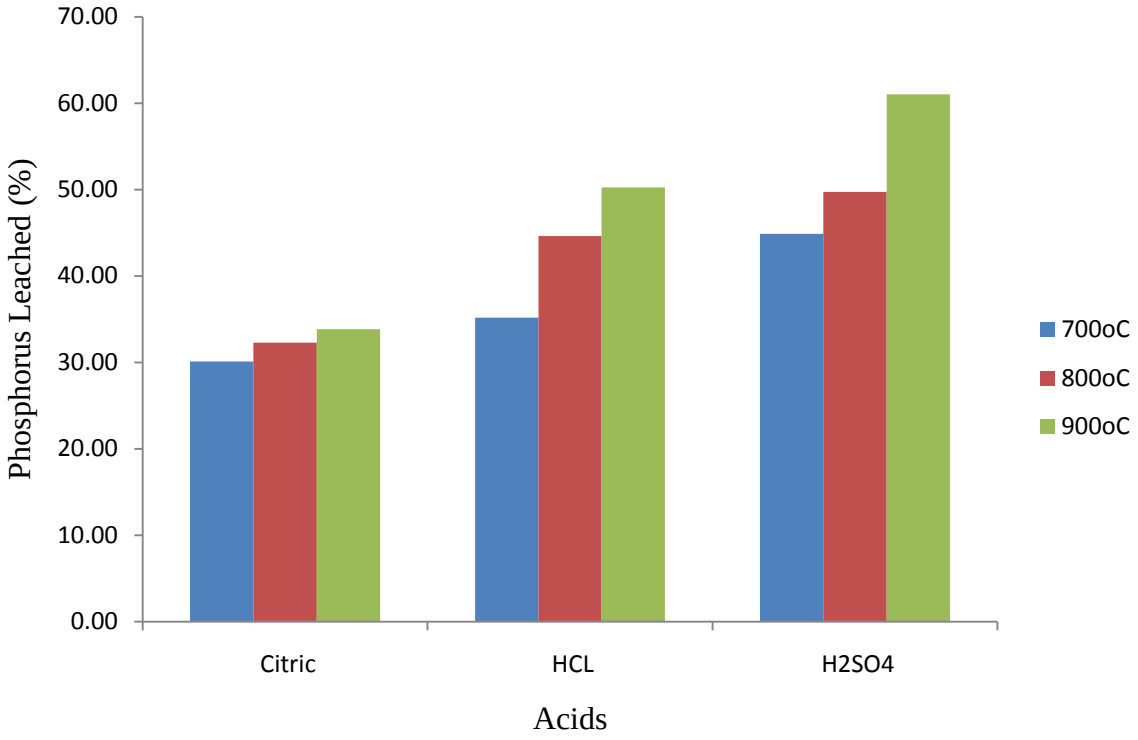


Figure 4.22: Effects of different acids on the leaching of -355 +250µm particle size with the optimum leaching concentration after calcinations.

Table 4.26: Results of leaching the -180 +125µm particle size with the optimum leaching conditions after calcination.

	Citric	**HCL**	**H_2SO_4**
700°C	31.89	37.84	49.19
800°C	32.43	46.49	60.54
900°C	35.14	57.30	73.51

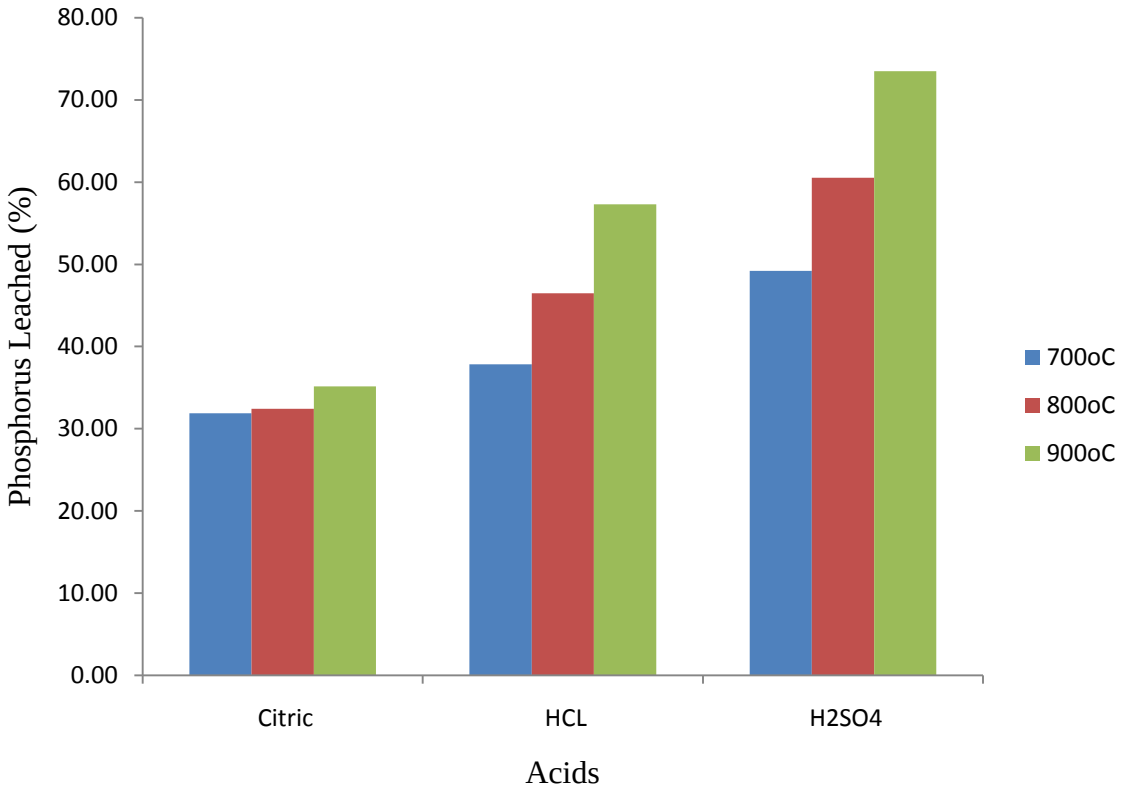


Figure 4.23: Effects of different acids on the leaching of -180 +125µm particle size with the optimum leaching concentration after calcinations.

4.11 COMPARISON OF OPTIMUM LEACHING CONDITIONS.

Table 4.27 and Figure 4.24 show the results for the comparison of the optimum leaching condition before and after calcinations at different temperatures.

Table 4.27: Summary of optimum leaching conditions for the various particle sizes.

ACID AND PHOSPHORUS LEACHED (%)						
	CITRIC		HYDROCHLORIC		SULPHURIC	
	-355 +250	-180 +125	-355+255	-180+125	-355+255	-180+125
Initially	27.27	29.73	33.84	35.13	41.41	45.4
Calcined at 700°C	30.1	31.89	35.2	37.84	44.9	49.19
Calcined at 800°C	32.31	32.43	44.62	46.49	49.74	60.54
Calcined at 900°C	33.85	35.14	50.26	57.3	61.03	73.51

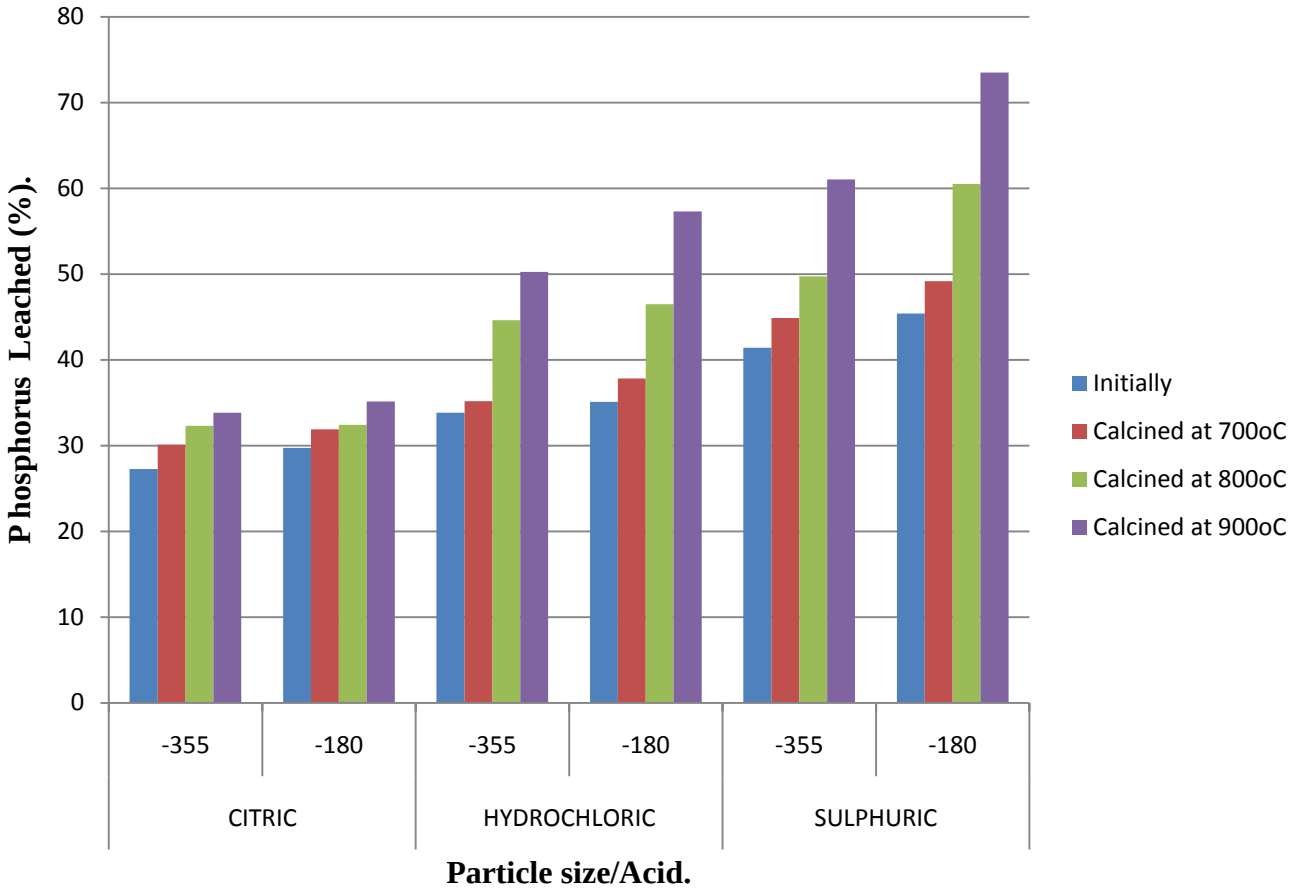


Figure 4.24: Comparative chart for various optimum leaching conditions with different acids and particle sizes before and after calcination.

4.12 DETERMINATION OF LOSSES TO THE LEACH SOLUTION.

Tables 4.28 – 4.30 show the results of inductive coupled plasma optical emission spectroscopy (ICPOES) analysis, carried out on the acids before and after leaching to determine the amount of losses to the solution after leaching with optimum concentrations for -180 +125µm particle size.

Table 4.28: ICPOES analysis of Citric acid before and after leaching at optimum leaching concentration.

	Concentration (mg/l)			Percentage(%)	
	Before	After	Cal @ 900	After	Cal @ 900
Al	0.0257	85.774	96.836	0.0089	0.0097
Fe	3.0625	14.4779	17.639	0.0011	0.0015
Mn	1.1998	4.4109	6.631	0.0003	0.0005
Si	232.91	540.411	620.531	0.0308	0.0388
Pb	0.1416	0.5568	0.6201	4.2×10^{-5}	4.8×10^{-5}
Co	0.4384	0.5293	0.5861	9.1×10^{-6}	1.5×10^{-5}
Ni	0.334	0.3575	0.4003	2.4×10^{-6}	6.6×10^{-6}

Table 4.29: ICPOES analysis of Hydrochloric acid before and after leaching at optimum leaching concentration.

	Concentration (mg/l)			Percentage(%)	
	Before	After	Cal @ 900	After	Cal @ 900
Al	0.0691	603.784	724.916	0.0604	0.0725
Fe	3.3087	282.132	392.315	0.0279	0.0389
Mn	1.2075	25.006	28.781	0.0024	0.0028
Si	102.139	2995.57	3669.07	0.2893	0.3567
Pb	0.0696	1.6595	2.0162	1.6×10^{-4}	2.0×10^{-4}
Co	0.4388	1.0511	1.1123	6.1×10^{-5}	6.7×10^{-5}
Ni	0.266	0.3617	0.4113	9.6×10^{-6}	1.5×10^{-5}

Table 4.30: ICPOES analysis of Sulphuric acid before and after leaching at optimum leaching concentration.

	Concentration (mg/l)			Percentage(%)	
	Before	After	Cal @ 900	After	Cal @ 900
Al	0.7962	467.61	526.724	0.0467	0.0526
Fe	3.1892	110.189	195.513	0.0107	0.0195
Mn	1.2052	16.0269	21.0346	0.0015	0.00198
Si	216.21	2442.49	2891.68	0.2226	0.2675
Pb	0.0268	0.0738	0.0839	4.7×10^{-6}	5.7×10^{-6}
Co	0.4299	0.8006	0.9107	3.7×10^{-5}	4.8×10^{-5}
Ni	0.2502	0.346	0.4231	9.6×10^{-6}	1.7×10^{-5}

4.13 DETERMINATION OF THE pH VALUES OF ACIDS BEFORE AND AFTER LEACHING

Tables 4.31 – 4.34 show the pH values for the acids before and after leaching for -355 +250 and -180 +125µm particle sizes.

Table 4.31: pH values of acid before and after initial leaching at optimum conditions for -355 +250µm particle size. (19.3^{o}C)

	Before	After
Citric	1.7	1.74
Hydrochloric	0.31	0.24
Sulphuric	0.7	0.76

Table 4.32: pH values of acid before and after Initial leaching at optimum conditions for -180 +125µm particle size. (2.17 ^{o}C)

	Before	After
Citric	1.45	1.51
Hydrochloric	0.48	0.42
Sulphuric	0.51	0.59

Table 4.33: pH values of acid before and after leaching at optimum conditions for -355 +250µm particle size after calcinations at 900^{o}C. (2.17 ^{o}C)

	Before	Cal @ 900
Citric	1.45	1.69
Hydrochloric	0.48	0.27
Sulphuric	0.51	0.61

Table 4.34: pH values of acid before and after leaching at optimum conditions for -180 +125µm particle size after calcinations at 900^{o}C.. (2.17 ^{o}C)

	Before	Cal @ 900
Citric	1.45	1.74
Hydrochloric	0.48	0.24
Sulphuric	0.51	0.63

4.14 KINETICS OF LEACHING.

4.14.1 Determination of rate constants (k) and the Activation energy (E_a) for the optimum leaching conditions.

Tables 4.35 – 4.37 show the rate constants (k) and the Activation energy (E_a) for the optimum leaching conditions with the various acids and particle sizes.

Table 4.35: The rate constants (k) and the Activation energy (E_a) for Citric Acid as a leachant

	-355 +250		-180 +125	
	k	Ea (KJ/mol)	k	Ea (KJ/mol)
Initially	5.0345×10^{-3}	13.34	5.5473×10^{-3}	13.09
Cal. at 700°C	5.6254×10^{-3}	13.05	6.0075×10^{-3}	12.85
Cal. at 800°C	6.0981×10^{-3}	12.85	6.1240×10^{-3}	12.84
Cal. at 900°C	6.4335×10^{-3}	12.71	6.7185×10^{-3}	12.6

Table 4.36: The rate constants (k) and the Activation energy (E_a) for Hydrochloric Acid as a leachant

	-355 +250		-180 +125	
	k	Ea (KJ/mol)	k	Ea (KJ/mol)
Initially	1.2607×10^{-4}	32.62	1.3692×10^{-4}	32.41
Cal. at 700°C	1.375×10^{-4}	32.4	1.6151×10^{-4}	32
Cal. at 800°C	2.3463×10^{-4}	31.05	2.5797×10^{-4}	30.82
Cal. at 900°C	3.0964×10^{-4}	30.36	4.2459×10^{-4}	29.56

Table 4.37: The rate constants (k) and the Activation energy (E_a) for Sulphuric Acid as a leachant

	-355 +250		**-180 +125**	
	k	Ea (KJ/mol)	k	Ea (KJ/mol)
Initially	2.9678×10^{-4}	30.46	3.6629×10^{-4}	29.93
Cal. at 700 °C	3.5705×10^{-4}	29.96	4.4149×10^{-4}	29.46
Cal. at 800 °C	4.5319×10^{-4}	29.4	7.3013×10^{-4}	28.19
Cal. at 900 °C	7.4508×10^{-4}	28.14	1.2183×10^{-3}	26.9

CHAPTER FIVE

5.0 DISCUSSION OF RESULTS.

5.1 X – Ray Fluorescent (XRF) analysis of Head sample.

From Table 4.1, the XRF analysis of the head sample shows that the major constituents of the iron ore include Fe_2O_3 – 67.02%, SiO_2 – 15.49%, Al_2O_3 – 13.76%, P_2O_5 – 1.81%, MnO – 0.41%, MgO – 0.41%, CaO – 0.26%, TiO_2 – 0.20% and others in trace. This is in line with initial reports by Astier et al (1988) and Uwadiale 1984.

5.2 X – Ray Diffraction (XRD) pattern of Head sample.

Figure 4.1 shows the XRD pattern of the head sample. The peaks show that the major iron bearing mineral is Goethite (FeO(OH)), Quartz (SiO_2), Alumina (Al_2O_3) and Berlinite ($AlPO_4$) with Magnetite (Fe_3O_4) and Hematite (Fe_2O_3) as minor constituents. The quantitative analysis using the Rietveld method in Table 4.2 shows among others that within the mineral phase Goethite constitutes 81.54% of the iron ore with 1.13% berlinite.

5.3 Scanning Electron Micrograph (SEM) of Head Sample.

Plate I shows the SEM image of the head sample with Energy Dispersion Spectroscopy (EDS) point analysis. The image shows the distribution of mainly Goethite and quartz as dark background while the white patches show Hematite and magnetite. The EDS point analysis carried out on the selected points on the SEM image is on Figure 4.2a – 4.2e. They all show the presence of Fe, Mg, P, Si, O, and K among others on most of the points analyzed.

Plates IIa – IIj show the SEM mapping for the various elements in the SEM image which confirms the presence of Fe, Al, Mg, P, Si, Mn, Ti, K, and Ca. This also confirms the initial results from XRF and XRD. Table 4.3 gives a summary of the counts for individual elements from the SEM showing the major constituents to be 54.29% - Fe, 15.93% - Al, 12.57% - Si, 1.24% - P, 0.51% - Ca, and 0.14% - Mg. within their weight percent error as presented.

5.4 X – Ray Fluorescent (XRF) analysis of the various particle sizes.

Table 4.4 shows the XRF analysis of the various particle sizes (+355, -355 +250, -255 +180, -180 +125, -125 +90, -90 +50, -50µm) considering the distribution of the major constituents: Fe_2O_3 has its highest value of 69.81% recorded on the -180 +125 µm followed by 67.73% recorded on -355 +250µm with the least value of 60.67% occurring on -90 +50µm. SiO_2 is distributed with minor fluctuations within the particle sizes. Its highest value of 17.33% is found on -250 +180µm particle size while the least value of 13.69% occurs with -120 +90µm sizes. The distribution of Al_2O_3 increases as the particle size decreases with 11.76% at +355µm to 18.44% for -50µm. The distribution of P_2O_5 within the iron ore varies slightly, its highest value of 1.98% occurs on -355 +250µm followed by 1.88% on -90 +50µm, then 1.85% for -180 +125µm. MgO, V_2O_5, and TiO_2 almost have uniform distribution within the particle sizes. This is in line with earlier research (Thomas 2008). Based on the distribution of the iron and phosphorus within the particle sizes, -355 +250µm and -180 +125µm particle sizes were selected for leaching. Particle size of -355 +250µm containing the highest amount of P_2O_5(1.98%) is selected to allow maximum exposure of phosphorus to the

leaching condition, while -180 +125µm was selected to investigate the effect of particle size on the leaching with respect to the highest distribution of iron (69.81%) which is also the liberation size as earlier reported elsewhere (Thomas 2008).

5.5 X – Ray Diffraction (XRD) pattern of the selected particle sizes.

Figures 4.3 and 4.5 show the XRD peaks for the selected particle sizes (-355 +250µm and -180 +125µm) respectively. Both figures show the presence of Goethite (FeO(OH)) as the major iron bearing mineral, while Magnetite (Fe_3O_4) and Hematite (Fe_2O_3) are minor constituents. It also shows the presence of Quartz (SiO_2) and Berlinite ($AlPO_4$). This line with the analysis from the head sample.

Table 4.5 shows the quantitative analysis for -355 +250µm particle size given by the reitveld method. It reveals 81.01% Goethite within the iron content with 3.17% Hematite and 0.72% Magnetite as minor constituents while 13.87% Quartz and 1.25% Berlinite are also present. Table 4.7 for -180 +125µm particle size given by the reitveld method shows that the mineral phase contains 82.19% Goethite, 3.32% Hematite, 0.72% Magnetite with 12.61% Quartz and 1.18% Berlinite.

5.6 Scanning Electron Microscopy (SEM) image of the selected particle sizes.

Plates III and V show the SEM of -355 +250µm and -180 +125µm particle sizes respectively with selected points of EDS Point analysis. They both show mainly a dark background of Quartz and Goethite with white patches of hematite and magnetite. Figures 4.4a – 4.4e and Figure 4.6a – 4.6e show the EDS point analysis of -355 +250µm and -180 +125µm particle sizes respectively. These

show the presence of Fe, Mg, P, Si, O, and Al with Fe presenting the highest count in both samples.

Plates IVa – IVj show the mapping for the individual elements in the SEM image which confirms the presence of Fe, Ca, Al, Si, P, Mg, and Mn as also given by other analysis. Table 4.6 gives a summary of the count of the individual elements on SEM for -355 +250µm particle size as 59.70% Fe, 18.76%Al, 14.78%Si, 1.60%Ca, and 3.83%P. Table 4.8 gives a summary of the count of the individual elements on SEM for -180 +125µm particle size as 61.76% Fe, 18.80%Al, 15.46%Si, 0.7%Ca, and 1.95%P all within their various percent weight errors as presented in the tables.

5.7 Distribution of phosphorus within the head sample and the selected particle sizes for leaching.

From the XRF result on Table 4.1, the head sample contains 1.81%-P_2O_5 (0.79%-P). From Table 4, -355 +250 particle size contains 1.98%-P_2O_5 (0.8644%-P) and -180 +125 particle size contains 1.85%-P_2O_5 (0.8177%-P). Figure 4.1 and Table 4.2 show the XRD peaks and rietveld estimation for the head sample and reveals that the head sample contains 1.13%-$AlPO_4$ (0.281%-P) which constitutes 36.33% of the total phosphorus (P) in the head sample. For -355 +250 particle size, Figure 4.3 and Table 4.5 reveal 1.25%-$AlPO_4$ (0.3176%-P) which constitutes 36.74% of the total phosphorus (P) in this particle size. -180 +125 particle size (Figure 4.5 and Table 4.7) indicated 1.18%-$AlPO_4$ (0.2997%-P) which constitutes 36.65% of the total phosphorus (P) in this particle size. From the above, it

concluded that 36.33%-P, 36.74%-P and 36.65%-P are contained in the $AlPO_4$ phase for the Head sample, -355 +250µm and -180 +125µm particle size respectively, while 63.67%-P, 63.26%-P and 63.35%-P are contained in the iron phase in solid solution with Goethite for the Head sample, -355 +250µm and -180 +125µm particle size respectively. This helps to explain the almost uniform distribution of phosphorus within the various particle sizes as observed in Table 4.4.

5.8 LEACHING OF -355 +250µm PARTICLE SIZE.

5.8.1 Variation of Agitation on leaching of -355 +250µm particle size.

The leaching of -355 +250µm particle size was carried out in various stages. The first stage was to investigate the effect of variation of agitation. The agitation was varied from 100 – 500prm at constant time of one (1) hour, temperature of 30^{o}C and 0.3M acid concentration for sulphuric acid while 0.5M concentration was used for hydrochloric and citric acid.

Table 4.9 and Figure 4.7 show the effect of the variation of agitation on the amount of phosphorus leached for the three acids used. For sulphuric acid the least percentage of phosphorus leached (10.10%) is obtained at 100rpm while the highest phosphorus leaching (23.75%) is obtained at 500rpm. With Hydrochloric acid, the least amount of phosphorus leached was obtained at 100rpm (8.08%) while the best phosphorus leaching (20.70%) was obtained at 300rpm, while with citric acid the phosphorus leaching of (6.51%) was least at 200rpm and the highest leaching of phosphorus (19.7%) was obtained at 400rpm. Figure 4.7

shows the result clearly from which sulphuric acid gave the best leaching rate at 500rpm, hydrochloric at 300rpm and citric at 400prm. This is in line with earlier reports by Jin Yong-shi et al 2006. They reported that when the speed exceeds the optimum revolution the phosphorus extraction decreases. That is because the iron ore samples are fine ground, and they could be easily driven by the whirlpool of the leaching solution at high speed of agitator, and in this way, the relative refresh velocity of the leaching solution on the surface of the ore particles decreases.

5.8.2 Variation of Temperature on leaching of -355 +250µm particle size.

The effect of the variation of temperature on the leaching of -355 +250µm particle size was the second stage of the leaching. The temperature was varied from 30 – 80^{o}C at an interval of 10 ^{o}C and a constant time of one (1) hour and concentration of 0.3M with agitation of 500rpm for sulphuric acid, 0.5M concentration 300rpm for hydrochloric acid and 0.5M concentration, 400rpm for Citric acid.

Table 4.10 and Figure 4.8 show the result for the variation of temperature on the phosphorus leaching for the three acids used. From the results all the acids perform better at 30^{o}C with phosphorus leaching of 23.74% for sulphuric acid, 20.71% for hydrochloric acid and 19.7% for citric acid. The phosphorus leaching drops as the temperature increases and can be clearly seen in Figure 4.8. This is in line with initial reports (Xia et. al 2011).

5.8.3 Variation of Concentration and time on leaching of -355 +250µm particle size.

The effect of the variation of concentration and time on the leaching of -355 +250µm particle size is the third stage of the leaching. It involved the variation of time from 20 – 120minutes on an interval of 20mins and concentration from 0.15 – 1.2M for sulphuric acid and 0.5 – 2.5M concentration for Hydrochloric and Citric acid. The leaching was carried out at constant temperature of 30^{o}C, and agitation of 500, 300, and 400rpm for sulphuric, hydrochloric and citric acid respectively as earlier established.

Tables 4.11 – 4.13 and Figures 4.9 – 4.11 show the effects of variation of time and concentration on the selective leaching of phosphorus with sulphuric, hydrochloric and citric acid respectively from the iron ore. The result shows clearly on Figure 4.9 that the best leaching rate was obtained at 0.9M concentration at a time of 80minutes with Sulphuric acid . Figure 10 shows that the best leaching rate is obtained after 120minutes with 2.0M Concentration of Hydrochloric acid, while Figure 4.11 reveals the best leaching condition at 0.5M concentration at a time of 20minutes when leaching with Citric acid. The results obtained were recorded as the optimum leaching conditions and summarized in Table 5.1

Table 5.1: The developed optimum leaching conditions for the selective leaching of Phosphorus from -355 +250 particle size of the Koton-karfe iron ore.

ACIDS	CONDITIONS			
	Temp. (^{o}C)	Conc. (M)	Time (mins)	Agitation (rpm)
Sulphuric	30	0.9	80	500
Hydrochloric	30	2.0	120	300
Citric	30	0.5	20	400

5.9 FACTORIAL DESIGN FOR THE LEACHING RATE OF -355 +250 PARTILE SIZE AND THE VARIOUS ACIDS USED.

Tables 4.14 – 4.16 show the experimental design layout and response data for the leaching rate of the various acids from which the analysis of variance (ANOVA) was used to determine the design parameters which significantly affect the leaching rate (response) under certain conditions. Tables 4.17 – 4.19 show the ANOVA results for the various acids used.

The last column of Tables 4.17 – 4.19 show the contribution (P) of each parameter (time and concentration) on the response (leaching rate). It is observed from Table 4.17 for sulphuric acid that the time (A) with a value of 1812.09 was the most significant parameter having the highest statistical influence on the leaching rate then followed by the concentration (B) having a value of 118.43. From Table 4.18, hydrochloric acid concentration (B) has the highest statistical influence with a value of 4383.54 followed by time (A) with a value of 135.14.

However the influence of both time and concentration is very minimal 1.53 and 0.58 respectively with Citric acid as seen on Table 4.19. These effects can be seen clearly on figures 4.12 - 4.14 (maps).

The model statistical influence (F-value) of 965.26 and 2259.34 for sulphuric and hydrochloric acid respectively implies that the models are significant. With only 2.28% chance for sulphuric acid and 1.49% chance for hydrochloric acid that model values this high can occur due to error. The model F-value of 1.06 for citric acid implies the model is not significant relative to error, there is a 56.66% chance that a model F-value this large could occur due to error.

Contribution (P) values less than 0.0500 indicates that model terms are significant while P values greater than 0.1000 indicates that the model terms are not significant. From Tables 4.17 and 4.18 for sulphuric acid with P values of 0.0150 for time and 0.0583 for concentration and hydrochloric acid with P values of 0.0546 for time and 0.0096 for concentration respectively show that both model terms are significant. From Table 4.19 for citric acid, the P values value of 0.4324 for time and 0.5854 for concentration show that the model terms are not significant.

The regression coefficient (R^2) calculated is 0.9917 (99.17%) for sulphuric acid, 0.8987 (89.87%) for hydrochloric acid, and 0.0231 (2.31%) for citric acid. When R^2 approaches unity, a better response model results and it fits the actual data. From R^2 for sulphuric acid and that for hydrochloric acid it indicates an adequate signal, which shows that the model can be used to navigate the design space. The ratio of 2.31% for citric acid indicates an inadequate signal, hence the model

should not be used to navigate the design space. This supports the attainment of the optimum leaching condition within the navigation for hydrochloric and sulphuric acid. Navigation within the conditions of citric acid does not yield any better result as predicted by the model.

Based on these validations by the ANOVA, the optimum conditions obtained from the -355 +250µm particle size were used for further leaching.

5.10 Leaching of -180 +125 particle size

The developed leaching conditions were used to leach -180 +125µm particle size with all the acids under investigation. Table 4.20 and Figure 4.15 show the results. They reveal that 45.40%, 35.13% and 29.73% leaching of phosphorus is obtained with sulphuric, hydrochloric and citric acid respectively. This shows an improvement from what was recorded from the leaching of -355 +250µm particle size (41.41% for Sulphuric, 33.84% for Hydrochloric and 27.27% for citric acid). The improvement in selective leaching of phosphorus with the -180 +125µm particle size is attributed to the increase in surface area which aids the exposure of more mineral to the leach liquor and therefore increases the leaching of phosphorus.

5.11 CALCINATION OF THE IRON ORE

The selected particle sizes for leaching (-355 +250µm and -180 +125µm) were calcined at 700, 800, and 900^{o}C. Table 4.21 and 4.22 show the XRF results for -355 +250µm and -180 +125µm particle sizes respectively. From both tables it is

observed that the major constituents still remain Fe_2O_3, SiO_2, Al_2O_3 and P_2O_5, while P_2O_5, MnO and MgO are still uniformly distributed within the particle sizes.

5.12 XRD results after Calcination.

Figures 4.16 – 4.18 show the XRD results for -355 +250µm particle size after calcinations. They reveal basically Quartz and Hematite and Table 4.23 shows the rietveld relative phase estimation for the various calcination temperatures. It shows that at 700 and 800 ^oC the hematite content is almost the same (84.33 and 84.3) but at 900^oC the hematite content rises to 86.73%.

Figures 4.19 – 4.21 show the XRD pattern for -180 +125µm particle size after calcinations. It also reveals basically Quartz and Hematite. Table 4.24 shows the rietveld relative phase estimation and shows that the Hematite content increases from 84.9% at 700 ^oC to 87.49% at 800 ^oC and to 88.39% at 900 ^oC.

The transformation of the major iron bearing mineral from Goethite to Hematite is as a result of the dissociation of Goethite at high temperature by the reaction:

$$2FeOOH = Fe_2O_3 + H_2O_{(g)} \qquad 5.1$$

which also liberates the phosphorus in an acid soluble compound. Several acid soluble compounds are possible, including magnesium phosphate, manganese phosphate and aluminium phosphate (Dukino 1997). The chemical analysis of the ore indicated the formation of aluminium phosphate as shown in equation 5.2 below

$$2(FeO)_3PO_4 + Al_2O_3 = 2AlPO_4 + 3Fe_2O_3 \quad 5.2$$

This is in line with earlier reports by Dukino 1997 and Cheng et al 1999.

5.13 LEACHING OF CALCINED IRON ORE.

Table 4.25 and Figure 4.22 show the result obtained from leaching the calcined -355 +250µm particle size with Citric, Hydrochloric and Sulphuric acid with the optimum leaching conditions developed for the acids. Table 4.25 shows that with citric acid, there is little difference in leaching rate from 30.10% at 700^{o}C to 33.85% at 900^{o}C. Hydrochloric acid gives a leaching rate of 35.20% for 700^{o}C which increases to 44.62% for 800^{o}C and finally to 50.26% for 900^{o}C. For sulphuric acid it is 44.90% leaching rate for 700^{o}C, 49.74% for 800^{o}C and 61.03% for 900^{o}C. This variation is can be observed in Figure 4.22.

Table 4.26 and Figure 4.23 show the result of leaching the calcined -180 +125µm particle size with the optimum leaching conditions developed for the acids. For Citric acid the leaching improves from 31.89% for 700 to 35.14% for 900. Hydrochloric acid shows a leaching rate of 37.84% for 700 to 46.49% for 800 and 57.30% for 900. Sulphuric acid shows a leaching rate of 49.19% for 700 to 60.54% for 800 and finally 73.51% for 900. The increase is clearly observed in Figure 4.23.

The increase in the selective leaching of phosphorus from the iron ore after calcination is attributed to the dissociation of Goethite to Hematite which also leads to the release of phosphorus initially in solid solution with Goethite since phosphorus is less soluble in hematite than in goethite, liberating the phosphorus

in acid soluble form. Also after calcination, there is a conspicuous increase in micropores of the iron ore thereby increasing the interfacial contact area for the acid, and enhancing the removal of phosphorus. This is in line with earlier reports (Lenintov et. al, 2007 and Peixoto 1991).

5.14 COMPARISON OF OPTIMUM PHOSPHORUS LEACHED FOR THE VARIOUS PARTICLE SIZES AND THE ACIDS USED.

Table 4.27 and Figure 4.24 show clearly the summary and comparison of the optimum phosphorus leached for the particle sizes respectively with the various acids used for leaching. These show clearly with all the acids (Citric, Hydrochloric and Sulphuric) that there is an improvement on the leaching rate of P with variation of particle size (i.e from -355 +250 to -180 +125µm). This variation is attributed to the fact that with -180 +125µm particle size there is an increase in the surface area thereby increasing the rate of contact between the acid and the particles of the ore, hence increasing the leaching of phosphorus.

From Table 4.27 it is seen that initially citric and hydrochloric acid leached 27.27 and 38.84% P for -355 +250µm particle size and 29.73 and 35.13% P for -180 +125µm particle size respectively. Therefore it is concluded that initially, citric and hydrochloric acid could only leach phosphorus associated with the $AlPO_4$ phase. Sulphuric acid was only able to leach a little out of the P associated with the Goethite phase, with 41.41% P leached with -355 +250µm particle size (i.e 4.6% above 36.74%P in $AlPO_4$) and 45.40% P leached with -180 +125µm particle size (i.e 8.75% above 36.65% P in $AlPO_4$).

On calcination at 700, 800 and 900^{o}C the leaching rate of the acids improved. Citric acid had the least increase in leaching rate from 27.27% initially to 33.85% after calcination at 900^{o}C for the -355 +250µm particle size and from 29.73% to 35.14% after calcinations at 900^{o}C for the -180 +125µm particle size. Hydrochloric acid with phosphorus leaching increasing from 33.84% initially to 50.26% after calcination at 900^{o}C for the -355 +250µm particle size and from 35.13% to 57.30% after calcination at 900^{o}C for the -180 +125µm particle size. Sulphuric acid showed the best results with phosphorus leaching increasing from 41.41% initially to 61.03% after calcinations at 900^{o}C for the -355 +250µm particle size, and equally from 45.40% to 73.51% after calcination at 900^{o}C for the -180 +125µm particle size. The general improvement in leaching could be associated with increase in microporosity associated with the iron ore after calcination and the structural rearrangement associated with the dissociation of goethite and liberation of P which enhances the leaching ability of the acid.

5.15 IONISATION OF ACIDS USED FOR LEACHING

The ionisation of the acids used for leaching shows that sulphuric acid is dibasic i.e it can donate two moles of protons per mol of acid, while hydrochloric acid is monobasic and citric acid tribasic. See equation 5.3 – 5.5

$$H_2SO_4 \rightarrow 2H^+ + SO_4^{2-} \qquad 5.3$$

$$HCl \rightarrow H^+ + Cl^- \qquad 5.4$$

$$C_6H_8O_7 \rightarrow 3H^+ + C_6H_5O_7^{3-} \qquad 5.5$$

5.16 EQUATIONS OF REACTIONS.

$$2AlPO_{4(s)} + 3H_2SO_{4\,(aq)} \rightarrow Al_2(SO4)_3 + 2H_3PO_{4(aq)} \quad 5.6$$

$$AlPO_{4\,(s)} + 3HCl_{(aq)} \rightarrow AlCl_{3\,(aq)} + H_3PO_{4(aq)} \quad 5.7$$

$$AlPO_{4(s)} + C_6H_8O_{7(aq)} \rightarrow (C_6H_5O_7)Al_{(aq)} + H_3PO_{4(aq)} \quad 5.8$$

Equation 5.6 shows that three (3) moles of sulphuric acid react with two (2) moles of aluminum phosphate, while equation 5.7 shows 3 moles of hydrochloric acid react with one mole of aluminum phosphate and 5.8 and shows 1 mole of citric acid reacts with one mole of aluminum phosphate. This explains why sulphuric acid leaches phosphorus better than hydrochloric acid even though they are both strong mineral acids while citric acid though tribasic, is a weak organic acid and leached the least amount of phosphorus.

5.17 DISSOLUTION OF IRON DURING LEACHING.

Tables 4.28 – 4.30 show the ICPOES analysis for the -180 +125µm particle size which shows the dissolution of elements in the various acids during the initial leaching and leaching after calcination at 900^{o}C. The results revealed that the major elements dissolved in the acids are Si, Al, and Fe while other elements Mn, Pb, Co, and Ni are dissolved in negligible amount. For Citric acid on Table 4.28 it revealed the dissolution of 0.031%Si, 0.009%Al, and 0.001%Fe initially and 0.039%Si, 0.010%Al, and 0.0015%Fe after calcination at 900^{o}C. The result for

hydrochloric acid on Table 4.29 revealed that 0.29%Si, 0.06%Al, and 0.028%Fe is dissolved initially and 0.357%Si, 0.073%Al, and 0.039%Fe is dissolved after calcinations. Table 4.30 for sulphuric acid reveals dissolution of 0.22%Si, 0.047%Al, and 0.011%Fe initially and 0.27%Si, 0.047%Al, and 0.02%Fe after calcinations at 900^{o}C. This indicates that the highest amount of Si and Iron dissolved are associated with Hydrochloric acid followed by sulphuric and then citric acid. The high dissolution of Silicon associated with hydrochloric and sulphuric acid is confirmed by the observation of the formation of a light grey jelly like substance which is suspected to be amorphous colloidal silicon in the course of leaching at higher concentration of these acids and it is noticed more with hydrochloric acid than sulphuric acid. Hence the dissolution of iron associated with sulphuric acid at optimum leaching condition is said to be minimal.

5.18 pH VALUES OF ACID AFTER LEACHING.

Tables 4.31 – 4.34 show the pH values of the acids before and after leaching. They reveal that the amount of acid used up for the leaching of the -180 +125µm is more than that used for the -355 +250µm and the leaching of the -180 +125µm after calcination gives the most expended acid. This is in line with the initial results obtained from Table 4.27. From the pH values it can therefore be concluded that minimum amount of sulphuric acid is used up for leaching. Therefore the used up acid can be treated to reclaim the sulphuric acid and can be recycled.

5.19 KINETICS OF LEACHING.

5.19.1 The rate constant (k) and the Activation energy (E_a) for the optimum leaching conditions.

The rate constant (k) and Activation energy (E_a) were calculated from equations 3.3 – 3.5 and as modified elsewhere (Olanipekun 2000 and Sultana et al 2012).

Tables 4.35 – 4.37 show the results of rate constant (k) and the Activation energy (E_a). The results show a reduction in activation energy with decrease in particle size and increase in calcination temperature. Table 4.35 shows that the result for citric acid, E_a decreases from 13.34 to 13.09KJ/mol for -355 +250µm particle size and -180 +125µm particle size initially. After calcination at 900^{o}C and leaching, E_a decreases from the initial value to 12.71 and 12.6KJ/mol for -355 +250µm particle size and -180 +125µm particle sizes respectively. Table 4.36 shows the result for Hydrochloric acid, where an initial decrease is observed from 32.62 to 32.41KJ/mol for -355 +250µm particle size and -180 +125µm particle sizes respectively and then further decreases from the initial values to 30.36 and 29.56KJ/mol for -355 +250µm particle size and -180 +125µm particle sizes respectively after calcination at 900^{o}C and leaching. From Table 4.37 for Sulphuric acid a decrease from 30.46 to 29.93KJ/mol is observed initially for -355 +250µm particle size and -180 +125µm particle sizes respectively and a further decrease from the initial values to 28.14 and 26.91KJ/mol for -355 +250µm particle size and -180 +125µm particle size after calcination at 900^{o}C and leaching.

From the results of Ea it is concluded that leaching with citric acid for both particle sizes is diffusion controlled. This means that the chemical reaction at the interface is much faster than the diffusion, this also confirms the attainment of the optimum leaching condition time of 20minutes. Leaching with hydrochloric and sulphuric acid is intermediate controlled (i.e both chemical and diffusion controlled, which implies the chemical reaction on the particle surface is approximately the same rate as the diffusion) in line with Habashi (1999). This explains why leaching with sulphuric and hydrochloric acid takes a longer time to attain the optimum phosphorus leaching from the Iron ore.

The decrease in activation energy with increase in calcination temperatures and phosphorus leaching rate confirms the dissociation of goethite to hematite, and the structural transformation that leads to increase in the amount of phosphorus leached with decrease in activation energy.

5.20 ACID CONSUMPTION COST

The acid consumption for leaching using 0.9M sulphuric acid was approximately 192litres/tonne, 680litres/tonne of ore using 2.0M hydrochloric acid and 452Kg/tonne of ore leaching with 0.5M citric acid. The cost of acid consumption is N192,000/tonne, N544,000/tonne, N452,000/tonne of ore using sulphuric, hydrochloric and citric acid respectively. It shows clearly that sulphuric acid is also the cheapest acid for leaching. With a treatment plant to enable recycle of sulphuric acid the cost of acid will even be cheaper.

CHAPTER SIX

6.0 CONCLUSIONS AND RECOMMENDATIONS

6.1 Conclusions

From the analysis and discussions of the results of characterization and leaching of the iron ore the following conclusions are drawn:

1). The ore contains Quartz, Alumina, Goethite, phosphorus as major constituent with Magnetite, hematite and other compounds in minor amounts. The head sample of the ore has a total iron content of 46.91%Fe (67.02% Fe_2O_3).

2). Some of the Phosphorus in the iron ore occur in the form of berlinite ($AlPO_4$) in a separate phase while most of the phosphorus is present in solid solution with Goethite, and is almost uniformly distributed within the various particle sizes.

3). The optimum leaching conditions prior to calcination for the removal of phosphorus for all the three acids were attained at the particle size fraction -180 +125µm at which 45.40, 35.13 and 27.73% phosphorus removal rate for sulphuric, hydrochloric and citric acids were attained respectively.

4). After calcination at 900^{o}C and leaching at the optimum conditions, phosphorus removal rate of 73.51%, 61.03%, 35.14% were obtained for sulphuric, hydrochloric and citric acids respectively at particle size fraction -180 +125µm .

5). Calcinations of the iron ore at 700, 800 and 900^{o}C converted the Goethite in the ore to hematite and caused a structural rearrangement thereby partially releasing the phosphorus contained in solid solution with Goethite.

6). The kinetic study results reveal that leaching with Citric acid is a diffusion controlled process while leaching with hydrochloric and sulphuric acid are intermediate controlled processes before and after calcination of the ore.

7). Sulphuric acid proved to be the best acid for the leaching of phosphorus from the iron ore resulting in the removal of 73.51% of the total phosphorus content in the ore thereby reducing Phosphorus contained in the ore from 0.81% P to 0.21% P at -180 +125µm particle size fraction.

8). The iron that dissolved in the leach solution is minimal 0.011% and 0.02% of the total Fe before and after calcinations of the ore at 900^{o}C respectively and leaching with sulphuric acid.

6.2 RECOMMENDATIONS.

It is recommend that:

1). Scrubbing and leaching of the iron ore and a study of the chemical reactions that occur in the course of leaching and how they can be possibly modified, i.e possible use of catalyst to improve the selective leaching of phosphorus, should be investigated.

2). Thermochemical cyclic leaching of the Koton-karfe iron ore to investigate the effect of this method on the selective leaching of phosphorus should also be investigated.

3). Investigation into the possible pressure and vacuum leaching of the Koton-karfe iron ore should be carried out.

4). The effect of temperatures less than $30^{o}C$ on the leaching condition should also be investigated.

REFERENCES

Also A. K and Yakubu N. A (1995): Local raw materials for steel production: The case of Ajaokuta. Proceeding of the second National Engineering Conference, Kaduna, Pp 16 – 22.

Amadi, N. J., Odunaike, A. A., and Mathur, G. P.,(1983): Preliminary bench scale beneficiation studieswith three lumps of Iron ore samples from Agbaja. Central Metallurgical Research and Development Institute, Research Report. 17pp.

Anyakwo, C. N., and Obot, O. W.. (2008):Phosphorus removal from Nigeria's Agbaja Iron Ore by Aspregillus niger. International Research Journal in Engineering Science and Technology. Vol. 5(1), Pp54 – 58.

Astier .J.E., Donzeau. M and Uwadiale .G.G.O.O. (1989): The lokoja Oolitic ironstone deposit: Possible use in the Ajaokuta iron and steel plant. Journal of mining and geology. Vol. 25. No 1. Pp 111 – 120.

Ates, S., Dingil, N., Bayraktar, E., Mehmetoglu, U., 2002:Enhancement of citric acid production by immobilized and freely suspended Aspergillus niger using silicone oil. Proceedings of Biochemistry 38, 433 - 436.

Baba, A.A, Adekola, F.A and Folashade, A.O. (2005). Quantitative Leaching of a Nigerian Iron Ore in Hydrochloric Acid: Journal of Applied Sciences and Environment Management, 9(3), 15 – 20.

Babich. A, Senk. D, Gudenau. H. W and Mavrommatis. K . Th. (2008):Ironmaking Textbook. Die Deustech Publikation in der Deutschen.

Barbour, A. R (1973): Distribution of phosphorus in iron ore deposit of Itabira, Minas Gerais, Brazil. Economic Geology. Vol 68 Pp 1 – 5.

Belikov,V.V.,Ogorodov,V.B.,Yadryshnikov,A.O., and Mikhailovina, N.A. (2003): Dephosphorisation of Brown iron ores concentrates. Obogashchenie Rud, No.3 Pp. 8 – 12.

Braithwaite .A .C., Eaton .A .C, and Groom .P .S (1990): Factors affecting the solubility of phosphate rock residue in 2% citric acid and 2% formic acid. Fertilizer research 23; 37 – 42.

BRGM NIG LTD. (1983): Preliminary Geological Reconnaisance survey, interim Report I, Submitted to the office of the Executive President Steel Development Department. (Re; Contract for survey of the Agbaja-Lokoja-Koton karfe-Bassa Nge Iron ore Deposits) 32pp.

Burkin, A.R. (1986). The Chemistry of Hydrometallurgical Processes, London: E and F.N.

Cheng .C.Y., Mishra .V.N., Clough .J. and Mun .R (1999): Dephophorization of western Australian iron ore by hydrometallurgical process. Minerals Engineering, Vol 12, No. 9, Pp 1083 – 1092.

Chenier, Philip J. (1987). Survey of Industrial Chemistry. New York: John Wiley & Sons. pp. 45–57. ISBN 0-471-01077-4.

Corbridge D.E.C. (1980): Phophorus: An Outline of Its Chemistry, Biochemistry and Technology (2nd ed). Amsterdam: Elsevier Scientific Publishing Company. Vol (2).

Davenport, William George and King, Matthew J. (2006). Sulfuric acid manufacture: analysis, control and optimization. Elsevier. pp. 8, 13. ISBN 978-0-08-044428-4.

Dennis W.H. (1983): Metallurgy of the Ferrous Metals. Sir Isaac Pitman and Sons Ltd. London.

Drouillon .M and Merckx .R (2003): The role of Citric acid as a Phosphorus mobilization mechanism in highly phosphorus fixing soils. Gayana Botanica 60(1): 55 – 62.

Dukino, R. D.(1997): Phosphorus in Hamersley range iron ore. BHP internal report.

Dukino, R. D., England, B.M., Kneeshaw, M., 2000: Phosphorous distribution in BIF-derived iron ores of Hamersley Province, Western Australia. Trans Instn Min Metall (Sect B: Applied Earth Science) 109, B168 – B176.

Famuboni, A. D. (1990): Sourcing of mineral raw materials for the Nigerian iron and steel Industries. Distinguished lecture programme, Department of mining Engineering and Applied Geology, College of Engineering Kaduna Polytechnic.

Feyza Cavus and Soner Kuslu (2005):Dissolution kinetics of colemanite in citric acid solutions assisted by mechanical agitation and microwaves. Industrial Eng. Chem. Res. Vol 44, Pp 8164 – 8170.

Forssberg R., Asolfsson G.(1981): Dephosphorization of high phosphorous iron ore by means of acid leaching. Erzmetal, (34) 316 – 322. English translation by BHP Central research laboratories, No. CRL/T 13278.

Frank H. Verhoff (2005), "Citric Acid", Ullmann's Encyclopedia of Industrial Chemistry, Weinheim: Wiley-VCH

Garba Ussma(1999):Research and Development efforts at NMDC Jos, towards arresting the decline fortunes of the Nigerian metallurgical Industry. 10th Annual Conference, Jos, Nigeria pp.14 – 16.

Ghosh Ahindra and Chartterjee Amit (2008): Ironmaking and Steelmaking theory and practice. Prentice-Hall of India Private limited, New Delhi.

Ghosh, A., Ray, H.S. (1991). Principles of Extractive metallurgy (2nd edition). New Delhi:

Gooden, J. E. A., Walker, W. M. and Allen, R. J.(1974): A chemical process for the dephosphorization of iron ore. Proceedings of National Chemical Engineering Conference, Queensland, 21 – 23.

Graham, J. (1973): Phosphorus in iron ore from the Hamersley formation. Proceedings of the Australian Institute of Mining and Metallurgy, No 246, 41 – 42.

Greenwood, N. N.; Earnshaw, A. (1997). Chemistry of the Elements (2nd ed.). Butterworth–Heinemann. p. 653. ISBN 0080379419.

Habashi Fathi. (1980). Principle of Extractive Metallurgy: Hydrometallurgy. New York: Gordon and Breach Science Publisher, Inc., Vol. (2)

Habashi Fathi. (1993): A Textbook of hydrometallurgy. Metallurgie Extractive Quebec

Habashi Fathi. (1999). Kinetics of metallurgical processes. Metallurgie Extractive Quebec

Harmet. M. (1879): Journal of Iron and steel Institute. Pp 150 – 153.

Haroyushi Tanabe and Masayuki Nakada 2003: Steelmaking Technologies, contributing to steel industries. NKK Technical review No 88. Pp 18 – 27.

http://en.wikipedia.org/Hydrochloric_acid.

http://en.wikipedia.org/Sulfuric_acid.

Information on *http://en.m.wikipedia.org*

Jian, N., Sharma, D.K., 2004: Biohydrometallurgy for non-sulphide minerals a review. Geomicrobiology journal 21, 135-144.

Jiang. X, Chen. Z, Lu. Z, Zhang. G and Zhong. Z (2007): Development and application of BRP technology in Baosteel. Revue de Metallurgie, Vol 104(1), Pp 29 – 34.

Jian-ping Duan, Yong-liang Zhang and Xue-min Yang (2009): Electric Arc Furnace steelmaking process with increasing hot metal charging ratio and improving slagging regime. International journal of Minerals, Metallurgy and Materials. Vol. 16 No 4. Pp 375 – 382.

Jin Yong-shi, Jiang Tao, Yang Yong-bin, Li Qian, Li Guang-hui and Guo Yu-feng (2006): Removal of phosphorus from Changde iron ore by chemical leaching. Journal of Central South University of Tecchnology. Vol. 13 No 6. Pp 673 – 677.

Kokal . H. R. (1990): The origin of Phosphorus in ironmaking raw materials and methods of removal. A review. Proceedings of the 63rd Annual Meeting – The Minnesota section AIME and 51st Annual Mining Symposium, Duluh – Minnesota. Pp 225 – 258.

Kokal. H. R., Singh, M. P., Naydyonov, V. A.,(2003): Removal of phosphorus from Lisakovsky iron ore by roast leach process. Proceeding of the 5th International symposium. Honouring Prof. Ian .M. Ritchie. Hydrometallurgy.

Kudrin, V. (1985):*Steel Making*. Moscow: MIR Publishers, pp 82 – 83.

Lenintov. B. L., Mirko. V.A., Kantemirov .M .D., Klimushkin .A .N., Naidenov .V.A., and Bohir .A.V.(2007): Structure of Oolitic brown Iron ores and their influence on the thermochemical Enrichment of lisakovsk concentrate. Steel in translation, vol 37, No. 8, Pp 681 – 685.

Maton, Anthea; Jean Hopkins, Charles William McLaughlin, Susan Johnson, Maryanna Quon Warner, David LaHart, Jill D. Wright (1993). Human Biology and Health. Englewood Cliffs, New Jersey, USA: Prentice Hall. ISBN 0-13-981176-1.

Matsuo,S., Ikeda, R. and Inaga, S., (1980):Method of dephosphurizing ore, Japanese patent 57-67136, English translation by BHP Central research laboratories.

Minerals and industry in Nigeria(1987): History of geological survey in Nigeria. Federal Ministry of Mines and power, Lagos Nigeria. Pp 5 – 7.

Monaghan. B.J., Pomfret R.J., and Coley. K.S., (1998): The kinetics of dephosphorization of carbon saturated iron using an oxidizing slag. Metallurgical and Materials transaction B. Vol 29B(1) Pp 111 – 118.

Morris, R.C (1973): A pilot study of phosphorus distribution in parts of the Brockman iron formation. Hamersley Group Internal report.

Muhammed Mamoun and Zhang Yu, (1989): A hydrometallurgical process for the dephosphorization of iron ore. Hydrometallurgy, 21. Pp 277 – 292.

Naito. K and Wakoh. M (2005): Recent change in refining process in Nippon Steel corporation and Metallurgical phenomenon in the new process. Scandinavian Journal of Metallurgy. Vol. 34(6). Pp 326 – 333.

Norton, S (2008). "A Brief History of Potable Gold". Molecular Interventions **8** (3): 120–3. DOI:10.1124/mi.8.3.1. PMID 18693188

Nwoye, C.I.(2008): Model for predicting the time of dissolution of pre-quantified concentration of phosphorus during leaching with Oxalic acid. International Journal of Natural and Applied Science. 4(3): 168 – 174.

Nwoye, C.I., Amara,G.N., and Onyemaobi, O.O.(2008): Model for Evaluating dissolved iron during leaching of iron oxide in sulphuric acid solution. International Journal of Natural and Applied Science. 4(2): 209 – 211.

Olanipekun .E .O. (2000): Kinetics of leaching laterite. International Journal of Mineral processing. Vol 60. Pp 9 – 14.

Oloche, O.B. and Hirse, P., (1995): Feasibility of using some Nigerian Iron Ores as Raw Materials for the Midrex Direct Reduction Process, Proceedings of Kaduna Polytechnic, Vol.2, pp. 71-75.

Oyeyinka, A., (1997): Chemical Compositions of some major Nigerian Iron Ore Deposits, Journal of the Raw Material Research Development Council, Vol.2, No.1, pp. 23-28.

Peixoto, G. (1991):Improvement of the reduction process in phosphorus content and other gangue in iron ore and its agglomerates. International patent 1991, No 93/10271.

Penniston KL, Nakada SY, Holmes RP, Assimos DG (2008). "Quantitative Assessment of Citric Acid in Lemon Juice, Lime Juice, and Commercially-Available Fruit Juice Products". *Journal of Endourology* **22** (3): 567–570.

Perry, R.; Green D., Maloney J. (1984). *Perry's Chemical Engineers' Handbook* (6th ed.). McGraw-Hill Book Company. ISBN 0-07-049479-7.

Povermo, J.(2005): Raw material challenges for blast furnace and direct reduction iron making. Proceeding of the 5th IAS Ironmaking Conference. Argentinian steelmaking Institute (IAS) Argentina. Pp 239 – 248.

Rawlings D.E (2007):Chemical leaching of Sishen iron ore using a range of oxidative chemicals. University of Pretoria. S.A.

Sahin.Y (2005): The prediction of wear resistance model for the metal matrix composites, wear 258, 1717 – 1722.

Sanchez-Reira .F (1999):Production of organic Acids. Biotechnology-Vol. V. Bio-Technical Resources, Wisconsin, USA.

Serdar Z.E. (1999): Classification of steel. Pp 1 – 5. Spon Ltd.

Snelus G.J. (1879): On the removal of Phosphorus and sulphur during the Bessemer and Siemens – Martin processes of steel manufacture.Journal of Iron and steel Institute. Pp 135 – 143.

Somnath Basu (2007): Studies on dephosphorization during steel making. School of Industrial Engineering and Management. Department of Material Science and Engineering, Division of material process science. Royal institute of technology. Stockholm. Sweden. Ph.D Dissetation.

Sultana .U. K. Fahmida Gulshan and Kurny .A .S. W. (2012):Kinetics of leaching of iron oxide in clay in oxalic acid and in Hydrochloric acid solution. International Journal of Electrical Engineering and Technology. Vol 1 Pp 1 – 14.

Sun, D. And Yang, Y.(1997): Method for microbial-chemical dephosphorization of iron ore. Chinese patent No CN 1107518 A.

Thomas S.G and Gilchrist P.G. (1879): Elimination of phosphorus in the Bessemer Converter. Journal of Iron and steel Institute. Pp 120 – 134.

Thomas(2012): Determination of the work indexes of the run-off mine and calcined Koton karfe iron ore. Nigerian Journal of Engineering. Vol 18. No. 2.

Thomas, D.G. (2008). Development of Process Route for the Beneficiation of Koton-Karfe Iron Deposit: Seminar on PhD Dissertation, Dept. of Metallurgical and Materials Engineering, Ahmadu Bello University, Zaria.

Thomas, D.G., (2002): Beneficiation of the Toto Muro Iron Ore Deposit, Department of Metallurgical Engineering, A. B. U. Zaria. M.Sc. Thesis, Unpublished.

Uwadiale, G. G. O. O. (1984): Beneficiation studies of Agbaja Iron ore. Ph.D thesis. Department of pure and applied chemistry, University of Strathclyde Glasgow.

Uwadiale, G.G.O.O. (1989): Up-grading of Nigerian Iron Ore, Journal of Mineral and Metallurgical Processing, vol.2, No.3, pp34-37.

Van Wazer, R.J. (1988). Phosphorus and Its Compounds. New York: Interscience Publishers, Inc., Vol. (3)

Wang, J., Liu, P., 1996: Comparison of citric acid production by aspergillus niger immobilized in gels and cryogels of polycrylamide. Journal of industrial Microbiology 16, 351 - 353.

Wang, W. X. (1997): Research background of the mineral processing group at Wuhan Yejin University of science and technology. Private communication.

Ward, R.G. (1982). An Introduction to the Physical Chemistry of Iron and Steel making. London: Edward Arnold (Publishers) Ltd.Wiley Eastern Limited.

Weast, R. (1981): CRC Handbook of Chemistry and Physics. 60th edition. Pp. B87.

Williams.P. J and Cloete T.E. (2008): The use of Aspergillus niger for the removal of phosphorous and potassium from the iron ore of the Sishen Iron ore Mine. Proceedings of Grahamstown Conference, South Africa.

Xia Wen-tang, Ren Zheng-de, and Gao Yi-feng (2011):Removal of phosphorus from high phosphorus iron ores by selective hydrochloric acid leaching. Journal of Iron nd Steel Research, International 18(5) 01 – 04.

Yusfin, Y. S., Chernousov, P. I., Garten, V., Karpov, Y. A. and Petelin, A. L. (1999): The role of alkali's and conserving resources in blast-furnace smelting. Metallurgist 43: 54-58.

Zhang Yu, Muhammed Mamoun 1988(a): Extraction of phosphoric acid from nitrate solutions with isoamyl alcohol. Solvent extraction. Ion exchange. 6(6) Pp 973

Zhang Yu, Muhammed Mamoun 1988(b): Removal of nitric acid from concentrated phosphoric acid by extraction with methyl isobutyl ketone in aromatic diluents. Solvent extraction. Ion exchange. 6(6) Pp 993.

Zhang Yu, Muhammed Mamoun 1989: the removal of phosphorus from iron ore by leaching with nitric acid (J). Hydrometallurgy, (21): 255 – 275.

Zhang Yu, Muhammed Mamoun 1990: An integrated process for the treatment of apatite obtained from the dephosphorization of iron ore. Journal of chemical technology Biotechnology, 47, 47-60.

APPENDIX

APPENDIX A

Table A1: XRF result for the variation of agitation rate on leaching of -355 +250µm particle size with Sulphuric acid.

	AGITATION (rpm)					
Constituent	Control	100	200	300	400	500
SiO_2	15.81	16.27	15.44	15.99	13.95	15.31
TiO_2	0.24	0.21	0.21	0.22	0.22	0.21
Al_2O_3	12.20	11.31	11.73	11.33	10.31	11.77
Fe_2O_3	67.73	67.90	68.71	68.10	66.36	68.42
MnO	0.45	0.40	0.40	0.39	0.38	0.40
MgO	0.47	0.53	0.39	0.40	0.30	0.36
CaO	0.35	0.16	0.14	0.14	0.13	0.14
Na_2O	*<0.01*	*<0.01*	*<0.01*	*<0.01*	*<0.01*	*<0.01*
K_2O	0.08	0.03	0.03	0.03	0.03	0.03
P_2O_5	1.98	1.78	1.55	1.76	1.53	1.51
Cr_2O_3	0.02	0.01	0.01	0.02	0.01	0.01
NiO	0.02	0.01	0.02	0.01	0.02	0.02
V_2O_5	0.07	0.07	0.07	0.07	0.07	0.07
ZrO_2	0.01	0.01	0.01	0.01	0.01	0.01
SO_3	0.15	0.90	0.79	0.74	0.70	0.70
WO_3	0.07	0.05	0.03	0.04	0.03	0.04
BaO	0.07	0.06	0.06	0.06	*<0.01*	*<0.01*
Cl	0.06	0.08	0.03	0.03	0.04	0.05
CuO	*<0.01*	0.01	*<0.01*	*<0.01*	0.01	0.01
ZnO	0.05	0.05	0.05	0.05	0.04	0.04
Co_3O_4	0.07	0.09	0.08	0.07	0.07	0.07
SrO	0.05	0.04	0.04	0.04	0.03	0.03
MoO3	0.02	*<0.01*	0.02	*<0.01*	*<0.01*	*<0.01*

Table A2: XRF result for the variation of agitation rate on leaching of -355 +250µm particle size with 0.5M Hydrochloric acid.

		AGITATION (rpm)				
Constituent	Control	100	200	300	400	500
SiO_2	15.81	16.19	16.00	15.97	15.87	16.08
TiO_2	0.24	0.22	0.22	0.22	0.21	0.21
Al_2O_3	12.20	11.56	11.84	11.74	11.49	11.47
Fe_2O_3	67.73	67.44	67.86	68.28	68.20	68.22
MnO	0.45	0.40	0.40	0.41	0.40	0.41
MgO	0.47	0.60	0.48	0.42	0.57	0.56
CaO	0.35	0.18	0.16	0.14	0.16	0.16
Na_2O	*<0.01*	*<0.01*	*<0.01*	*<0.01*	*<0.01*	*<0.01*
K_2O	0.08	0.03	0.03	0.02	0.03	0.03
P_2O_5	1.98	1.82	1.58	1.57	1.84	1.57
Cr_2O_3	0.02	0.02	0.02	0.02	0.02	0.02
NiO	0.02	0.02	0.02	0.02	0.02	0.02
V_2O_5	0.07	0.07	0.07	0.07	0.06	0.07
ZrO_2	0.01	0.01	0.01	0.01	0.01	0.01
SO_3	0.15	0.13	0.10	0.11	0.11	0.09
WO_3	0.07	0.05	0.05	0.04	0.05	0.05
BaO	0.07	0.06	0.06	0.06	0.06	0.06
Cl	0.06	1.01	0.70	0.52	0.66	0.62
CuO	*<0.01*	0.01	0.01	0.01	0.01	*<0.01*
ZnO	0.05	0.05	0.05	0.04	0.05	0.05
Co_3O_4	0.07	0.07	0.08	0.07	0.08	0.08
SrO	0.05	0.04	0.04	0.04	0.04	0.04
MoO3	0.02	0.01	0.01	0.02	0.02	0.01

Table A3 : XRF result for the variation of agitation rate on leaching of -355 +250µm particle size with 0.5M Citric acid.

	AGITATION (rpm)					
Constituent	Control	100	200	300	400	500
SiO_2	15.81	16.74	16.04	15.63	15.48	15.74
TiO_2	0.24	0.22	0.22	0.23	0.23	0.22
Al_2O_3	12.20	11.52	11.69	12.07	12.04	11.96
Fe_2O_3	67.73	68.07	68.53	67.81	68.45	68.71
MnO	0.45	0.39	0.40	0.43	0.41	0.40
MgO	0.47	0.39	0.44	0.59	0.51	0.42
CaO	0.35	0.16	0.17	0.21	0.19	0.18
Na_2O	*<0.01*	*<0.01*	*<0.01*	*<0.01*	*<0.01*	*<0.01*
K_2O	0.08	0.03	0.03	0.03	0.03	0.03
P_2O_5	1.98	1.83	1.85	1.86	1.59	1.60
Cr_2O_3	0.02	0.02	0.02	0.02	0.02	0.02
NiO	0.02	0.02	0.02	0.02	0.03	0.02
V_2O_5	0.07	0.07	0.07	0.07	0.06	0.07
ZrO_2	0.01	0.01	0.01	0.01	0.01	0.01
SO_3	0.15	0.16	0.15	0.09	0.09	0.10
WO_3	0.07	0.04	0.04	0.08	0.05	0.04
BaO	0.07	0.06	0.06	0.06	0.06	0.06
Cl	0.06	0.05	0.07	0.53	0.34	0.04
CuO	*<0.01*	0.01	0.01	0.01	0.00	0.01
ZnO	0.05	0.05	0.04	0.05	0.05	0.05
Co_3O_4	0.07	0.06	0.06	0.09	0.06	0.06
SrO	0.05	0.04	0.04	0.04	0.04	0.04
MoO3	0.02	*<0.01*	0.02	0.02	0.02	0.01

APPENDIX B

Table B1: XRF result for the variation of Temperature on leaching of -355 +250µm particle size with 0.3M Sulphuric acid.

				TEMPT (°C)			
Constituent	Control	30	40	50	60	70	80
SiO_2	15.81	15.31	14.97	14.67	14.27	14.82	14.61
TiO_2	0.24	0.21	0.23	0.23	0.22	0.23	0.23
Al_2O_3	12.20	11.77	12.25	12.38	11.26	11.96	11.80
Fe_2O_3	67.73	68.42	68.48	68.32	69.65	68.22	68.35
MnO	0.45	0.40	0.39	0.39	0.38	0.37	0.36
MgO	0.47	0.36	0.42	0.47	0.52	0.52	0.57
CaO	0.35	0.14	0.17	0.18	0.17	0.18	0.18
Na_2O	*<0.01*	*<0.01*	0.08	0.09	0.11	0.08	0.08
K_2O	0.08	0.03	0.03	0.03	0.03	0.03	0.03
P_2O_5	1.98	1.51	1.63	1.74	1.76	1.87	1.82
Cr_2O_3	0.02	0.01	0.02	0.02	0.02	0.02	0.02
NiO	0.02	0.02	0.01	0.01	0.01	0.01	0.02
V_2O_5	0.07	0.07	0.06	0.06	0.07	0.06	0.07
ZrO_2	0.01	0.01	0.01	0.01	0.01	0.01	0.01
SO_3	0.15	0.70	0.92	1.06	1.18	1.30	1.51
WO_3	0.07	0.04	0.02	0.02	0.02	0.02	0.02
BaO	0.07	*<0.01*	0.06	0.06	0.07	0.07	0.07
Cl	0.06	0.05	0.04	0.04	0.05	0.03	0.03
CuO	*<0.01*	0.01	*<0.01*	*<0.01*	*<0.01*	*<0.01*	*<0.01*
ZnO	0.05	0.04	0.03	0.04	0.04	0.03	0.03
Co_3O_4	0.07	0.07	0.06	0.06	0.06	0.07	0.07
SrO	0.05	0.03	0.05	0.05	0.04	0.05	0.05
MoO3	0.02	*<0.01*	*<0.01*	0.02	0.02	0.02	0.02

Table B2: XRF result for the variation of Temperature on leaching of -355 +250µm particle size with 0.5M Hydrochloric acid.

	TEMPT (°C)						
Constituent	Control	30	40	50	60	70	80
SiO_2	15.81	15.97	14.55	14.78	14.69	14.49	15.11
TiO_2	0.24	0.22	0.23	0.22	0.23	0.23	0.24
Al_2O_3	12.20	11.74	12.78	12.63	12.67	12.29	12.33
Fe_2O_3	67.73	68.28	68.09	68.22	68.00	68.71	67.85
MnO	0.45	0.41	0.43	0.40	0.40	0.36	0.33
MgO	0.47	0.42	0.51	0.53	0.52	0.47	0.51
CaO	0.35	0.14	0.19	0.18	0.18	0.17	0.18
Na_2O	*<0.01*	*<0.01*	0.11	0.10	0.11	0.09	0.11
K_2O	0.08	0.02	0.02	0.03	0.03	0.02	0.02
P_2O_5	1.98	1.57	1.92	1.69	1.93	1.93	1.96
Cr_2O_3	0.02	0.02	0.02	0.02	0.02	0.02	0.02
NiO	0.02	0.02	0.01	0.01	0.02	0.01	0.01
V_2O_5	0.07	0.07	0.07	0.07	0.07	0.07	0.07
ZrO_2	0.01	0.01	0.01	0.01	0.01	0.01	0.01
SO_3	0.15	0.11	0.12	0.10	0.09	0.09	0.11
WO_3	0.07	0.04	0.02	0.02	0.02	0.03	0.03
BaO	0.07	0.06	0.06	0.06	0.06	0.06	0.06
Cl	0.06	0.52	0.61	0.65	0.72	0.72	0.84
CuO	*<0.01*	0.01	*<0.01*	*<0.01*	*<0.01*	*<0.01*	*<0.01*
ZnO	0.05	0.04	0.04	0.04	0.03	0.04	0.03
Co_3O_4	0.07	0.07	0.07	0.08	0.07	0.08	0.08
SrO	0.05	0.04	0.05	0.05	0.05	0.05	0.05
MoO3	0.02	0.02	0.02	0.02	*<0.01*	0.02	0.01

Table B3: XRF result for the variation of Temperature on leaching of -355 +250µm particle size with 0.5M Citric acid.

	TEMPT (°C)						
Constituent	Control	30	40	50	60	70	80
SiO_2	15.81	15.48	15.05	15.01	14.95	14.72	14.59
TiO_2	0.24	0.23	0.23	0.23	0.23	0.23	0.23
Al_2O_3	12.20	12.04	12.54	12.55	12.59	12.06	12.35
Fe_2O_3	67.73	68.45	68.80	68.70	68.80	69.56	69.40
MnO	0.45	0.41	0.41	0.38	0.36	0.34	0.30
MgO	0.47	0.51	0.37	0.39	0.37	0.38	0.40
CaO	0.35	0.19	0.17	0.17	0.16	0.17	0.15
Na_2O	*<0.01*	*<0.01*	0.09	0.11	0.10	0.12	0.09
K_2O	0.08	0.03	0.03	0.03	0.03	0.03	0.03
P_2O_5	1.98	1.59	1.63	1.90	1.92	1.87	1.93
Cr_2O_3	0.02	0.02	0.02	0.02	0.02	0.02	0.01
NiO	0.02	0.03	0.02	0.01	0.01	0.01	0.01
V_2O_5	0.07	0.06	0.06	0.07	0.06	0.07	0.07
ZrO_2	0.01	0.01	0.01	0.01	0.01	0.01	0.01
SO_3	0.15	0.09	0.12	0.11	0.12	0.09	0.10
WO_3	0.07	0.05	0.02	0.02	0.02	0.02	0.02
BaO	0.07	0.06	0.06	0.05	0.05	0.05	0.05
Cl	0.06	0.34	0.03	0.04	0.03	0.04	0.03
CuO	*<0.01*	0.00	*<0.01*	*<0.01*	*<0.01*	*<0.01*	*<0.01*
ZnO	0.05	0.05	0.03	0.04	0.03	0.04	0.04
Co_3O_4	0.07	0.06	0.05	0.05	0.05	0.05	0.07
SrO	0.05	0.04	0.05	0.05	0.04	0.04	0.04
MoO3	0.02	0.02	0.02	0.01	0.01	0.01	0.02

APPENDIX C

Table C1: XRF result showing the effect of 0.15M concentration of Sulphuric acid and variation of time on the leaching of -355 +250 µm particle size

		TIME(Mins)					
Constituent	Control	20	40	60	80	100	120
SiO_2	15.81	16.67	16.61	16.68	16.33	15.88	16.08
TiO_2	0.24	0.22	0.23	0.22	0.22	0.23	0.23
Al_2O_3	12.20	11.33	11.73	11.39	11.78	12.12	12.45
Fe_2O_3	67.73	67.97	67.77	67.93	67.97	68.14	67.63
MnO	0.45	0.40	0.39	0.40	0.37	0.35	0.32
MgO	0.47	0.41	0.40	0.40	0.39	0.38	0.38
CaO	0.35	0.13	0.14	0.14	0.14	0.14	0.14
Na_2O	*<0.01*	*<0.01*	*<0.01*	*<0.01*	*<0.01*	*<0.01*	*<0.01*
K_2O	0.08	0.02	0.03	0.03	0.02	0.02	0.03
P_2O_5	1.98	1.83	1.57	1.79	1.83	1.59	1.61
Cr_2O_3	0.02	0.02	0.02	0.02	0.02	0.02	0.02
NiO	0.02	0.02	0.03	0.02	0.03	0.02	0.02
V_2O_5	0.07	0.07	0.07	0.06	0.06	0.07	0.06
ZrO_2	0.01	0.01	0.01	0.01	0.01	0.01	0.01
SO_3	0.15	0.48	0.50	0.56	0.50	0.52	0.55
WO_3	0.07	0.06	0.05	0.05	0.04	0.04	0.03
BaO	0.07	0.06	0.06	0.06	0.06	0.06	0.06
Cl	0.06	0.01	0.01	0.01	0.01	0.01	0.01
CuO	*<0.01*	0.01	0.01	0.01	0.01	0.01	*<0.01*
ZnO	0.05	0.05	0.05	0.05	0.05	0.05	0.05
Co_3O_4	0.07	0.07	0.07	0.06	0.06	0.07	0.08
SrO	0.05	0.04	0.04	0.04	0.04	0.05	0.04
MoO3	0.02	0.01	0.02	0.01	0.01	0.01	0.01

Table C2: XRF result showing the effect of 0.3M concentration of Sulphuric acid and variation of time on the leaching of -355 +250 µm particle size.

		TIME(Mins)					
Constituent	Control	20	40	60	80	100	120
SiO_2	15.81	15.32	15.85	15.31	16.97	17.29	16.25
TiO_2	0.24	0.23	0.23	0.21	0.23	0.22	0.23
Al_2O_3	12.20	11.87	12.01	11.77	11.67	11.85	12.32
Fe_2O_3	67.73	68.71	68.07	68.42	67.42	66.83	67.45
MnO	0.45	0.41	0.40	0.40	0.40	0.38	0.40
MgO	0.47	0.40	0.38	0.36	0.38	0.38	0.37
CaO	0.35	0.14	0.14	0.14	0.15	0.14	0.15
Na_2O	*<0.01*	*<0.01*	*<0.01*	*<0.01*	*<0.01*	*<0.01*	*<0.01*
K_2O	0.08	0.03	0.03	0.03	0.03	0.03	0.03
P_2O_5	1.98	1.85	1.84	1.51	1.53	1.82	1.57
Cr_2O_3	0.02	0.02	0.02	0.01	0.02	0.01	0.02
NiO	0.02	0.02	0.02	0.02	0.02	0.02	0.02
V_2O_5	0.07	0.07	0.07	0.07	0.07	0.06	0.06
ZrO_2	0.01	0.01	0.01	0.01	0.01	0.01	0.01
SO_3	0.15	0.57	0.58	0.70	0.57	0.60	0.63
WO_3	0.07	0.04	0.04	0.04	0.06	0.04	0.03
BaO	0.07	0.07	0.06	*<0.01*	0.06	0.06	0.07
Cl	0.06	0.01	0.01	0.05	0.01	0.01	0.01
CuO	*<0.01*	0.01	0.01	0.01	0.01	0.01	*<0.01*
ZnO	0.05	0.05	0.05	0.04	0.05	0.05	0.04
Co_3O_4	0.07	0.06	0.06	0.07	0.06	0.06	0.06
SrO	0.05	0.04	0.04	0.03	0.04	0.04	0.05
MoO3	0.02	0.02	0.01	*<0.01*	0.02	0.02	0.01

Table C3: XRF result showing the effect of 0.6M concentration of Sulphuric acid and variation of time on the leaching of -355 +250 µm particle size.

		TIME(Mins)					
Constituent	Control	20	40	60	80	100	120
SiO_2	15.81	15.28	15.72	15.48	15.38	15.06	16.12
TiO_2	0.24	0.23	0.23	0.23	0.23	0.24	0.23
Al_2O_3	12.20	11.64	11.72	12.31	12.03	12.47	11.52
Fe_2O_3	67.73	68.88	68.24	67.86	68.21	68.23	68.02
MnO	0.45	0.40	0.40	0.39	0.39	0.39	0.39
MgO	0.47	0.42	0.43	0.41	0.41	0.40	0.42
CaO	0.35	0.15	0.15	0.15	0.15	0.16	0.15
Na_2O	*<0.01*	*<0.01*	*<0.01*	*<0.01*	*<0.01*	*<0.01*	*<0.01*
K_2O	0.08	0.03	0.03	0.03	0.03	0.03	0.03
P_2O_5	1.98	1.57	1.83	1.86	1.84	1.56	1.83
Cr_2O_3	0.02	0.02	0.02	0.02	0.02	0.02	0.02
NiO	0.02	0.02	0.02	0.03	0.03	0.02	0.02
V_2O_5	0.07	0.07	0.06	0.07	0.07	0.07	0.06
ZrO_2	0.01	0.01	0.01	0.01	0.01	0.01	0.01
SO_3	0.15	0.80	0.81	0.78	0.81	0.83	0.81
WO_3	0.07	0.04	0.03	0.04	0.06	0.03	0.05
BaO	0.07	0.06	0.06	0.06	0.06	0.07	0.06
Cl	0.06	0.01	0.01	0.01	0.01	0.01	0.01
CuO	*<0.01*	0.01	0.01	0.01	0.01	0.01	0.01
ZnO	0.05	0.05	0.05	0.05	0.05	0.05	0.05
Co_3O_4	0.07	0.08	0.08	0.08	0.08	0.07	0.09
SrO	0.05	0.04	0.05	0.05	0.05	0.05	0.04
MoO3	0.02	*<0.01*	0.02	0.02	0.02	0.02	0.02

Table C4: XRF result showing the effect of 0.9M concentration of Sulphuric acid and variation of time on the leaching of -355 +250 µm particle size.

		TIME(Mins)					
Constituent	Control	20	40	60	80	100	120
SiO_2	15.81	15.79	16.23	16.41	16.55	16.27	16.88
TiO_2	0.24	0.21	0.22	0.23	0.22	0.22	0.23
Al_2O_3	12.20	11.22	11.42	11.83	11.24	11.88	11.72
Fe_2O_3	67.73	68.73	68.47	67.94	68.54	67.96	67.23
MnO	0.45	0.40	0.39	0.39	0.39	0.38	0.37
MgO	0.47	0.41	0.40	0.39	0.42	0.39	0.37
CaO	0.35	0.13	0.14	0.14	0.13	0.14	0.15
Na_2O	*<0.01*	*<0.01*	*<0.01*	*<0.01*	*<0.01*	*<0.01*	*<0.01*
K_2O	0.08	0.02	0.03	0.03	0.03	0.03	0.03
P_2O_5	1.98	1.79	1.47	1.31	1.16	1.33	1.59
Cr_2O_3	0.02	0.02	0.02	0.02	0.02	0.02	0.02
NiO	0.02	0.02	0.02	0.02	0.02	0.02	0.02
V_2O_5	0.07	0.06	0.07	0.07	0.07	0.06	0.06
ZrO_2	0.01	0.01	0.01	0.01	0.01	0.01	0.01
SO_3	0.15	0.77	0.79	0.83	0.78	0.79	0.81
WO_3	0.07	0.04	0.05	0.05	0.04	0.04	0.05
BaO	0.07	0.05	0.06	0.06	0.06	0.06	0.07
Cl	0.06	0.01	0.02	0.01	0.01	0.01	0.02
CuO	*<0.01*	0.01	0.01	0.01	0.01	0.01	0.01
ZnO	0.05	0.05	0.05	0.05	0.05	0.05	0.05
Co_3O_4	0.07	0.07	0.08	0.08	0.06	0.07	0.07
SrO	0.05	0.04	0.04	0.04	0.04	0.04	0.05
MoO3	0.02	0.02	0.01	0.01	0.01	0.02	0.02

Table C5: XRF result showing the effect of 1.2M concentration of Sulphuric acid and variation of time on the leaching of -355 +250 µm particle size.

		TIME(Mins)					
Constituent	Control	20	40	60	80	100	120
SiO_2	15.81	16.86	16.76	16.52	16.83	16.63	16.50
TiO_2	0.24	0.23	0.23	0.22	0.23	0.23	0.23
Al_2O_3	12.20	11.25	11.47	11.01	11.00	11.28	11.79
Fe_2O_3	67.73	67.71	67.53	68.31	68.20	67.95	67.66
MnO	0.45	0.38	0.36	0.34	0.33	0.30	0.26
MgO	0.47	0.40	0.41	0.41	0.43	0.40	0.38
CaO	0.35	0.14	0.15	0.14	0.14	0.14	0.14
Na_2O	*<0.01*	*<0.01*	*<0.01*	*<0.01*	*<0.01*	*<0.01*	*<0.01*
K_2O	0.08	0.02	0.02	0.02	0.02	0.03	0.02
P_2O_5	1.98	1.77	1.78	1.76	1.47	1.78	1.56
Cr_2O_3	0.02	0.02	0.02	0.02	0.02	0.02	0.02
NiO	0.02	0.02	0.03	0.02	0.02	0.02	0.03
V_2O_5	0.07	0.07	0.06	0.06	0.07	0.06	0.06
ZrO_2	0.01	0.01	0.01	0.01	0.01	0.01	0.01
SO_3	0.15	0.78	0.78	0.76	0.75	0.75	0.81
WO_3	0.07	0.05	0.05	0.04	0.04	0.03	0.03
BaO	0.07	0.06	0.05	0.06	0.06	0.06	0.06
Cl	0.06	0.01	0.01	0.01	0.01	0.01	0.01
CuO	*<0.01*	0.01	0.01	0.01	*<0.01*	0.01	0.01
ZnO	0.05	0.05	0.05	0.05	0.05	0.05	0.05
Co_3O_4	0.07	0.06	0.06	0.06	0.06	0.06	0.07
SrO	0.05	0.04	0.04	0.04	0.04	0.04	0.04
MoO3	0.02	*<0.01*	0.01	0.02	0.01	0.02	0.02

Table C6: XRF result showing the effect of 0.5M concentration of Hydrochloric acid and variation of time on the leaching of -355 +250 µm particle size.

		TIME(Mins)					
Constituent	Control	20	40	60	80	100	120
SiO_2	15.81	16.86	16.52	15.97	16.84	16.48	16.15
TiO_2	0.24	0.22	0.22	0.22	0.23	0.24	0.22
Al_2O_3	12.20	11.49	11.90	11.74	12.36	12.43	12.28
Fe_2O_3	67.73	67.90	68.13	68.28	67.37	67.60	67.82
MnO	0.45	0.41	0.40	0.41	0.39	0.38	0.38
MgO	0.47	0.39	0.39	0.42	0.37	0.38	0.37
CaO	0.35	0.14	0.13	0.14	0.15	0.15	0.14
Na_2O	*<0.01*	*<0.01*	*<0.01*	*<0.01*	*<0.01*	*<0.01*	*<0.01*
K_2O	0.08	0.03	0.03	0.02	0.03	0.02	0.03
P_2O_5	1.98	1.85	1.57	1.57	1.53	1.61	1.91
Cr_2O_3	0.02	0.02	0.02	0.02	0.02	0.02	0.02
NiO	0.02	0.02	0.02	0.02	0.02	0.02	0.02
V_2O_5	0.07	0.07	0.07	0.07	0.06	0.06	0.07
ZrO_2	0.01	0.01	0.01	0.01	0.01	0.01	0.01
SO_3	0.15	0.06	0.07	0.11	0.07	0.07	0.06
WO_3	0.07	0.06	0.04	0.04	0.05	0.04	0.04
BaO	0.07	0.06	0.05	0.06	0.06	0.06	0.06
Cl	0.06	0.19	0.22	0.52	0.16	0.18	0.21
CuO	*<0.01*	0.01	0.01	0.01	0.01	0.01	0.01
ZnO	0.05	0.05	0.05	0.04	0.05	0.05	0.05
Co_3O_4	0.07	0.07	0.06	0.07	0.06	0.07	0.06
SrO	0.05	0.04	0.04	0.04	0.05	0.05	0.04
MoO3	0.02	0.01	0.02	0.02	0.01	0.01	0.01

Table C7: XRF result showing the effect of 1.0M concentration of Hydrochloric acid and variation of time on the leaching of -355 +250 µm particle size.

		TIME(Mins)					
Constituent	Control	20	40	60	80	100	120
SiO_2	15.81	17.42	17.40	17.34	17.58	17.01	16.20
TiO_2	0.24	0.21	0.22	0.21	0.21	0.22	0.22
Al_2O_3	12.20	11.21	11.51	11.48	11.65	11.90	12.53
Fe_2O_3	67.73	67.89	67.55	67.50	67.45	67.40	67.59
MnO	0.45	0.39	0.38	0.38	0.37	0.38	0.37
MgO	0.47	0.39	0.37	0.36	0.37	0.35	0.33
CaO	0.35	0.13	0.13	0.13	0.13	0.14	0.13
Na_2O	*<0.01*	*<0.01*	*<0.01*	*<0.01*	*<0.01*	*<0.01*	*<0.01*
K_2O	0.08	0.03	0.03	0.02	0.02	0.02	0.02
P_2O_5	1.98	1.81	1.55	1.84	1.55	1.86	1.91
Cr_2O_3	0.02	0.02	0.02	0.02	0.02	0.02	0.02
NiO	0.02	0.02	0.02	0.02	0.02	0.02	0.02
V_2O_5	0.07	0.07	0.07	0.07	0.07	0.06	0.07
ZrO_2	0.01	0.01	0.01	0.01	0.01	0.01	0.01
SO_3	0.15	0.06	0.07	0.06	0.07	0.07	0.07
WO_3	0.07	0.04	0.06	0.04	0.04	0.05	0.03
BaO	0.07	0.05	0.06	0.05	0.05	0.05	0.05
Cl	0.06	0.20	0.18	0.20	0.19	0.18	0.22
CuO	*<0.01*	0.01	0.01	0.01	0.01	0.00	0.01
ZnO	0.05	0.04	0.04	0.05	0.04	0.04	0.05
Co_3O_4	0.07	0.06	0.06	0.06	0.06	0.06	0.05
SrO	0.05	0.04	0.04	0.04	0.04	0.04	0.04
MoO3	0.02	0.00	0.02	0.02	0.01	0.02	*<0.01*

Table C8: XRF result showing the effect of 1.5M concentration of Hydrochloric acid and variation of time on the leaching of -355 +250 µm particle size.

		TIME(Mins)					
Constituent	Control	20	40	60	80	100	120
SiO_2	15.81	17.00	16.89	17.22	16.82	16.54	16.33
TiO_2	0.24	0.22	0.22	0.22	0.22	0.22	0.22
Al_2O_3	12.20	11.23	11.18	11.53	11.68	11.87	12.16
Fe_2O_3	67.73	68.26	68.17	67.51	68.01	68.17	67.87
MnO	0.45	0.38	0.39	0.38	0.39	0.38	0.38
MgO	0.47	0.40	0.39	0.36	0.37	0.37	0.37
CaO	0.35	0.13	0.12	0.13	0.13	0.13	0.14
Na_2O	*<0.01*	*<0.01*	*<0.01*	*<0.01*	*<0.01*	*<0.01*	*<0.01*
K_2O	0.08	0.02	0.02	0.02	0.02	0.02	0.02
P_2O_5	1.98	1.54	1.83	1.84	1.60	1.56	1.89
Cr_2O_3	0.02	0.02	0.02	0.02	0.02	0.02	0.02
NiO	0.02	0.02	0.02	0.02	0.02	0.02	0.02
V_2O_5	0.07	0.07	0.07	0.06	0.06	0.07	0.06
ZrO_2	0.01	0.01	0.01	0.01	0.01	0.01	0.01
SO_3	0.15	0.06	0.06	0.07	0.06	0.05	0.07
WO_3	0.07	0.05	0.06	0.05	0.04	0.04	0.05
BaO	0.07	0.05	0.05	0.05	0.06	0.05	0.06
Cl	0.06	0.28	0.26	0.24	0.24	0.25	0.25
CuO	*<0.01*	0.01	0.01	0.00	0.01	0.01	0.01
ZnO	0.05	0.05	0.05	0.05	0.04	0.04	0.05
Co_3O_4	0.07	0.07	0.06	0.07	0.07	0.07	0.09
SrO	0.05	0.04	0.04	0.04	0.04	0.04	0.04
MoO3	0.02	0.02	0.02	0.02	0.02	0.02	0.02

Table C9: XRF result showing the effect of 2.0M concentration of Hydrochloric acid and variation of time on the leaching of -355 +250 µm particle size.

		TIME(Mins)					
Constituent	Control	20	40	60	80	100	120
SiO_2	15.81	16.94	16.76	17.36	17.63	17.73	16.45
TiO_2	0.24	0.21	0.21	0.21	0.21	0.22	0.21
Al_2O_3	12.20	11.08	11.38	11.53	11.58	11.47	12.14
Fe_2O_3	67.73	68.16	68.08	67.49	67.38	67.33	67.95
MnO	0.45	0.38	0.38	0.36	0.36	0.36	0.36
MgO	0.47	0.36	0.36	0.36	0.34	0.35	0.34
CaO	0.35	0.13	0.12	0.12	0.13	0.13	0.12
Na_2O	*<0.01*	*<0.01*	*<0.01*	*<0.01*	*<0.01*	*<0.01*	*<0.01*
K_2O	0.08	0.02	0.02	0.02	0.02	0.03	0.02
P_2O_5	1.98	1.81	1.83	1.55	1.53	1.52	1.31
Cr_2O_3	0.02	0.02	0.02	0.02	0.02	0.02	0.01
NiO	0.02	0.02	*<0.01*	0.02	*<0.01*	0.02	0.02
V_2O_5	0.07	0.07	0.07	0.07	0.06	0.06	0.06
ZrO_2	0.01	0.01	0.01	0.01	0.01	0.01	0.01
SO_3	0.15	0.07	0.07	0.06	0.08	0.07	0.06
WO_3	0.07	0.05	0.05	0.05	0.06	0.06	0.04
BaO	0.07	0.06	0.05	0.05	0.05	0.05	0.05
Cl	0.06	0.36	0.37	0.34	0.31	0.34	0.40
CuO	*<0.01*	*<0.01*	0.01	*<0.01*	0.01	*<0.01*	0.01
ZnO	0.05	0.05	0.04	0.05	0.05	0.05	0.04
Co_3O_4	0.07	0.07	0.05	0.07	0.05	0.07	0.08
SrO	0.05	0.04	0.04	0.04	0.04	0.04	0.04
MoO3	0.02	0.02	0.01	0.02	0.01	0.01	0.02

Table C10: XRF result showing the effect of 2.5M concentration of Hydrochloric acid and variation of time on the leaching of -355 +250µm particle size.

		TIME(Mins)					
Constituent	Control	20	40	60	80	100	120
SiO_2	15.81	17.21	17.42	17.12	17.22	17.10	16.72
TiO_2	0.24	0.20	0.22	0.21	0.21	0.22	0.22
Al_2O_3	12.20	10.96	11.32	11.47	11.24	11.61	12.41
Fe_2O_3	67.73	68.31	67.62	67.64	67.90	67.75	67.34
MnO	0.45	0.38	0.36	0.36	0.36	0.36	0.34
MgO	0.47	0.37	0.35	0.37	0.35	0.35	0.33
CaO	0.35	0.12	0.12	0.12	0.12	0.12	0.13
Na_2O	*<0.01*	*<0.01*	*<0.01*	*<0.01*	*<0.01*	*<0.01*	*<0.01*
K_2O	0.08	0.02	0.02	0.02	0.02	0.02	0.02
P_2O_5	1.98	1.54	1.82	1.84	1.83	1.55	1.59
Cr_2O_3	0.02	0.02	0.02	0.02	0.02	0.02	0.02
NiO	0.02	0.02	0.02	0.02	0.02	0.02	0.02
V_2O_5	0.07	0.07	0.07	0.07	0.07	0.07	0.06
ZrO_2	0.01	0.01	0.01	0.01	0.01	0.01	0.01
SO_3	0.15	0.06	0.07	0.07	0.06	0.07	0.07
WO_3	0.07	0.06	0.05	0.04	0.04	0.04	0.04
BaO	0.07	0.05	0.06	0.05	0.05	0.05	0.05
Cl	0.06	0.24	0.23	0.24	0.23	0.24	0.22
CuO	*<0.01*	0.01	*<0.01*	0.01	0.01	0.01	0.01
ZnO	0.05	0.05	0.04	0.05	0.05	0.05	0.05
Co_3O_4	0.07	0.07	0.09	0.08	0.08	0.08	0.08
SrO	0.05	0.04	0.04	0.04	0.04	0.04	0.04
MoO3	0.02	0.02	0.02	0.01	0.02	0.01	0.01

Table C11: XRF result showing the effect of 0.5M concentration of Citric acid and variation of time on the leaching of -355 +250µm particle size.

		TIME(Mins)					
Constituent	Control	20	40	60	80	100	120
SiO_2	15.81	16.45	16.64	15.48	16.40	16.28	15.03
TiO_2	0.24	0.21	0.21	0.23	0.22	0.23	0.22
Al_2O_3	12.20	11.40	11.58	12.04	11.75	11.95	12.34
Fe_2O_3	67.73	68.85	68.42	68.45	68.27	68.23	68.98
MnO	0.45	0.40	0.41	0.41	0.40	0.39	0.40
MgO	0.47	0.41	0.40	0.51	0.40	0.39	0.39
CaO	0.35	0.15	0.15	0.19	0.15	0.15	0.15
Na_2O	*<0.01*	*<0.01*	*<0.01*	*<0.01*	*<0.01*	*<0.01*	*<0.01*
K_2O	0.08	0.03	0.03	0.03	0.03	0.03	0.03
P_2O_5	1.98	1.44	1.48	1.59	1.86	1.63	1.91
Cr_2O_3	0.02	0.02	0.02	0.02	0.02	0.02	0.02
NiO	0.02	0.02	0.03	0.03	0.02	0.03	0.01
V_2O_5	0.07	0.07	0.06	0.06	0.06	0.07	0.07
ZrO_2	0.01	0.01	0.01	0.01	0.01	0.01	0.01
SO_3	0.15	0.06	0.06	0.09	0.05	0.04	0.07
WO_3	0.07	0.06	0.05	0.05	0.04	0.04	0.02
BaO	0.07	0.05	0.06	0.06	0.05	0.06	0.05
Cl	0.06	0.01	0.01	0.34	0.01	0.01	0.01
CuO	*<0.01*	0.01	0.01	0.00	0.01	0.00	0.01
ZnO	0.05	0.05	0.05	0.05	0.06	0.05	0.05
Co_3O_4	0.07	0.07	0.07	0.06	0.07	0.08	0.06
SrO	0.05	0.04	0.04	0.04	0.04	0.04	0.04
MoO3	0.02	0.01	0.02	0.02	0.01	0.01	0.02

Table C12: XRF result showing the effect of 1.0M concentration of Citric acid and variation of time on the leaching of -355 +250µm particle size.

	TIME(Mins)						
Constituent	Control	20	40	60	80	100	120
SiO_2	15.81	16.54	16.68	16.74	16.84	16.40	15.98
TiO_2	0.24	0.22	0.22	0.22	0.23	0.22	0.22
Al_2O_3	12.20	11.67	11.51	11.66	11.81	11.63	11.96
Fe_2O_3	67.73	67.80	68.28	68.05	67.91	68.38	68.47
MnO	0.45	0.39	0.39	0.39	0.39	0.38	0.38
MgO	0.47	0.38	0.39	0.39	0.38	0.39	0.38
CaO	0.35	0.15	0.15	0.14	0.15	0.15	0.15
Na_2O	*<0.01*	*<0.01*	*<0.01*	*<0.01*	*<0.01*	*<0.01*	*<0.01*
K_2O	0.08	0.03	0.03	0.03	0.03	0.03	0.03
P_2O_5	1.98	1.84	1.85	1.86	1.61	1.87	1.89
Cr_2O_3	0.02	0.02	0.02	0.02	0.02	0.02	0.02
NiO	0.02	0.03	0.02	0.02	0.02	0.02	0.02
V_2O_5	0.07	0.07	0.07	0.06	0.06	0.07	0.07
ZrO_2	0.01	0.01	0.01	0.01	0.01	0.01	0.01
SO_3	0.15	0.06	0.06	0.06	0.06	0.06	0.07
WO_3	0.07	0.04	0.04	0.04	0.05	0.04	0.03
BaO	0.07	0.05	0.05	0.06	0.05	0.05	0.05
Cl	0.06	0.01	0.02	0.01	0.02	0.01	0.01
CuO	*<0.01*	0.01	0.01	0.01	0.01	0.00	0.01
ZnO	0.05	0.05	0.05	0.05	0.05	0.05	0.05
Co_3O_4	0.07	0.06	0.06	0.06	0.06	0.06	0.06
SrO	0.05	0.04	0.04	0.04	0.04	0.04	0.04
MoO3	0.02	0.01	0.02	0.01	0.01	*<0.01*	0.02

Table C13: XRF result showing the effect of 1.5M concentration of Citric acid and variation of time on the leaching of -355 +250µm particle size.

	TIME(Mins)						
Constituent	Control	20	40	60	80	100	120
SiO_2	15.81	15.91	15.97	16.68	16.63	16.75	15.98
TiO_2	0.24	0.21	0.23	0.22	0.23	0.23	0.23
Al_2O_3	12.20	11.08	11.44	11.58	11.95	12.08	12.83
Fe_2O_3	67.73	69.50	69.31	68.18	67.87	67.61	67.62
MnO	0.45	0.39	0.39	0.38	0.38	0.36	0.36
MgO	0.47	0.43	0.41	0.40	0.38	0.38	0.38
CaO	0.35	0.14	0.14	0.15	0.16	0.16	0.16
Na_2O	*<0.01*	*<0.01*	*<0.01*	*<0.01*	*<0.01*	*<0.01*	*<0.01*
K_2O	0.08	0.02	0.02	0.03	0.03	0.03	0.03
P_2O_5	1.98	1.83	1.49	1.86	1.87	1.89	1.67
Cr_2O_3	0.02	0.02	0.02	0.02	0.02	0.02	0.02
NiO	0.02	0.02	*<0.01*	0.02	0.02	0.03	0.02
V_2O_5	0.07	0.06	0.07	0.07	0.07	0.07	0.06
ZrO_2	0.01	0.01	0.01	0.01	0.01	0.01	0.01
SO_3	0.15	0.06	0.06	0.06	0.05	0.06	0.05
WO_3	0.07	0.03	0.03	0.04	0.05	0.04	0.03
BaO	0.07	0.05	0.05	0.05	0.06	0.06	0.05
Cl	0.06	0.01	0.01	0.01	0.02	0.01	0.02
CuO	*<0.01*	*<0.01*	0.01	0.01	0.01	0.01	0.01
ZnO	0.05	0.05	0.05	0.05	0.05	0.05	0.05
Co_3O_4	0.07	0.06	0.03	0.06	0.06	0.06	0.06
SrO	0.05	0.04	0.04	0.04	0.05	0.05	0.05
MoO3	0.02	0.01	0.02	0.02	0.01	0.01	0.02

Table C14: XRF result showing the effect of 2.0M concentration of Citric acid and variation of time on the leaching of -355 +250µm particle size.

	TIME(Mins)						
Constituent	Control	20	40	60	80	100	120
SiO_2	15.81	18.23	18.10	18.02	18.04	18.77	17.21
TiO_2	0.24	0.21	0.21	0.21	0.21	0.20	0.21
Al_2O_3	12.20	10.52	10.27	10.62	10.24	9.44	12.03
Fe_2O_3	67.73	67.84	68.40	68.15	68.41	68.41	67.38
MnO	0.45	0.39	0.35	0.36	0.35	0.34	0.32
MgO	0.47	0.39	0.39	0.38	0.39	0.40	0.33
CaO	0.35	0.12	0.12	0.12	0.12	0.12	0.13
Na_2O	*<0.01*	*<0.01*	*<0.01*	*<0.01*	*<0.01*	*<0.01*	*<0.01*
K_2O	0.08	0.02	0.02	0.02	0.02	0.02	0.02
P_2O_5	1.98	1.77	1.62	1.53	1.52	1.75	1.84
Cr_2O_3	0.02	0.02	0.02	0.02	0.02	0.01	0.02
NiO	0.02	0.02	0.02	*<0.01*	0.02	0.03	0.02
V_2O_5	0.07	0.07	0.06	0.07	0.06	0.07	0.06
ZrO_2	0.01	0.01	0.01	0.01	0.01	0.01	0.01
SO_3	0.15	0.06	0.07	0.07	0.07	0.07	0.08
WO_3	0.07	0.06	0.05	0.05	0.05	0.09	0.02
BaO	0.07	0.05	0.05	0.05	0.05	0.04	0.04
Cl	0.06	0.01	0.02	0.01	0.02	0.01	0.02
CuO	*<0.01*	*<0.01*	0.01	0.01	0.01	0.01	0.01
ZnO	0.05	0.05	0.05	0.05	0.05	0.05	0.05
Co_3O_4	0.07	0.06	0.06	0.04	0.06	0.07	0.06
SrO	0.05	0.03	0.03	0.03	0.03	0.03	0.04
MoO3	0.02	0.01	0.00	0.01	0.00	0.02	0.02

Table C15: XRF result showing the effect of 2.5M concentration of Citric acid and variation of time on the leaching of -355 +250µm particle size.

	TIME(Mins)						
Constituent	Control	20	40	60	80	100	120
SiO_2	15.81	17.45	17.84	17.67	17.51	17.39	17.25
TiO_2	0.24	0.21	0.21	0.21	0.21	0.21	0.22
Al_2O_3	12.20	11.02	10.79	10.65	10.74	10.39	11.92
Fe_2O_3	67.73	68.06	67.95	68.26	68.38	68.84	67.41
MnO	0.45	0.38	0.38	0.37	0.37	0.36	0.33
MgO	0.47	0.39	0.38	0.38	0.39	0.43	0.35
CaO	0.35	0.13	0.13	0.13	0.13	0.12	0.14
Na_2O	*<0.01*	*<0.01*	*<0.01*	*<0.01*	*<0.01*	*<0.01*	*<0.01*
K_2O	0.08	0.02	0.02	0.02	0.02	0.02	0.02
P_2O_5	1.98	1.81	1.80	1.78	1.81	1.56	1.86
Cr_2O_3	0.02	0.02	0.01	0.02	0.02	0.02	0.02
NiO	0.02	0.02	0.02	0.03	0.02	0.02	0.02
V_2O_5	0.07	0.07	0.07	0.07	0.06	0.07	0.07
ZrO_2	0.01	0.01	0.01	0.01	0.01	0.01	0.01
SO_3	0.15	0.05	0.05	0.05	0.05	0.07	0.06
WO_3	0.07	0.05	0.05	0.06	0.03	0.04	0.02
BaO	0.07	0.05	0.05	0.05	0.04	0.04	0.05
Cl	0.06	0.02	0.01	0.01	0.01	0.01	0.02
CuO	*<0.01*	0.01	0.01	0.01	0.00	0.01	0.01
ZnO	0.05	0.05	0.05	0.05	0.05	0.05	0.05
Co_3O_4	0.07	0.07	0.06	0.07	0.06	0.06	0.06
SrO	0.05	0.03	0.04	0.03	0.04	0.03	0.04
MoO3	0.02	0.01	0.01	0.01	*<0.01*	0.01	0.01

APPENDIX D

Table D1: XRF Results for the leaching of of -180 +125 µm particle size under optimum leaching conditions.

Constituent	Control	Sulphuric	Hydrochloric	Citric
SiO_2	14.06	14.63	14.25	14.97
TiO_2	0.22	0.22	0.22	0.21
Al_2O_3	12.25	12.05	12.13	11.11
Fe_2O_3	69.81	70.03	70.13	70.96
MnO	0.43	0.39	0.35	0.40
MgO	0.39	0.33	0.26	0.38
CaO	0.22	0.13	0.12	0.13
Na_2O	*<0.01*	*<0.01*	*<0.01*	*<0.01*
K_2O	0.08	0.02	0.02	0.02
P_2O_5	1.85	1.01	1.20	1.30
Cr_2O_3	0.02	0.02	0.02	0.02
NiO	0.02	0.02	0.02	0.02
V_2O_5	0.07	0.07	0.07	0.07
ZrO_2	0.01	0.01	0.01	0.01
SO_3	0.17	0.75	0.10	0.07
WO_3	0.05	0.03	0.03	0.03
BaO	0.07	0.06	0.05	0.05
Cl	0.05	0.01	0.32	0.01
CuO	0.01	0.01	0.01	0.01
ZnO	0.05	0.05	0.04	0.05
Co_3O_4	0.07	0.05	0.06	0.06
SrO	0.05	0.04	0.04	0.04
MoO3	0.02	0.02	0.02	0.01

APPENDIX E.

Table E1: XRF result for leaching of -355 +250µm particle size with the optimum leaching conditions after calcinations at 700^{o}C

Constituents	**Control**	**citric**	**HCL**	**H_2SO_4**
SiO2	16.61	17.30	18.03	18.79
TiO2	0.22	0.23	0.25	0.24
Al2O3	13.29	11.19	9.90	8.02
Fe2O3	66.11	68.77	69.42	70.07
MnO	0.42	0.37	0.21	0.26
MgO	0.40	0.21	0.22	0.21
CaO	0.32	0.11	0.03	0.04
Na2O	*<0.01*	*<0.01*	*<0.01*	*<0.01*
K2O	0.08	0.06	0.05	0.04
P2O5	1.96	1.37	1.27	1.08
Cr2O3	0.02	0.02	0.02	0.01
NiO	0.02	0.02	0.02	0.02
V2O5	0.06	0.07	0.04	0.04
ZrO2	0.01	0.01	0.02	0.01
SO3	0.07	0.03	0.10	0.94
WO3	0.04	0.02	0.05	0.04
BaO	0.06	0.05	*<0.01*	0.05
Cl	0.01	*<0.01*	0.10	0.01
CuO	0.01	0.01	0.01	0.01
ZnO	0.05	0.03	0.02	0.03
Co3O4	0.05	0.08	0.07	0.06
CeO2	0.01	0.01	*<0.01*	*<0.01*
SrO	0.04	0.02	*<0.01*	0.01
MoO3	0.01	0.01	0.01	0.01

Table E2: XRF result for leaching of -355 +250µm particle size with the optimum leaching conditions after calcinations at 800^{o}C

Constituents	Control	citric	HCL	H_2SO_4
SiO2	17.56	17.67	18.54	18.11
TiO2	0.22	0.23	0.25	0.23
Al2O3	12.64	10.78	9.09	8.96
Fe2O3	65.91	68.86	69.76	70.04
MnO	0.40	0.36	0.36	0.36
MgO	0.37	0.19	0.19	0.16
CaO	0.29	0.10	0.05	0.04
Na2O	*<0.01*	*<0.01*	*<0.01*	*<0.01*
K2O	0.09	0.06	0.05	0.05
P2O5	1.95	1.32	1.08	0.98
Cr2O3	0.02	0.02	0.02	0.02
NiO	0.02	0.02	0.02	0.02
V2O5	0.07	0.06	0.05	0.05
ZrO2	0.01	0.01	0.01	0.01
SO3	0.06	0.02	0.09	0.71
WO3	0.05	0.03	0.05	0.04
BaO	0.06	0.04	0.01	0.05
Cl	0.01	0.01	0.09	0.01
CuO	0.01	0.01	0.01	0.01
ZnO	0.05	0.03	0.02	0.02
Co3O4	0.05	0.07	0.08	0.06
CeO2	0.02	*<0.01*	*<0.01*	*<0.01*
SrO	0.04	0.02	*<0.01*	0.01
MoO3	0.01	0.01	0.01	0.01

Table E3: XRF result for leaching of -355 +250µm particle size with the optimum leaching conditions after calcinations at 900^{o}C

Constituents	Control	citric	HCL	H_2SO_4
SiO2	17.38	17.58	17.48	17.41
TiO2	0.23	0.24	0.25	0.25
Al2O3	12.85	11.30	10.20	9.97
Fe2O3	65.81	68.54	70.13	70.44
MnO	0.43	0.36	0.32	0.32
MgO	0.41	0.16	0.14	0.13
CaO	0.34	0.09	0.05	0.05
Na2O	*<0.01*	*<0.01*	*<0.01*	*<0.01*
K2O	0.08	0.06	0.05	0.05
P2O5	1.95	1.29	0.97	0.76
Cr2O3	0.02	0.02	0.02	0.02
NiO	0.02	0.02	0.02	*<0.01*
V2O5	0.07	0.04	0.03	0.03
ZrO2	0.01	0.01	0.01	0.01
SO3	0.05	0.01	0.07	0.33
WO3	0.04	0.05	0.04	0.03
BaO	0.06	0.03	*<0.01*	0.05
Cl	*<0.01*	0.01	0.04	0.01
CuO	0.01	0.01	0.01	*<0.01*
ZnO	0.05	0.03	0.02	0.02
Co3O4	0.06	0.07	0.07	0.05
CeO2	*<0.01*	*<0.01*	*<0.01*	*<0.01*
SrO	0.05	0.01	*<0.01*	0.01
MoO3	0.01	0.01	0.01	0.01

Table E4: XRF result for leaching of -180 +125µm particle size with the optimum leaching conditions after calcinations at 700^{o}C

Constituents	Control	citric	HCL	H_2SO_4
SiO2	18.20	15.87	17.67	16.52
TiO2	0.22	0.23	0.23	0.24
Al2O3	13.66	10.76	9.06	8.80
Fe2O3	64.62	70.70	70.69	71.51
MnO	0.38	0.37	0.27	0.39
MgO	0.27	0.19	0.19	0.19
CaO	0.21	0.09	0.04	0.03
Na2O	*<0.01*	*<0.01*	*<0.01*	*<0.01*
K2O	0.10	0.05	0.05	0.04
P2O5	1.85	1.26	1.15	0.94
Cr2O3	0.02	0.01	0.02	0.02
NiO	0.02	0.02	*<0.01*	0.02
V2O5	0.07	0.08	0.04	0.06
ZrO2	0.02	0.01	0.01	0.02
SO3	0.07	0.03	0.12	0.90
WO3	0.04	0.04	0.04	0.04
BaO	0.06	0.05	*<0.01*	0.06
Cl	0.02	*<0.01*	0.27	*<0.01*
CuO	0.01	0.01	*<0.01*	0.01
ZnO	0.04	0.03	0.02	0.03
Co3O4	0.06	0.09	0.06	0.06
CeO2	0.01	*<0.01*	*<0.01*	*<0.01*
SrO	0.04	0.02	*<0.01*	0.01
MoO3	*<0.01*	0.02	0.01	0.02

Table E5: XRF result for leaching of -180 +125µm particle size with the optimum leaching conditions after calcinations at 800^{o}C

Constituents	Control	citric	HCL	H_2SO_4
SiO2	16.78	15.62	16.95	16.84
TiO2	0.22	0.22	0.24	0.23
Al2O3	13.20	10.75	9.17	8.84
Fe2O3	66.33	70.86	71.62	71.72
MnO	0.42	0.38	0.28	0.29
MgO	0.34	0.19	0.16	0.16
CaO	0.21	0.10	0.04	0.04
Na2O	*<0.01*	*<0.01*	*<0.01*	*<0.01*
K2O	0.08	0.06	0.04	0.05
P2O5	1.85	1.25	0.99	0.73
Cr2O3	0.02	0.02	0.02	0.02
NiO	0.02	0.02	0.02	0.02
V2O5	0.07	0.06	0.03	0.03
ZrO2	0.01	0.01	0.01	0.01
SO3	0.08	0.02	0.08	0.70
WO3	0.03	0.03	0.04	0.04
BaO	0.06	0.05	*<0.01*	0.06
Cl	0.01	*<0.01*	0.10	0.01
CuO	0.01	0.01	0.01	0.01
ZnO	0.05	0.03	0.02	0.02
Co3O4	0.06	0.08	0.07	0.06
CeO2	0.01	0.02	*<0.01*	*<0.01*
SrO	0.04	0.02	*<0.01*	0.01
MoO3	0.02	0.01	0.01	0.01

Table E6: XRF result for leaching of -180 +125µm particle size with the optimum leaching conditions after calcinations at 900^{o}C.

Constituents	**Control**	**citric**	**HCL**	**H_2SO_4**
SiO2	16.31	16.53	16.24	16.51
TiO2	0.22	0.22	0.23	0.24
Al2O3	13.12	10.61	10.08	8.58
Fe2O3	67.01	70.40	71.65	72.96
MnO	0.41	0.37	0.35	0.30
MgO	0.32	0.14	0.11	0.10
CaO	0.22	0.07	0.05	0.04
Na2O	*<0.01*	*<0.01*	*<0.01*	*<0.01*
K2O	0.09	0.05	0.05	0.04
P2O5	1.85	1.20	0.79	0.49
Cr2O3	0.02	0.02	0.03	0.02
NiO	0.01	0.02	0.02	0.02
V2O5	0.07	0.04	0.05	0.03
ZrO2	0.02	0.01	0.02	0.02
SO3	0.04	0.02	0.07	0.35
WO3	0.02	0.05	0.04	0.03
BaO	0.06	0.03	0.01	0.05
Cl	0.01	*<0.01*	0.04	0.01
CuO	0.01	0.01	0.01	0.01
ZnO	0.04	0.03	0.02	0.02
Co3O4	0.05	0.07	0.06	0.07
CeO2	*<0.01*	*<0.01*	*<0.01*	*<0.01*
SrO	0.04	0.01	*<0.01*	0.01
MoO3	0.02	0.01	0.01	0.01